PROBABILISTIC SEISMIC HAZARD ASSESSMENT OF EASTERN MARMARA AND EVALUATION OF TURKISH EARTHQUAKE CODE REQUIREMENTS

A THESIS SUBMITTED TO
THE GRADUATE SCHOOL OF NATURAL AND APPLIED SCIENCES
OF
MIDDLE EAST TECHNICAL UNIVERSITY

BY

RECAİ SONER OCAK

IN PARTIAL FULFILLMENT OF THE REQUIREMENTS
FOR
THE DEGREE OF THE MASTER OF SCIENCE
IN
CIVIL ENGINEERING

NOVEMBER 2011

Approval of the thesis:

PROBABILISTIC SEISMIC HAZARD ASSESSMENT OF EASTERN MARMARA AND EVALUATION OF TURKISH EARTHQUAKE CODE REQUIREMENTS

submitted by **RECAİ SONER OCAK** in partial fulfillment of the requirements for the degree of **Master of Science in Civil Engineering Department, Middle East Technical University** by,

Prof. Dr. Canan Özgen _____
Dean, Graduate School of Natural and Applied Science

Prof. Dr. Güney Özcebe _____
Head of Department, Civil Engineering

Asst. Prof. Dr. Zeynep Gülerce _____
Supervisor, Civil Engineering Dept., METU

Examining Committee Members:

Prof. Dr. Yener Özkan _____
Civil Engineering Dept., METU

Asst. Prof. Dr. Zeynep Gülerce _____
Civil Engineering Dept., METU

Prof. Dr. Kemal Önder Çetin _____
Civil Engineering Dept., METU

Assoc. Prof. Dr. Aysegül Askan Gündoğan _____
Civil Engineering Dept., METU

Asst. Prof. Dr. Mustafa Tolga Yılmaz _____
Engineering Sciences Dept., METU

Date: **25.11.2011**

I hereby declare that all information in this document has been obtained and presented in accordance with academic rules and ethical conduct. I also declare that, as required by these rules and conduct, I have fully cited and referenced all material and results that are not original to this work.

Name, Last name : Recai Soner Ocak

Signature :

ABSTRACT

PROBABILISTIC SEISMIC HAZARD ASSESSMENT OF EASTERN MARMARA AND EVALUATION OF TURKISH EARTHQUAKE CODE REQUIREMENTS

Ocak, Recai Soner
M.Sc., Department of Civil Engineering
Supervisor: Asst. Prof. Dr. Zeynep Gülerce

November 2011, 108 pages

The primary objective of this study is to evaluate the seismic hazard in the Eastern Marmara Region using improved seismic source models and enhanced ground motion prediction models by probabilistic approach. Geometry of the fault zones (length, width, dip angle, segmentation points etc.) is determined by the help of available fault maps and traced source lines on the satellite images. State of the art rupture model proposed by USGS Working Group in 2003 is applied to the source system. Composite reoccurrence model is used for all seismic sources in the region to represent the characteristic behavior of North Anatolian Fault.

New and improved global ground motion models (NGA models) are used to model the ground motion variability for this study. Previous studies, in general, used regional models or older ground motion prediction models which were updated by their developers during the NGA project. New NGA models were improved in terms of additional prediction parameters (such as depth of the source, basin effects, site dependent standard deviations, etc.), improved statistical approach, and very well constrained global database.

The use of NGA models reduced the epistemic uncertainty in the total hazard incorporated by regional or older models using smaller datasets.

The results of the study is presented in terms of hazard curves, deaggregation of the hazard and uniform hazard spectrum for six main locations in the region (Adapazari, Duzce, Gölcük, İzmit, İznik, and Sapanca City Centers) to provide basis for seismic design of special structures in the area. Hazard maps of the region for rock site conditions at the accepted levels of risk by Turkish Earthquake Code (TEC-2007) are provided to allow the user perform site-specific hazard assessment for local site conditions and develop site-specific design spectrum. Comparison of TEC-2007 design spectrum with the uniform hazard spectrum developed for selected locations is also presented for future reference.

Keywords: Source model, probability distribution functions, slip rate, Ground Motion Prediction Equations, Probabilistic Seismic Hazard Assessment

ÖZ

DOĞU MARMARA 'DAKİ SİSMİK TEHLİKENİN OLASILIKSAL ANALİZİ VE TÜRK DEPREM ŞARTNAMESİ İLE KARŞILAŞTIRILMASI

Ocak, Recai Soner
Yüksek Lisans, İnşaat Mühendisliği Bölümü
Tez Yöneticisi: Yrd. Doç. Dr. Zeynep Gülerce

Kasım 2011, 108 sayfa

Bu çalışmanın en önemli amacı, Doğu Marmara Bölgesi'nde, gelişmiş kaynak modelleri ve yer hareketi tahmin denklemlerini kullanarak olasılıksal sismik tehlike analizi çalışmasının yapılmasıdır. Fay zonlarının geometrisi (boy, genişlik, dip açısı ve segmantasyon noktaları, vb.) mevcut fay haritaları ve uydu fotoğraflarındaki fay izleri yardımıyla bulunmuştur. USGS Çalışma Grubu'nun 2003 yılında önerdiği kırılma modelleri kaynak sistemine uygulanmıştır. Kuzey Anadolu Fayı'nın karakteristiğini temsil eden Komposit tekrarlanma modelleri bölgedeki bütün kaynaklar için kullanılmıştır.

Bu çalışmada yeni ve geliştirilmiş global yer hareketi tahmin denklemleri (NGA modelleri), yer hareketindeki değişkenliği modellemek için kullanılmıştır. Genel olarak eski çalışmalarda, bölgesel modeller ya da NGA çalışmasında güncellenmiş daha eski yer hareketi tahmin denklemleri kullanılmıştır. Yeni NGA modelleri, ilave tahmin parametreleri (kaynak derinliği, basen etkileri ve sahaya özgü standart sapma, vb.), geliştirilmiş istatistiksel yaklaşım ve çok detaylı oluşturulmuş veritabanı yardımıyla güncellenmiştir. NGA modellerinin kullanımı, toplam tehlike analizlerindeki bölgesel ya da eski modellerin kullandığı küçük veri tabanlarına bağlı epistemik belirsizliği azaltmıştır.

Bu çalışmanın sonucu olarak, tehlike eğrileri, girdi parametrelerinin (magnitüd ve uzaklık) tehlikeye katkıları ve bölgedeki altı noktada üniform tehlike spektrumu (Adapazarı, Düzce, Gölcük, İzmit, İznik ve Sapanca şehir merkezleri) sunulmuştur. Bu sonuçlar bölgedeki özel yapıların tasarımına katkı sağlayacaktır. Kaya zemin koşulları için bölgenin tehlike haritaları, Türk Deprem Şartnamesi'nde (2007) önerilen risk düzeylerine göre sunulmuştur. Bu haritalar, sahaya özgü tehlike analizlerinde ve sahaya özgü tasarım spektrumu üretilmesinde faydalı olacaktır.

Seçilen noktalar için üretilen üniform tehlike spektrumu, deprem şartnamesi ile karşılaştırılmış ve gelecekteki çalışmalar için sonuçlar sunulmuştur.

Anahtar Kelimeler: Kaynak Modeli, olasılıksal dağılım fonksiyonları, kayma oranı, Yer Hareketi Tahmin Denklemleri, Olasılıksal Sismik Tehlike Analizi

To My Beloved Family

ACKNOWLEDGEMENTS

I would like to thank my advisor Asst. Prof. Dr. Zeynep Gülerce for her guidance and support throughout the preparation of this thesis. I would also like to thank Dr. Norman Abrahamson, for his invaluable guidance in seismic source characterization and providing the hazard code.

I thank to our geologist partners Prof. Dr. Haluk Akgün, Asst. Prof. Dr. Mustafa Koçkar and Selim Cambazoglu for preparation of the source model used in this study.

I am very grateful to my friends, Onur Balal, Okan Çağrı Bozkurt, Emre Akyüz and Umut Akın for their priceless help and support at even the most desperate times during the preparation of this thesis.

Special thanks to my company Hidromark, for their understanding and tolerance throughout the preparation of this thesis.

I respectfully commemorate my grandmothers Bedia Koyuncu and Raife Ocak who we have lost during the preparation period of this thesis.

At last for this study but not the least for my life, sincere thanks to my beloved family Ragıp Ocak, Ayşın Ocak, İlker Ocak and my grandfather Hulusi Koyuncu who grow me up until now and who do not avoid their help, support, guidance, understanding and protection at any time during my life.

TABLE OF CONTENTS

ABSTRACT iv

ÖZ vi

ACKNOWLEDGEMENTS ix

TABLE OF CONTENTS x

LIST OF TABLES xiii

LIST OF FIGURES xv

CHAPTER

1. INTRODUCTION 1

1.1 Research Statement 2

1.2 Problem Significance and Limitations of Previous Studies 3

1.3 Scope 4

2. PREVIOUS HAZARD ASSESSMENT STUDIES IN THE REGION 6

2.1 Previous Studies in the Region 7

2.2 Turkish Earthquake Code (2007) 19

3. SEISMIC SOURCE CHARACTERIZATION FOR EASTERN MARMARA REGION 21

3.1 Definition of segment, source and scenario in PSHA 22

3.2 Seismic Source Characterization Procedure 23

3.2.2 Magnitude Distributions..... 25

3.2.3 Activity Rates and Reoccurrence Relations 28

3.3 Seismic Source Characterization of Eastern Marmara 29

3.3.1 Source Geometry and Mean Characteristic Magnitude for the Seismic Sources in the Region 30

3.3.2 Magnitude Distribution Models for the Sources in the Region.... 36

3.3.3 Activity Rates and Recurrence Relations for the Seismic Sources in the Region..... 40

4. SELECTION OF GROUND MOTION PREDICTION MODELS 45

4.1 Next Generation Attenuation Models 46

4.2 Available Strong Ground motion Recording in the Region and Preliminary Comparison 48

4.3 Preliminary Comparison of the NGA (2008) Models with the Strong Ground Motions of the Region..... 49

5. PROBABILISTIC SEISMIC HAZARD ASSESSMENT FOR EASTERN MARMARA REGION 67

5.1 Probabilistic Seismic Hazard Assessment Methodology 68

5.2 PSHA Results for Example Sites in the Study Area 70

5.3 Hazard Maps for Eastern Marmara Region 93

6. SUMMARY AND CONCLUSION 98

REFERENCES 104

LIST OF TABLES

TABLES

Table 2.1 Seismic zones and related effective ground acceleration coefficient (Ao) values suggested by TEC 2007. 20

Table 2.2 T_A and T_B coefficients assigned to different soil conditions by TEC 2007 20

Table 3.1 Fault segmentation of NAF_N 31

Table 3.2 Seismic Sources and Rupture Scenarios considered for NAF_N (Rows indicate rupture scenarios and columns show the seismic sources). 33

Table 3.3 Geometry of Düzce Fault 34

Table 3.4 Geometry of NAF_S 35

Table 3.5 Sources and Scenarios generated for Duzce Fault 35

Table 3.6 Sources and Scenarios generated for NAF_S 35

Table 3.7 Geometry of Geyve and Iznik Fault 35

Table 3.8 Sources and Scenarios generated for Geyve & Iznik Fault 36

Table 3.9 Distribution of magnitudes of the earthquakes within the catalog in the region (After Cambazoglu, 2011) 37

Table 3.10 Complete database intervals for different magnitude bins 38

Table 3.11 Maximum likelihood estimation of the recurrence parameter b .. 40

Table 4.1 Global Ground Motion Prediction Equations 47

Table 4.2 The number of earthquakes and recordings obtained from the events occurred in Turkey included to the databases of each NGA model.. 47
Table 5.1 Acceptable risk levels in TEC-2007 and other design codes 70
Table 5.2 PGA for different exceedance levels at six locations 80
Table 6.1 Parameters for Design Spectra 103

LIST OF FIGURES

FIGURES

Figure 2.1 The general study area and three different sources models proposed within the study Atakan et al., 2002. (After Atakan et al., 2002)..... 9

Figure 2.2 Source model proposed by the study of Erdik et al., 2004..... 10

Figure 2.3 Seismic source model used in the study of Parsons (2004) (After Parsons (2004) 11

Figure 2.4 Source model used in the study of Kalkan et al., 2009 (After Kalkan et al., 2009)..... 13

Figure 2.5 Hazard map generated from the combination of source model 3 and the attenuation model proposed by Ambraseys et al. (1996) (After Atakan et al., 2002)..... 15

Figure 2.6 Response spectra for acceleration values obtained by using three different source models and the attenuation model proposed by Ambraseys et al. (1996) for rock site (left) and soft sediment site (right) with 5% damping. (The bold dotted lines indicate the first model; gray dotted lines indicate the second model and the gray line indicate the third model) (Modified from Atakan et al., 2002)..... 15

Figure 2.7 PGA contour map for NEHRP B/C boundary site class for 10% probability of exceedance in 50 years (After Erdik et al., 2004) 16

Figure 2.8 The hazard curves showing comparison between PSHA and MCS methodologies for 2secs spectral acceleration for three municipalities in İstanbul (After Crowley and Bommer, 2006) 17
Figure 2.9 Hazard Map for PGA with a hazard level of 2% probability of exceedance in 50 years for uniform firm rock conditions. (The figure is taken from the study of Kalkan and Gülkan, 2009) 17
Figure 2.10 Hazard curves for the city of Istanbul at different spectral acceleration values for uniform firm rock condition. (After Kalkan and Gülkan, 2009) 18
Figure 2.11 Uniform design spectra for the city of Istanbul (After Kalkan and Gülkan, 2009) 18
Figure 2.12 Earthquake regions proposed by TEC 2007. The red regions indicate the first, the pink regions indicate the second, the yellow regions indicate the third and the light yellow regions indicate the fourth earthquake region. (Modified from TEC 2007) 19
Figure 2.13 Normalized spectrum coefficients proposed by TEC 2007. (The figure is taken from TEC 2007) 20
Figure 3.1 Illustration of the segment, source and scenario concepts 24
Figure 3.2 Magnitude distribution functions used in PSHA, truncated exponential, truncated normal (characteristic) and composite models (Y&C (1985) 27
Figure 3.3 Study area and the main seismic sources taken from active fault map of MTA (Saroglu et al., 1992) 30

Figure 3.4 The layout of NAFN, NAFS and Duzce Faults (After Barka et al., 2002) 30
Figure 3.5 The general layout of the sources and the slip rate assigned to each source used in this model. (This figure is modified from the study of Cambazoglu (2011)) 32
Figure 3.6 Catalogue completeness check (The circles imply the break points of the linear trend) 38
Figure 3.7 Comparison of recurrence relation and epicenter data for Duzce Fault 44
Figure 3.8 Comparison of recurrence relation and epicenter data for Geyve & Iznik Fault 44
Figure 4.1 The original (a) and processed (b) accelerogram obtained from the recording 19991112171644_9904 50
Figure 4.2 The response spectrum for the two horizontal components, geometric mean and GMRotI50 resultants obtained from the recording 19991112171644_9904 51
Figure 4.3 Residuals vs Magnitude at a)PGA, b) T =0.3 secs and c) T = 1.0 secs for A & S (2008) 52
Figure 4.4 Residuals vs Distance at a)PGA, b) T =0.3 secs and c) T = 1.0 secs for A & S (2008) 53
Figure 4.5 Residuals vs Vs30 at a)PGA, b) T =0.3 secs and c) T = 1.0 secs for A & S (2008) 54

Figure 4.6 Residuals vs Magnitude at a)PGA, b) T =0.3 secs and c) T = 1.0 secs for B & A (2008) 55
Figure 4.7 Residuals vs Distance at a)PGA, b) T =0.3 secs and c) T = 1.0 secs for B & A (2008) 56
Figure 4.8 Residuals vs Vs30 at a)PGA, b) T =0.3 secs and c) T = 1.0 secs for B & A (2008) 57
Figure 4.9 Residuals vs Magnitude at a)PGA, b) T =0.3 secs and c) T = 1.0 secs for C & B (2008) 58
Figure 4.10 Residuals vs Distance at a)PGA, b) T =0.3 secs and c) T = 1.0 secs for C & B (2008) 59
Figure 4.11 Residuals vs Vs30 at a)PGA, b) T =0.3 secs and c) T = 1.0 secs for C & B (2008) 60
Figure 4.12 Residuals vs Magnitude at a)PGA, b) T =0.3 secs and c) T = 1.0 secs for C & Y (2008) 61
Figure 4.13 Residuals vs Distance at a)PGA, b) T =0.3 secs and c) T = 1.0 secs for C & Y (2008) 62
Figure 4.14 Residuals vs Vs30 at a)PGA, b) T =0.3 secs and c) T = 1.0 secs for C & Y (2008) 63
Figure 4.15 Residuals vs Magnitude at a)PGA, b) T =0.3 secs and c) T = 1.0 secs for Idriss (2008) 64
Figure 4.16 Residuals vs Distance at a)PGA, b) T =0.3 secs and c) T = 1.0 secs for Idriss (2008) 65

Figure 4.17 Residuals vs Vs30 at a)PGA, b) T =0.3 secs and c) T = 1.0 secs for Idriss (2008) 66
Figure 5.1 The six locations where the analysis are performed 71
Figure 5.2 Hazard Curves for T = 0 secs 72
Figure 5.3 Hazard Curves for T = 0.01secs 72
Figure 5.4 Hazard Curves for T = 0.03 secs 73
Figure 5.5 Hazard Curves for T = 0.05 secs 73
Figure 5.6 Hazard Curves for T = 0.075 secs 74
Figure 5.7 Hazard Curves for T = 0.10 secs 74
Figure 5.8 Hazard Curves for T = 0.20 secs 75
Figure 5.9 Hazard Curves for T = 0.50 secs 75
Figure 5.10 Hazard Curves for T = 1.00 secs 76
Figure 5.11 Hazard Curves for T = 2.00 secs 76
Figure 5.12 Hazard Curves for T = 3.00 secs 77
Figure 5.13 Hazard Curves for T = 4.00 secs 77
Figure 5.14 Hazard Curves for T = 5.00 secs 78
Figure 5.15 Hazard Curves for T = 7.50 secs 78
Figure 5.16 Hazard Curves for T = 10.00 secs 79
Figure 5.17 Contribution of the sources to total hazard at Sapanca 80
Figure 5.18 Deaggregation for Adapazari 81
Figure 5.19 Deaggregation for Gemlik 82
Figure 5.20 Deaggregation for İzmit 82
Figure 5.21 Deaggregation for İznik 83

Figure 5.22 Deaggregation for Sapanca 83
Figure 5.23 Deaggregation for Duzce 84
Figure 5.24 Hazard Curves for different Ground Motion Prediction Models for the source of Adapazarı 85
Figure 5.25 Uniform Hazard Spectra for Duzce 87
Figure 5.26 Uniform Hazard Spectra for Adapazarı 87
Figure 5.27 Uniform Hazard Spectra for Gemlik 88
Figure 5.28 Uniform Hazard Spectra for İzmit 88
Figure 5.29 Uniform Hazard Spectra for İznik 89
Figure 5.30 Uniform Hazard Spectra for Sapanca 89
Figure 5.31 Uniform Hazard Spectra for Düzce 90
Figure 5.32 Uniform Hazard Spectra for Adapazarı 90
Figure 5.33 Uniform Hazard Spectra for Gemlik 91
Figure 5.34 Uniform Hazard Spectra for İzmit 91
Figure 5.35 Uniform Hazard Spectra for İznik 92
Figure 5.36 Uniform Hazard Spectra for Sapanca 92
Figure 5.37 Grids assigned to region 93
Figure 5.38 Hazard Map for PGA for a hazard level of 2% probability of exceedence in 50 years (g) 94
Figure 5.39 Hazard Map for PGA for a hazard level of 10% probability of exceedence in 50 years (g) 94
Figure 5.40 Hazard Map for PGA for a hazard level of 50% probability of exceedence in 50 years (g) 95

Figure 5.41 Hazard Map for T=0.2 secs for a hazard level of 2% probability of exceedence in 50 years (g)..... 95
Figure 5.42 Hazard Map for T=0.2 secs for a hazard level of 10% probability of exceedence in 50 years (g)..... 95
Figure 5.43 Hazard Map for T=0.2 secs for a hazard level of 50% probability of exceedence in 50 years (g)..... 96
Figure 5.44 Hazard Map for T=1.0 secs for a hazard level of 2% probability of exceedence in 50 years (g)..... 96
Figure 5.45 Hazard Map for T=1.0 secs for a hazard level of 10% probability of exceedence in 50 years (g)..... 96
Figure 5.46 Hazard Map for T=1.0 secs for a hazard level of 50% probability of exceedence in 50 years (g)..... 97
Figure 6.1 Design Spectrum for Rock Sites (Vs30 = 760 m/s)..... 102
Figure 6.2 Design Spectrum for Soil Sites (Vs30 = 270 m/s)..... 102

CHAPTER 1

INTRODUCTION

The formation of the Anatolia is shaped up by the tectonic interaction between African, Arabian and Eurasian plates, and this interaction results in seismic activity of the faults that exist in Turkey. As the interaction between the plates continues which means permanent seismic activity in Turkey, special care must be taken to reduce the hazard caused by earthquakes.

In 1999, two destructive earthquakes struck Marmara Region, the industrial center of Turkey, causing the loss of more than 17.000 lives and millions of dollars. The number of probabilistic seismic hazard assessment (PSHA) studies for the region, even for Turkey, was limited before these earthquakes. After the earthquakes, several researchers published valuable research results on the characteristic of seismic sources in the region and probabilistic seismic hazard assessment results for Marmara and Istanbul. In the past 12 years after the earthquakes, the region developed significantly in terms of increasing population and growing number of industrial and residential projects. Therefore, the accurate estimation of seismic hazard in the region using improved seismic source models and new ground motion attenuation models is very important to reduce the structural damage and loss of human lives from future earthquakes. At this point the methodology to follow while predicting the possible future earthquakes is very important. At the old days, people use deterministic methods to model future earthquakes.

This method is based on selecting a possible scenario that produces a possible earthquake. To decrease the uncertainty due to decision on selecting the design scenario, probabilistic methodology was proposed. In this methodology several earthquake scenarios are considered, and different ground motion levels are provided. Decision on these design levels are due to importance and economic life assigned to structure. This enables the designer to decide the proper performance levels for the design structure.

Although there exists design codes for the buildings to be constructed in seismically active regions, for more important structures (dams, bridges, high rise buildings, etc.) special care must be taken. By a better understanding over the seismic character of the sources within the area of interest, more specific analysis should be performed.

1.1 Research Statement

The primary objective of this study is to evaluate the seismic hazard in the Eastern Marmara Region using improved seismic source models and enhanced ground motion prediction models by probabilistic approach. The calculated hazard is used to assess the Turkish Earthquake Code (TEC-2007) requirements for the region. The results of the study is presented in terms of hazard curves, deaggregation of the hazard and uniform hazard spectrum for six main locations in the region (Adapazarı, Düzce, Gölcük, İzmit, İznik, and Sapanca City Centers) to provide basis for seismic design of special structures in the area. Hazard maps of the region for rock site conditions at the accepted levels of risk by TEC-2007 are provided to allow the user perform site-specific hazard assessment for local site conditions and develop site-specific design spectrum. Comparison of TEC-2007 design spectrum with the uniform hazard spectrum developed for selected locations is also presented for future reference.

Results of the study deviate from the earlier hazard studies performed in the region due to the improvements in the seismic source characterization of the

faults in the area and the employment of new ground motion prediction equations. The preliminary results of a complementary study to evaluate the applicability of the ground motion models used in this study to the region is also added to provide insight on the effect of ground motion models to the total hazard levels proposed by this study. These results may be improved by assessing the contribution of seismic sources outside the study area and modification of the ground motion model variables for seismo-tectonics properties of the region.

1.2 Problem Significance and Limitations of Previous Studies

Turkey is one of the most seismically active regions in the world therefore accurate evaluation of seismic hazard is crucial to reduce the structural damage and loss of lives in future earthquakes with a sensible and economical design practice. The main components of the probabilistic seismic hazard framework are the seismic source characterization and the ground motion prediction models. The total seismic hazard calculated for a site is quite sensitive to the parameters of these models thus; proper modeling of the seismic sources and selecting suitable and unbiased ground motion models will reduce the uncertainty in the hazard significantly.

Two significant improvements over the previous seismic hazard assessment practice were accomplished in this study; advanced seismic source models in terms of source geometry and reoccurrence relations were developed and improved global ground motion models were employed to represent the ground motion variability.

Geometry of the fault zones (length, width, dip angle, segmentation points etc.) were determined by the help of available fault maps and traced source lines on the satellite images. State of the art rupture model proposed by USGS Working Group in 2003 was applied to the source system. Composite reoccurrence model was used for all seismic sources in the region to represent the characteristic behavior of North Anatolian Fault. The benefits of

the source model used in this study when compared to the previously used source models are; (i) the use of linear fault zones instead of areal sources, (ii) employment of the state of the art fault rupture model, and (iii) proper representation of fault characterization in the earthquake reoccurrence models.

New and improved global ground motion models (NGA models) were used to model the ground motion variability for this study. Previous studies, in general, used regional models or older ground motion prediction models which were updated by their developers during the NGA project. New NGA models were improved in terms of additional prediction parameters (such as depth of the source, basin effects, site dependent standard deviations, etc.), statistical approach, and very well constrained global database. The use of NGA models reduced the epistemic uncertainty in the total hazard incorporated by regional or older models using smaller datasets. The representation of regional characteristics in global ground motion prediction models is a controversial topic therefore; a complementary study examining the applicability of these new models to the study area is also included to the scope of this study. Finally, the uncertainty level assigned to the ground motions for this study is increased to median± 3σ as the new seismic hazard practice commands whereas, previous studies use only median±1σ consistent with the deterministic approach.

1.3 Scope

The scope of this thesis can be summarized as follows;

In the first chapter general information about the concepts reviewed in this study are revised.

In the Chapter 2, the previous probabilistic seismic hazard studies performed for the study region are reviewed. The methods for finding the source and ground motion model parameters assumed by each study are compared.

In the third chapter, source characterization for the seismic zones in the region is provided. Generation of the source geometry model, selection of the recurrence relations and estimation of the characteristic earthquake magnitude for each source is explained.

In the Chapter 4, employed ground motion prediction equations are reviewed, and a preliminary comparison of the prediction models with the strong ground motions in the region is presented.

In the fifth chapter, the methodology of probabilistic seismic hazard analysis is explained and the results of the analysis are provided.

In the final chapter, the results of the analysis are discussed, and comparison between the results proposed by the national building code is provided.

CHAPTER 2

PREVIOUS HAZARD ASSESSMENT STUDIES IN THE REGION

In 1999, two destructive earthquakes struck Marmara Region, the industrial center of Turkey, causing the loss of more than 17.000 lives and millions of dollars. The number of probabilistic seismic hazard assessment (PSHA) studies for the region, even for Turkey, was limited before these earthquakes. After the earthquakes, several researchers published valuable research results on the characteristic of seismic sources in the region and probabilistic seismic hazard assessment results for Marmara and Istanbul. In the past 12 years after the earthquakes, the region developed significantly in terms of increasing population and growing number of industrial and residential projects. Therefore, the accurate estimation of seismic hazard in the region using improved seismic source models and new ground motion attenuation models is very important to reduce the structural damage and loss of human lives from future earthquakes.

In this chapter, the previous probabilistic seismic hazard assessment studies performed in the region were summarized. The focus of the chapter is on the seismic source, and ground motion prediction models used in these studies since the objective of this study is to enhance these critical elements of PSHA. Results of the previous studies were added to help the reader to compare the results of this study to the previous ones.

A short discussion on the Turkish Earthquake Code (TEC-2007) requirements is also added to the end of this chapter.

2.1 Previous Studies in the Region

The most critical elements in probabilistic seismic hazard assessment are the proper seismic source characterization and selection of ground motion prediction equations. Seismic source characterization involves the modeling the source geometry and definition of the source recurrence relation. In the previous studies, the researchers defined the sources either as areal or linear depending on the limits of the knowledge on the geometry of the fault planes (lengths, widths, dip angles, etc.). Uncertainties involved in these parameters forced the researchers to generalize the fault zones as areal sources.

Atakan et al., 2002 characterized the seismic sources in using three different models. In the first model, they divided the region into five areal sources and assumed that the earthquake occurrences follow the Poisson's process (Figure 2.1a). The earthquake recurrence relations of the areal sources were modeled with Guttenberg and Richter model (see Equation 3.2). The estimated b-value for each source ranges between 0.5-1.4 with an average of 1.0. In the second model, the sources were defined as linear sources with a buffer zone around them to treat the uncertainty in the exact location of the faults (Figure 2.1b). In this model the earthquake occurrence was assumed to follow time dependent renewal model. In the third model, linear sources were defined where exact locations of the faults were known, but linear sources with buffer zones were used if the exact location of the faults were unknown. Additionally, areal sources were defined where the fault traces cut-off by the Marmara Sea. Also in this model time dependent renewal model was used. (Figure 2.1c)

Erdik et al., 2004, characterized the seismic sources in the region by using 45 different linear fault zones. Multi segment ruptures were taken into account in Erdik et al., 2004 model (Figure 2.2). Together with the linear

sources, small areal sources were also defined where the knowledge about the exact locations of the sources was insufficient. An earthquake catalog including the events with magnitudes between 5.0 and 6.9 were used to represent the background seismicity of the region. The earthquake recurrence was assumed to follow Gutenberg and Richter exponential model and the b-value for the region was found as 0.80 using the maximum likelihood method.

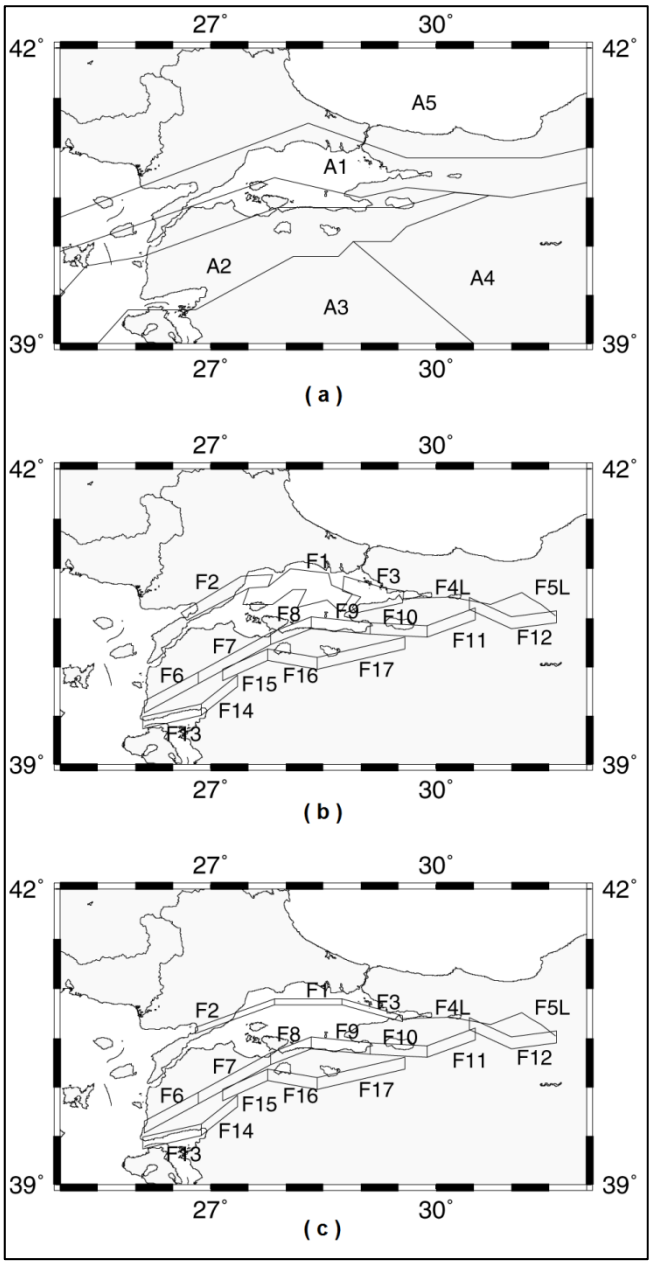

Figure 2.1 The general study area and three different sources models proposed within the study Atakan et al., 2002. (After Atakan et al., 2002)

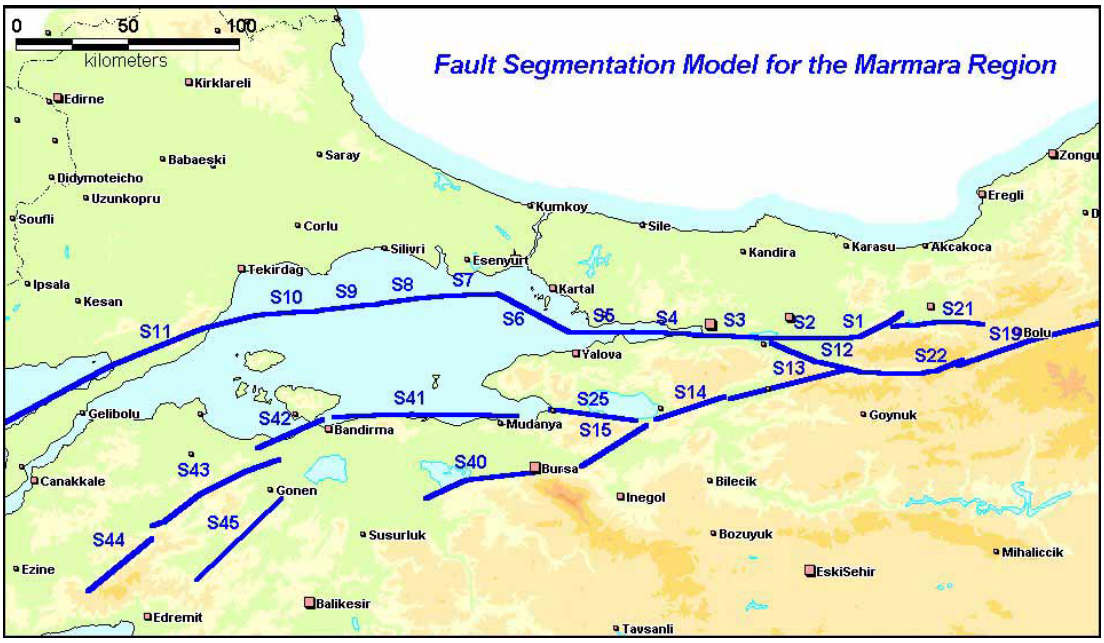

Figure 2.2 Source model proposed by the study of Erdik et al., 2004

Erdik et al., 2004 assumed that the earthquakes with magnitudes greater than 7.0 are generated by well defined linear sources, and the earthquake recurrence was controlled by characteristic model. They used the time dependent renewal model for obtaining the long term hazard levels. A comparison between Poisson's process and time dependent renewal model was also presented, showing that, the renewal model results were 1.1 to 1.3 times higher than the Poisson's process results for the regions with less seismic activity. However the renewal model results were 50% less than the Poison's process results for seismically active regions.

Parsons (2004) study was focused on finding the probability of events with magnitudes greater than 7.0 between years 2004 and 2034 in Marmara Sea region. The linear seismic source zones used in the study were the Ganos segment, Prince's Island segment and İzmit segment of the North Anatolian Fault (Figure 2.3). Additionally, a group of normal faults around Çinarcık basin representing the events with magnitudes greater than 7.0 that cannot be assigned to any of these linear sources were included in the analysis. The

b-value of the Guttenberg and Richter recurrence relation was found to be 1.4 for the region by using the maximum likelihood approach.

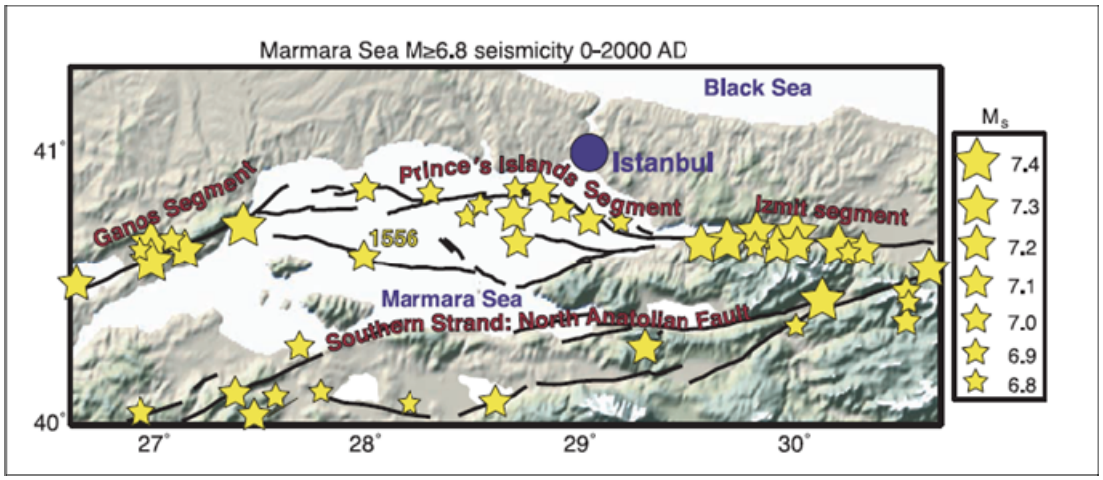

Figure 2.3 Seismic source model used in the study of Parsons (2004) (After Parsons (2004)

Crowley and Bommer (2006) examined the seismic hazard in the Marmara region with the conventional probabilistic seismic hazard assessment approach and the Monte Carlo Simulation approach. The earthquake catalog compiled in Global Seismic Hazard Assessment Program (GSHAP) that covers the earthquakes having magnitudes between 5.5 and 7.0 was used in their study. The authors utilized the Monte Carlo Simulations to develop a stochastic earthquake catalog of 500.000 years and to overcome the incompleteness in historical earthquake catalog. They used the source model proposed by Erdik et al. (2004). The events having magnitude greater than 7.0 were directly assigned to faults as suggested by Erdik et al. (2004). Since the earthquake interval of 5.5 to 7.0 was used, the authors found it unnecessary to sort out foreshocks and aftershocks, since they are rarely to happen within this range. For this range of events, the recurrence relation proposed by Gutenberg and Richter was used, and recurrence parameter b

was found to be 0.69. The events having magnitude greater than 7.0 are assumed to be characteristic which occur on the faults. The authors also developed loss exceedance curves by relating the hazard results with structural loss.

Kalkan et al., 2009, used a combination of two different seismic source models, smoothed gridded seismicity model and fault model. The events with magnitudes between 4.0 and 6.5 were used in the smoothed gridded seismicity model whereas the fault model was assumed to be responsible for the events with magnitudes greater than 6.5. For the smoothed gridded seismicity approach, the recurrence of earthquakes was modeled using the Gutenberg Richter exponential model and the recurrence parameter b was found to be 0.72 using the maximum likelihood method. For the fault model approach, both Gutenberg Richter exponential relation and Characteristic Model were used to model the recurrence of earthquakes by assigning equal weights and using a logic tree. They modeled the occurrence of earthquakes with the Poisson process (Figure 2.4).

The authors used an earthquake catalog that includes the events occurred between 1901 and 2004. The foreshocks and aftershocks were eliminated using the declustering methodology proposed by Gardner and Knopoff (1974). Also the catalog completeness intervals were checked for magnitude intervals, and for magnitude 4-5 earthquakes the catalogue was found to be complete for the last 40 years.

Another important part of seismic hazard assessment is selection of proper ground motion prediction equations.

Atakan et al., 2002 used four ground motion prediction equations (attenuation relations), namely, Boore et al. (1997), Campbell (1997), Sadigh et al. (1997) and Ambraseys *et al.* (1996).

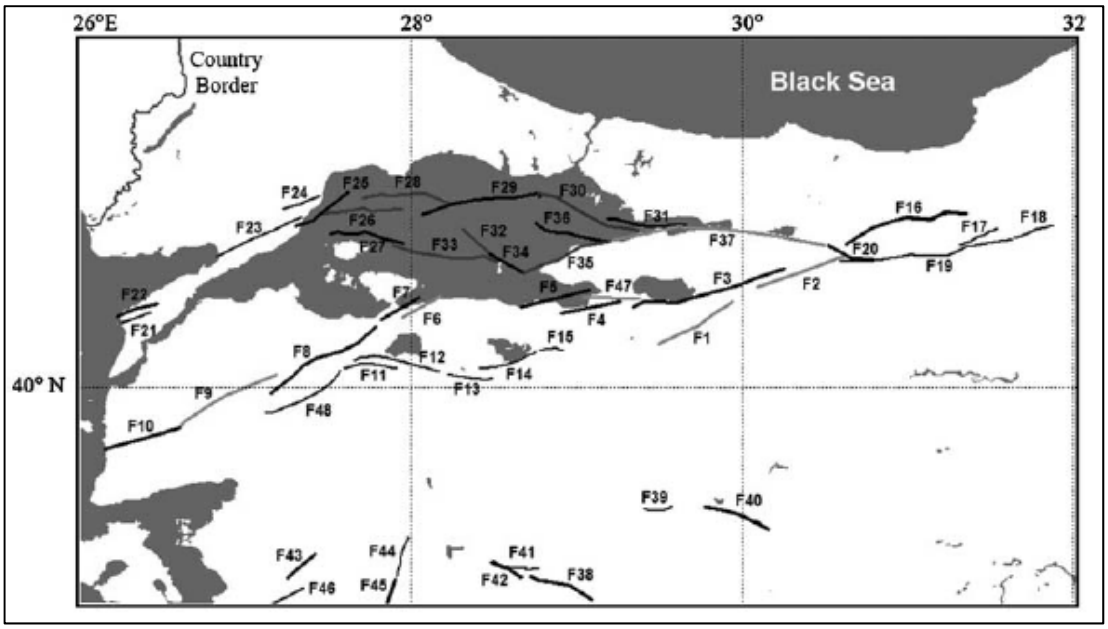

Figure 2.4 Source model used in the study of Kalkan et al., 2009 (After Kalkan et al., 2009)

Similarly in the study of **Erdik et al., 2004**, Boore et al. (1997), Campbell (1997) and Sadigh et al. (1997) ground motion prediction models were used. For estimating the peak ground acceleration (PGA), **Erdik et al., 2004** used the average of the Boore et al. (1997), Campbell (1997) and Sadigh et al. (1997) models, whereas, the average of only Boore et al. (1997) and Sadigh et al. (1997) models were used to compute the spectral accelerations at T=0.2 second and T = 1.0 second spectral periods.

Parsons (2004) used only the regional attenuation model proposed by Ambrasey (2002) and **Crowley and Bommer (2006)** used the Boore et al. (1997) model.

In 2008, new and improved ground motion prediction models by Abrahamon and Silva (2008), Boore and Atkinson (2008), Campbell and Bozorgnia (2008), Chiou and Youngs (2008), and Idriss(2008) were published. **Kalkan et al., 2009** used these new global models in addition to the ground motion

model developed for Turkey by the authors (Kalkan and Gülkan (2004)). 50% weight was assigned to the average of global NGA equations and 50% weight was assigned to Kalkan and Gülkan (2004) in the logic tree used by **Kalkan et al., 2009**. Since the NGA models use GMRotI50 (rotation independent ground motion components) and Kalkan and Gülkan (2004) uses the largest horizontal component the authors adjusted the Kalkan and Gülkan (2004) equations before calculating the ground motion models.

The results of the previous seismic hazard assessment studies were presented in terms of the hazard maps for different accepted risk levels or hazard curves for selected sites and spectral acceleration values.

Atakan et al., 2002 generated the hazard maps for peak ground acceleration (PGA) for 10% of chance of exceedance in 50 years risk level. Within the combinations of source models and GMPE's, the combination of the third source model with the Ambraseys et al. (1996) model resulted in the highest peak ground acceleration value (0.3g) for the region. (Figure 2.5)

475 years return period normalized response spectra were also generated for these different combinations and for different site conditions (hard rock and soft sediment). Again the combination of the third source model and Ambraseys *et al.* (1996) ground motion model yielded the highest values. The 0.5 second period spectral acceleration values exceeded 0.8g for the soil sites and 0.5g for the rock sites. (Figure 2.6)

Erdik et al., 2004, presented the hazard maps for PGA, T=0.2 second and T=1.0 second spectral acceleration considering 2% and 10% probability of exceedence in 50 years. The hazard map for PGA with 10% probability of exceedence in 50 years is given in Figure 2.7.

Parsons (2004) did not present any hazard map but the results of the study show that by using a time dependent model, the occurrence probability of an earthquake having magnitude greater than 7.0 between years 2004 and 2034 is 44%.

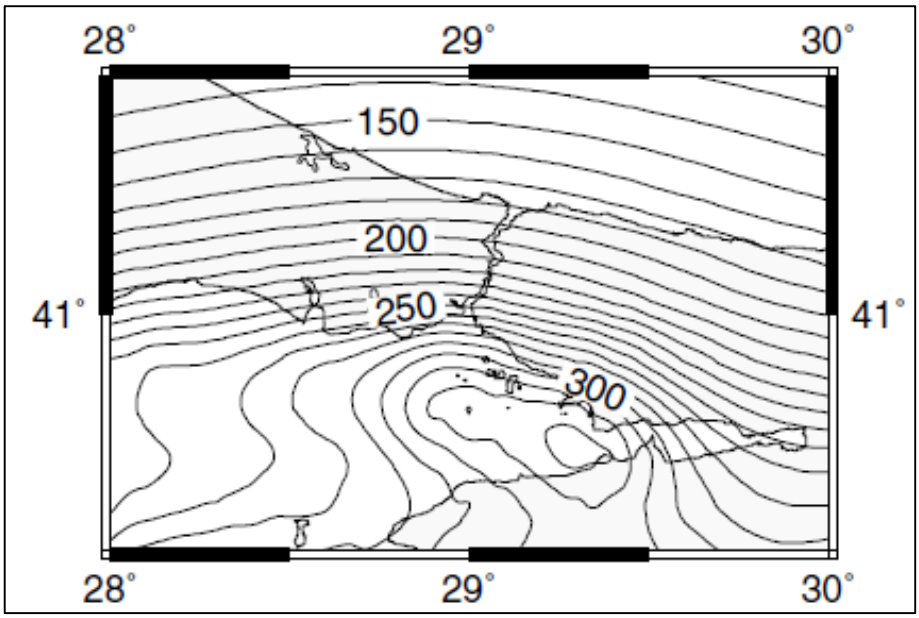

Figure 2.5 Hazard map generated from the combination of source model 3 and the attenuation model proposed by Ambraseys et al. (1996) (After Atakan et al., 2002)

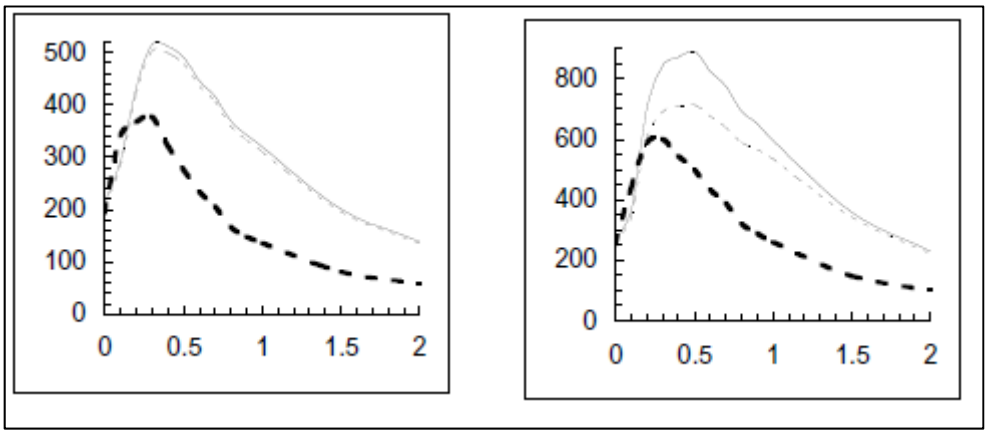

Figure 2.6 Response spectra for acceleration values obtained by using three different source models and the attenuation model proposed by Ambraseys et al. (1996) for rock site (left) and soft sediment site (right) with 5% damping. (The bold dotted lines indicate the first model; gray dotted lines indicate the second model and the gray line indicate the third model) (Modified from Atakan et al., 2002)

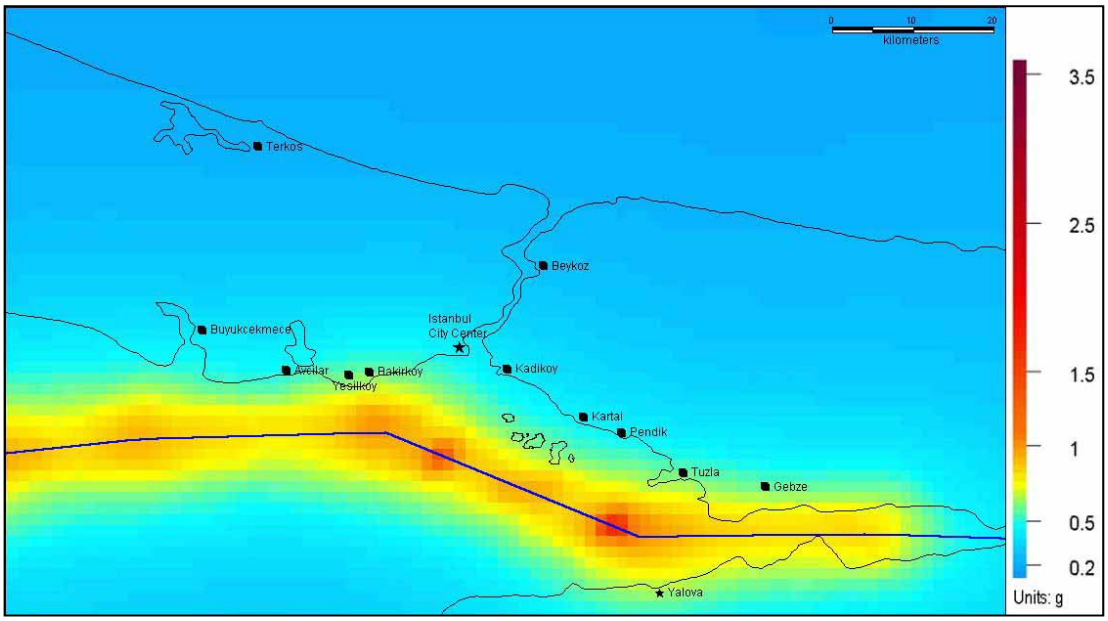

Figure 2.7 PGA contour map for NEHRP B/C boundary site class for 10% probability of exceedance in 50 years (After Erdik et al., 2004)

The results of the study performed by **Crowley and Bommer (2006)** were focused on comparing the conventional probabilistic seismic hazard assessment by the procedures described in FEMA 366 and Monte Carlo Simulation approach. Figure 2.8 presents the hazard curves for Adalar, Saray and Gölcük sites determined by PSHA and MCS methods.

Kalkan et al., 2009, the hazard maps of the region were generated for PGA , T=0.2 second and T=1.0 second spectral accelerations for firm rock (V_{s30} = 760 m/s) assuming a risk level of 2% and 10% probabilities of exceedance in 50 years. The maximum PGA was found to be around 1.6g for the region as shown in Figure 2.9. Hazard curves for different spectral periods for Istanbul were presented for rock, soil and soft-soil soil conditions (Figure 2.10). The design spectrum for Istanbul was also developed and compared to the spectrum recommended by Turkish Earthquake Code (2007) (Figure 2.11).

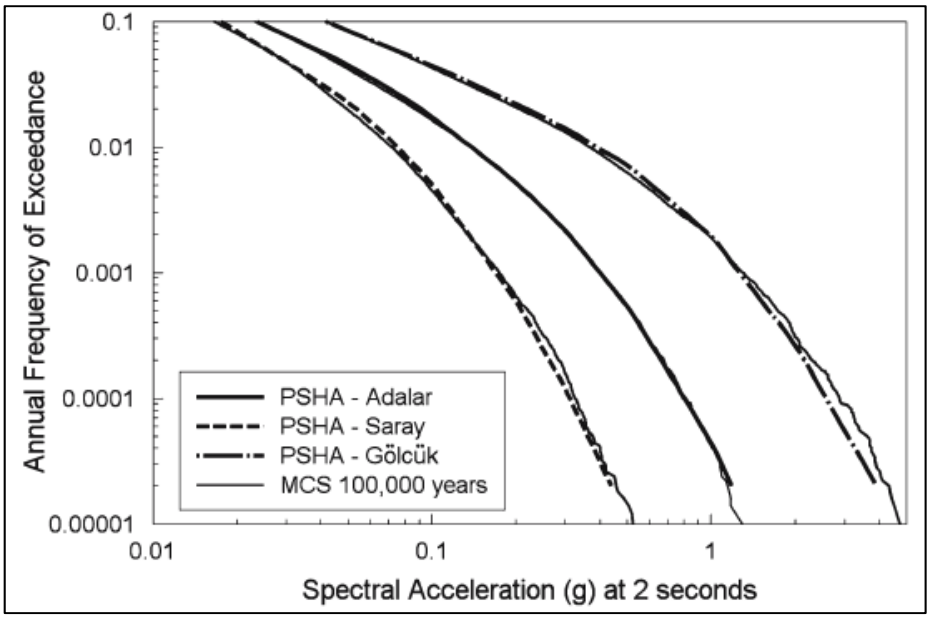

Figure 2.8 The hazard curves showing comparison between PSHA and MCS methodologies for 2secs spectral acceleration for three municipalities in İstanbul (After Crowley and Bommer, 2006)

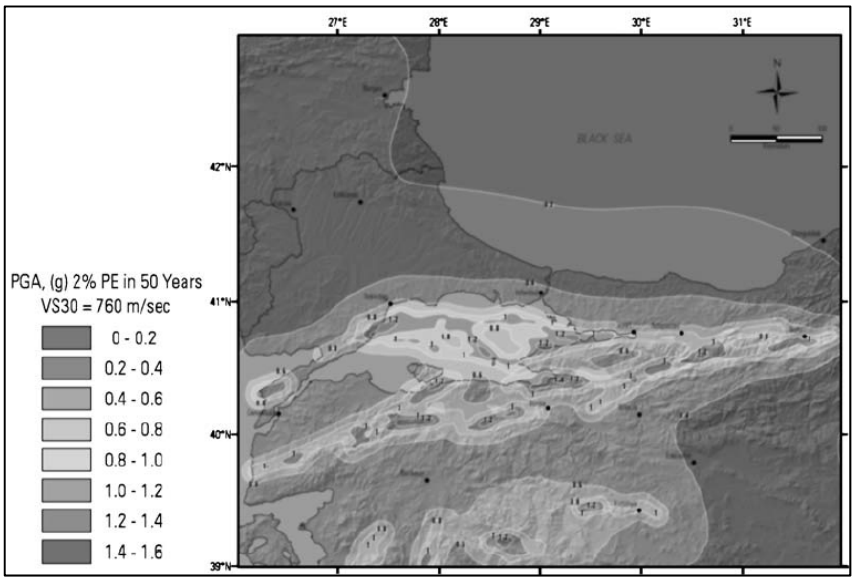

Figure 2.9 Hazard Map for PGA with a hazard level of 2% probability of exceedance in 50 years for uniform firm rock conditions. (The figure is taken from the study of Kalkan and Gülkan, 2009)

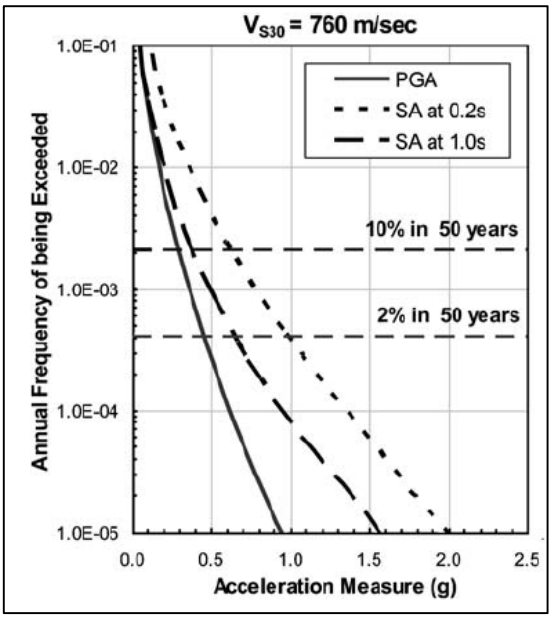

Figure 2.10 Hazard curves for the city of Istanbul at different spectral acceleration values for uniform firm rock condition. (After Kalkan and Gülkan, 2009)

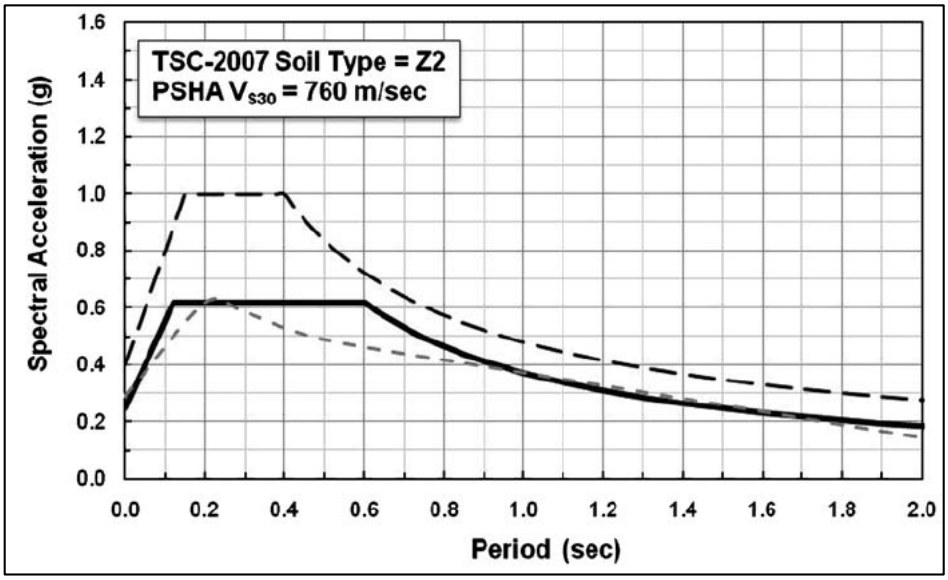

Figure 2.11 Uniform design spectra for the city of Istanbul (After Kalkan and Gülkan, 2009)

2.2 Turkish Earthquake Code (2007)

For the buildings constructed in seismic zones in Turkey, provisions given by the Turkish Earthquake Code, 2007 (TEC 2007) are used. The ground motion values are based on a risk level of 10% probability of exceedance in 50 years. For different performance levels, the accepted risk levels of 50% probability of exceedance in 50 years and 2% probability of exceedance in 50 years, multiplication factors are suggested. For the risk level of 50% probability of exceedance in 50 years 0.5 times, for the risk level of 2% probability of exceedance in 50 years, 1.5 times of the values given for the risk level of 10% probability of exceedance in 50 years are suggested.

In TEC 2007, Turkey is divided into four earthquake regions (Figure 2.12), and for each region an effective ground acceleration coefficient (Ao) is assigned (Table 2.1). These coefficients are multiplied by normalized spectrum coefficients (Figure 2.13) in order to estimate the ground motion values for different site conditions. The T_A and T_B coefficients are used in order to treat different site conditions.

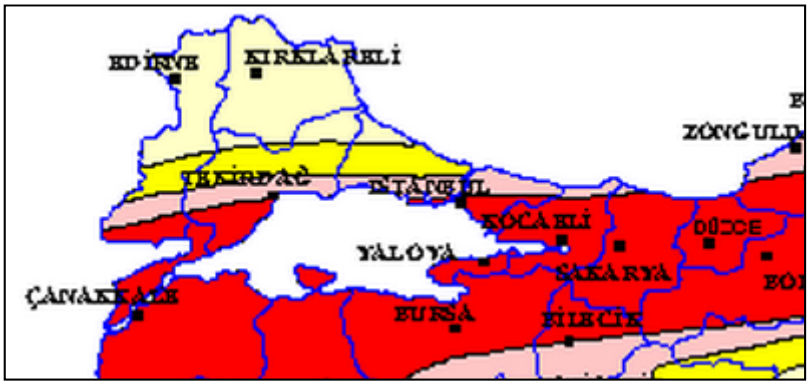

Figure 2.12 Earthquake regions proposed by TEC 2007. The red regions indicate the first, the pink regions indicate the second, the yellow regions indicate the third and the light yellow regions indicate the fourth earthquake region. (Modified from TEC 2007)

As the earthquake regions, the site conditions are divided into four groups, and for each group different T_A and T_B coefficients are assumed (Table 2.2).

Table 2.1 Seismic zones and related effective ground acceleration coefficient (Ao) values suggested by TEC 2007.

Seismic Zone	Ao
1	0.40
2	0.30
3	0.20
4	0.10

Table 2.2 T_A and T_B coefficients assigned to different soil conditions by TEC 2007

Soil Condition	T_A	T_B
Z1	0.10	0.30
Z2	0.15	0.40
Z3	0.15	0.60
Z4	0.20	0.90

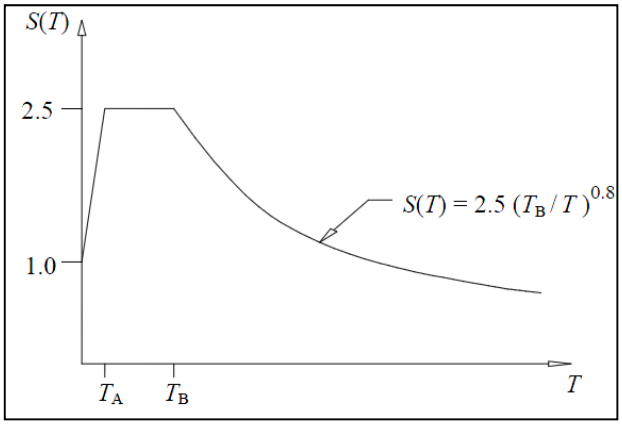

Figure 2.13 Normalized spectrum coefficients proposed by TEC 2007. (The figure is taken from TEC 2007)

CHAPTER 3

SEISMIC SOURCE CHARACTERIZATION FOR EASTERN MARMARA REGION

Characterization of the seismic sources for a probabilistic seismic hazard study includes the definition of the source geometry and modeling the earthquake recurrence relations of the source with the help of historic seismicity and available geological information about the source. Proper definition of the source geometry covers the description of the length, width, dip and strike angles of the fault plane, and identification of the segmentation point locations. This is a critical part of seismic source characterization since the estimated magnitudes of the future earthquake scenarios depend on this information. Therefore, expertise on structural geology, tectonics and seismology is required for proper and accurate modeling of the seismic source geometry. The geometry of the seismic sources in the area was modeled by a team of experts within the contents of the project **BAP-03032009**. Details of this study will be presented in **Cambazoglu (2011).** References to the group work are provided within the chapter where needed.

Other important parameters of the seismic sources such as the estimation of the activity rates and the reoccurrence relations were performed within the content of this study. In this chapter, a complete picture of seismic source characterization methodology is provided and the source parameters for each seismic zone in the study area are presented.

The use of these seismic source models in probabilistic seismic hazard assessment will be discussed in details at Chapter 5

3.1 Definition of segment, source and scenario in PSHA

In early seismic hazard assessment studies, the seismic source characterization was typically based on historical seismicity data using areal sources. In many parts of the world, particularly those without known faults, this is still the standard of practice. In regions with geological information on the faults (slip rates or recurrence intervals) are available, this information can be used to define fault sources. Fault sources were initially modeled as multi-linear line sources. Now they are more commonly modeled as multi-planar features (Abrahamson, 2000).

For this study, USGS Working Group for Earthquake Probabilities (2003) definitions for segment, source, and scenario are used. According to USGS_WG (2003):

A **segment** is defined as the shortest fault capable of rupture to produce large earthquakes repeatedly. Two criteria are used to define a segment; Kinematic and Dynamic. The Kinematic criteria include information about geometry and structure of the segments, whereas Dynamic criteria include information about previous earthquakes. The evidences for kinematic criteria are changes in strike, occurrence of restraining bends, intersection points, changes in fault complexity and major changes in lithology along the fault. These evidences alone are not enough to decide on a fault segment. The dynamic criteria should also be considered together with the kinematic criteria in order to decide on segmentation.

A **source** is defined as a fault segment or a combination of multiple adjacent fault segments that are possible to rupture and produce an earthquake in the future.

A **scenario** is defined as any possible combination of sources that describes a possible failure mode. Rupture scenario covers the decision of assigning either a single or a set of faults to be involved in rupture.

For illustration of the segment, source and scenario definitions in USGS_WG (2003), an example fault with three segments (A, B and C) is given in Figure 3.1. Six different rupture sources can be defined from these three segments such as individual fault segments (1,2 and 3 in b) (4 and 5 in Figure 3.1b) + fault groups consisting of two adjacent fault segments (2) + three segment rupture (1) (6 in Figure 3.1b). Using these rupture sources, rupture scenarios for future earthquakes can be defined as: (Rupture of the three segments individually (A,B,C) + Rupture of the first two segments together and the third segment (A+B,C) + Rupture of the last two segments together with the first segment (A, B+C) + Rupture of the three segments together (A+B+C) (Figure 3.1c)

A rupture **model** is the weighted combination of all possible scenarios produced from the seismic source. Assigning the weights to each scenario requires accurate knowledge on the historical seismic activity of the source.

3.2 Seismic Source Characterization Procedure

3.2.1 Source Geometry and Mean Characteristic Earthquake

The most important step in seismic source characterization is to define the length, width and dip angle of available active seismic sources in the region. Available tectonic maps may be digitized and used for this purpose or surface scars of the fault zones may be determined using satellite images. For the BAP-Project (03032009), satellite images of the region were gathered, de-lineament maps were prepared, the location and segmentation points for the linear sources were determined by a group of experts. Once the geometry (length, width and dip angle) of each source is determined, the characteristic magnitude of the source should be calculated using the magnitude – rupture area correlations. Among many available magnitude –

area relations, the equations proposed by Wells and Coppersmith (1994) is used in this study.

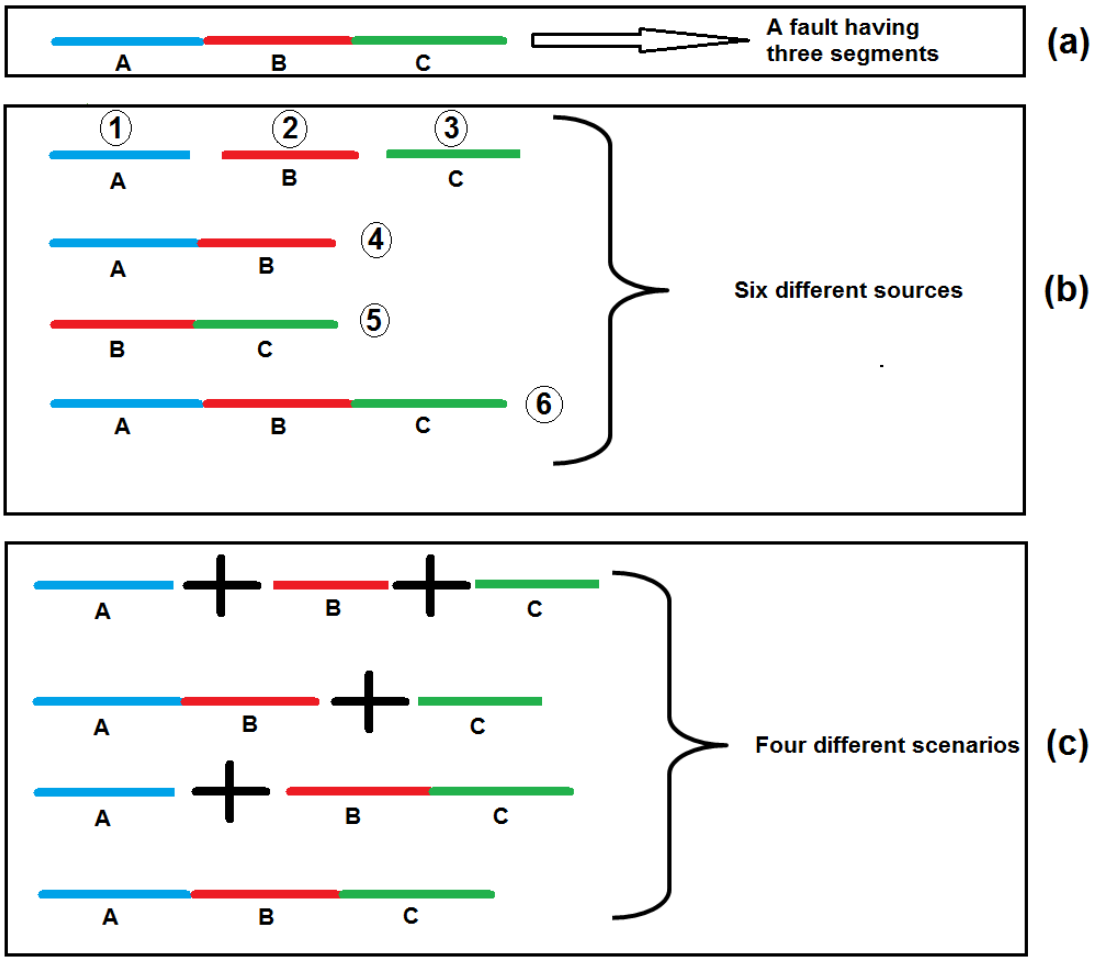

Figure 3.1 Illustration of the segment, source and scenario concepts

Since all the sources considered in this study are dominated by strike – slip motion, the Wells and Coppersmith (1994) equations for strike – slip faults are used as provided in Equations 3.1 to 3.3.

$$\text{Mchar} = 3.98 + 1.02\log(\text{RA}) \ (\pm 0.23) \qquad 3.1$$

$$\text{Mchar} = 5.16 + 1.12\log(\text{RL}) \ (\pm 0.28) \qquad 3.2$$

$$\mathrm{Mchar} = 3.80 + 2.59\log(\mathrm{RW}) \ (\pm 0.45) \qquad 3.3$$

Where Mchar represents the mean value of the characteristic magnitude, RA is the rupture area (in km²), RL is the rupture length (in km) and RW is the rupture width (in km).

3.2.2 Magnitude Distributions

A seismic source will generate a range of earthquake magnitudes. The magnitude distribution describes the relative number of large, moderate and small magnitude earthquakes that may occur on the seismic source. Typical magnitude distributions used in PSHA are;

1. Truncated Exponential Model
2. Truncated Normal Model (Characteristic Model)
3. Composite Model (Youngs & Coppersmith, 1985)

The basic magnitude recurrence relation proposed by Gutenberg – Richter (G-R) (1944) is;

$$\mathrm{Log\ N(M)} = \mathrm{a} - \mathrm{bM} \qquad 3.4$$

Where N (M) is the cumulative number of earthquakes greater than M, a and b are the constants that represent the rate and relative frequency of earthquakes. Since there is a maximum magnitude for the source and a minimum magnitude for engineering interest, the G – R (1944) distribution is typically truncated at both ends. The truncated exponential model is bounded at the minimum and maximum magnitude values and the distribution function is normalized to set the total probability value to unity as given in Equation 3.5.

$$fm(Mw) = \frac{\beta \exp\left(-\beta\ (\mathrm{Mw} - \mathrm{Mmin})\right)}{1 - \exp\left(-\beta\ (\ \mathrm{Mmax} - \mathrm{Mmin})\right)} \qquad 3.5$$

Where β is ln(10) times the b value. The exponential distribution is suitable for large regions or regions with multiple faults but in most cases does not work well for fault zones (Youngs and Coppersmith, 1985).

Schwartz and Coppersmith (1984) proposed the characteristic magnitude distribution model in which the faults tend to generate only characteristic (or maximum) size events depending on the fault geometry. In other words, seismic energy is released only by characteristic earthquakes in this model. The general form of the fully characteristic model is represented by truncated normal distribution. (Truncation is done according to the standard deviation in magnitude – rupture area relation.) (Figure 3.2)

Composite models combine the Truncated Exponential Model and the Characteristic Model where smaller size earthquakes are represented with the Truncated Exponential Model and larger size earthquakes are represented with Characteristic Model. For this study, the composite model proposed by Youngs and Coppersmith (1985) is used (Figure 3.2). The key feature of this model is; 94% of the seismic moment is released by the characteristic earthquakes, and the rest of the total seismic moment is released by the smaller size earthquakes due to the constraints of the distribution equation. (Equations 3.6 and 3.7) The changes in the b-value have an insignificant effect on the recurrence relation but the function is more sensitive to the changes in upper bound magnitude (Youngs and Coppersmith, 1985).

$$fm(Mw) = \begin{cases} \dfrac{\beta \exp\left(-\beta\ (\mathrm{Mw} - \mathrm{Mmin})\right)}{1 - \exp\left(-\beta\ (\ \mathrm{Mmax} - \Delta \mathrm{M}_2 - \ \mathrm{Mmin})\right)} \mathrm{x}\ \dfrac{1}{1 + \mathrm{c}}, & Mw \leq Mmax - 0.5\Delta M2 \\ \dfrac{\beta \exp\left(-\beta\ (\mathrm{Mmax} - \Delta \mathrm{M}_1 - \ \Delta \mathrm{M}_2 - \mathrm{Mmin}\ )\right)}{1 - \exp\left(-\beta\ (\ \mathrm{Mmax} - \Delta \mathrm{M}_2 - \ \mathrm{Mmin})\right)} \mathrm{x}\ \dfrac{1}{1 + \mathrm{c}}, & Mw > Mmax - 0.5\Delta M2 \end{cases} \qquad 3.6$$

In these equations;

$$c = \frac{\beta \exp\left(-\beta\ (\mathrm{Mmax} - \Delta M_1 - \ \Delta M_2 - \mathrm{Mmin}\ )\right)}{1 - \exp\left(-\beta\ (\ \mathrm{Mmax} - \Delta M_2 - \ \mathrm{Mmin})\right)} \mathrm{x}\ \Delta M_2 \qquad 3.7$$

$$\Delta M_1 = \ 1.0$$
$$\Delta M_2 = \ 0.5$$

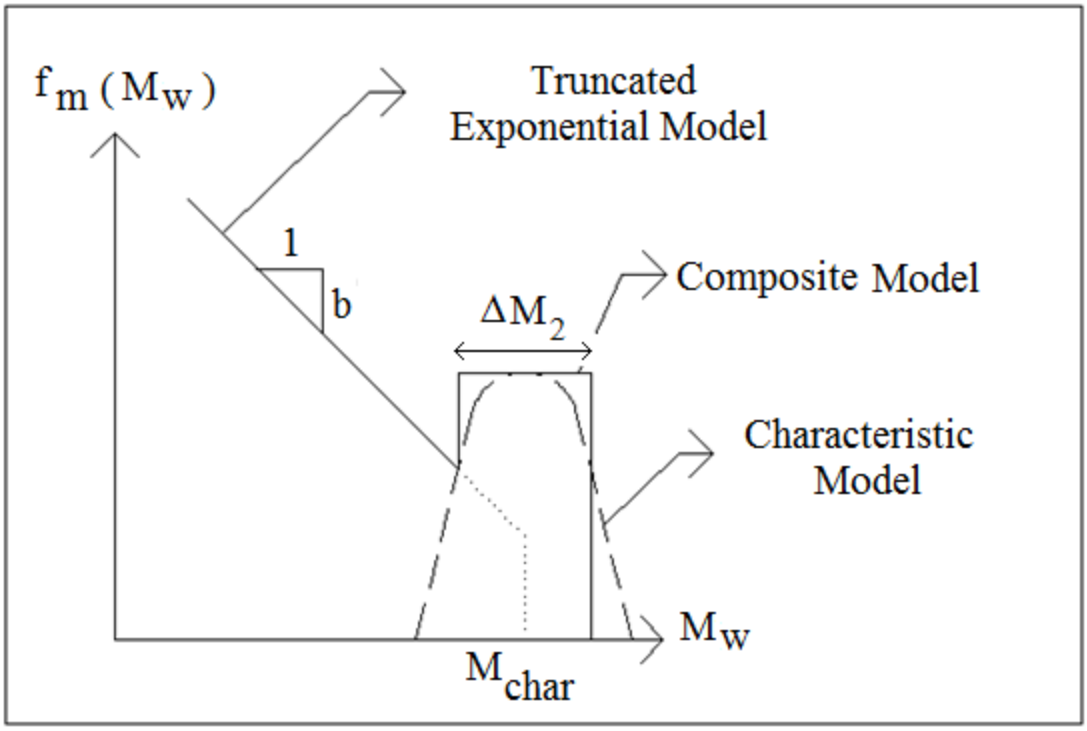

Figure 3.2 Magnitude distribution functions used in PSHA, truncated exponential, truncated normal (characteristic) and composite models (Y&C (1985)

3.2.3 Activity Rates and Reoccurrence Relations

To determine the magnitude reoccurrence relation of a seismic source, activity rate of the source should be estimated in addition to the magnitude distribution model. The activity rate of a source is defined as the rate of earthquakes above the minimum magnitude and denoted by N(Mmin). The activity rate can be estimated by either using the historical seismicity or the geological information about the fault. (Abrahamson, 2000)

Historical seismicity catalogues are used to calculate the activity rate for areal sources. The N(Mmin) is estimated by fitting the Truncated Exponential Model to the historical data. If geological (or geodetic) information will be used for estimating N(Mmin), the accumulation of the seismic moment should be balanced by the release of seismic moment in earthquakes. The total accumulated seismic moment (Mo) on a source is given by;

$$\mathrm{Mo} = \mu \,.\, \mathrm{A} \,.\, \mathrm{D} \qquad 3.8$$

Where, μ is the rigidity of the crust (~3 x 10^{11} dyne / cm²), A is the fault area (km²) and D is the average displacement.

By taking the time derivative the annual accumulating seismic moment is found as;

$$\frac{\partial \mathrm{Mo}}{\partial \mathrm{t}} = \mu \,.\, \mathrm{A} \,.\, \mathrm{s} \qquad 3.9$$

Where, s is the slip rate (cm/year). Seismic moment release during an earthquake is given by Equation 3.10.

$$\mathrm{Mr} = 10^{1.5\,\mathrm{M}+16.05} \qquad 3.10$$

Therefore the activity rate N(Mmin) is calculated by integrating the moment release per earthquake times the relative frequency of earthquakes as given in Equation 3.11

$$\mathrm{N(Mmin)} = \frac{\mu \,.\, \mathrm{A} \,.\, s}{\int_{\mathrm{Mmin}}^{\mathrm{Mmax}} fm(Mw)\ 10^{1.5\ \mathrm{Mw}+16.05}\ \mathrm{dm}} \qquad 3.11$$

The activity rate N(Mmin) is combined with the magnitude distribution function to develop the recurrence model N (M) for the source:

$$\mathrm{N(M)} = \mathrm{N(Mmin)} \int_{\mathrm{Mmin}}^{\mathrm{Mmax}} fm(Mw) \qquad 3.12$$

3.3 Seismic Source Characterization of Eastern Marmara

The boundary between the Eurasia and Anatolian plates, the North Anatolian Fault Zone (NAF), extends along the Northern Turkey for more than 1500 km and it is one of the most active fault systems in the world. During the last century, almost all of the NAF system was ruptured by large earthquakes (1939 Erzincan, 1942 Erbaa-Niksar, 1943 Tosya, 1944 Bolu-Gerede, 1957 Abant, 1967 Mudurnu, 1999 Kocaeli and 1999 Düzce) providing the most valuable information on the segments that tend to produce large earthquakes. The study area covers a large region bounded by Marmara Sea on the west and Bolu city limits on the east. The study area and the segments of NAF system in the region are shown in Figure 3.3. According to Figure 3.3, the four primary fault segments in the area are;

1. North Anatolian Fault Northern Strand (NAF_N)
2. North Anatolian Fault Southern Strand (NAF_S)
3. Düzce Fault
4. Geyve & Iznik Fault

Figure 3.3 Study area and the main seismic sources taken from active fault map of MTA (Saroglu et al., 1992)

The seismic source characterization for each fault zone will be explained by following the procedure provided in the previous section.

3.3.1 Source Geometry and Mean Characteristic Magnitude for the Seismic Sources in the Region

The location, geometry and slip distribution of North Anatolian Fault Northern Strand and Düzce fault has been studied extensively after the 1999 Kocaeli and Düzce Earthquakes (Barka et al. 2002, Stein et al. 1997, Langridge et al., 2002, Harris, 2002). The surface rupture of the 1999 Kocaeli Earthquake extended for almost 165 km and 4 distinct segments as shown in Figure 3.4. (Hersek Segment, Gölcük-Karamürsel-İzmit Segment, Sapanca-Akyazı segment and Karadere Segment) were ruptured (Barka et al., 2002).

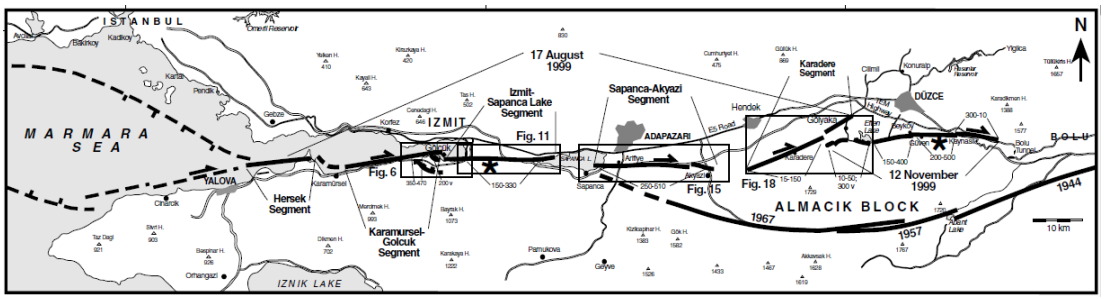

Figure 3.4 The layout of NAFN, NAFS and Duzce Faults (After Barka et al., 2002)

A segment of NAFN located on the boundary between the Marmara Sea and Çınarcık Block (shown by broken lines in Figure 3.4) was not ruptured during 1999 Kocaeli Earthquake. Cambazoğlu (2011) used the satellite images of the region to accurately define the location of the fault plane, segmentation points and lengths of the fault segments. Using the fault segmentation defined by Barka (2002) and Cambazoğlu (2011), NAF_N fault zone in the study region is divided into 6 segments (see Table 3.1 and Figure 3.5). The width of the fault zone is back calculated by the area – magnitude relations proposed by Wells and Coppersmith (1994) as 18 km. This value is reasonable since depth of 1999 Kocaeli Earthquake is around 17 km (Barka et al., 2002). The location and geometry of the Hendek segment is provided in details by Cambazoğlu (2011).

Table 3.1 Fault segmentation of NAF_N

SEGMENTS		**RL(km)**	**RW(km)**	**SR(mm/yr)**	**Mchar**
W1	Çınarcık segment	46.4	18	19	7.0
W2	Hersek segment	12.4	18	19	6.4
C	Gölcük-Karamürsel-İzmit	47.0	18	19	7.0
E1	Sapanca – Akyazı	21.6	18	10	6.6
E2	Karadere	26.6	18	10	6.7
H	Hendek segment	45.2	18	10	7.0

The six segments determined forms a rupture model which is composed of 19 seismic sources and 24 rupture scenarios according to the USGS_WG (2003) definitions. The seismic sources and rupture scenarios generated for NAF_N is presented in Table 3.2. While generating the scenarios, the eastern segments (E1 and E2) and Hendek (H) segment are assumed to behave dependently. Since they are parallel segments of the same source, simultaneous rupture of these faults is not taken into account.

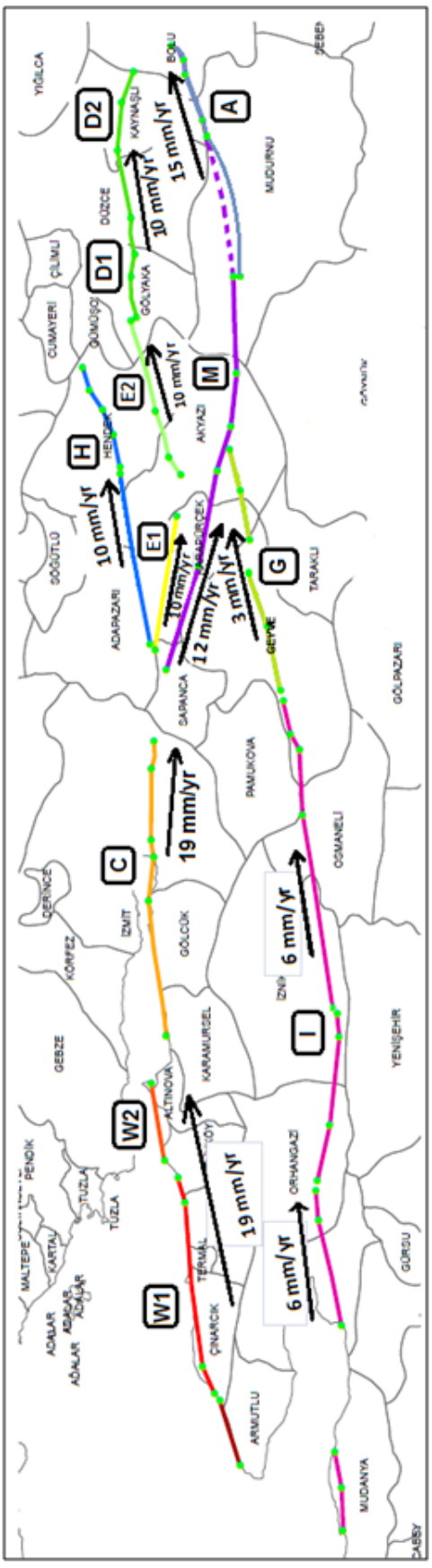

Figure 3.5 The general layout of the sources and the slip rate assigned to each source used in this model. (This figure is modified from the study of Cambazoglu (2011))

NAF - N	W1	W2	C	E1	E2	W1+W2	W2+C	C+E1	E1+E2	W1+W2+C	W2+C+E1	C+E1+E2	W1+W2+C+E1	W2+C+E1+E2	W1+W2+C+E1+E2	H	C+H	W2+C+H	W1+W2+C+H	
W1,W2,C,E1,E2	1	1	1	1	1	0	0	0	0	0	0	0	0	0	0	0	0	0	0	1
W1+W2,C,E1,E2	0	0	1	1	1	1	0	0	0	0	0	0	0	0	0	0	0	0	0	2
W1,W2+C,E1,E2	1	0	0	1	1	0	1	0	0	0	0	0	0	0	0	0	0	0	0	3
W1,W2,C+E1,E2	1	1	0	0	1	0	0	1	0	0	0	0	0	0	0	0	0	0	0	4
W1,W2,C,E1+E2	1	1	1	0	0	0	0	0	1	0	0	0	0	0	0	0	0	0	0	5
W1+W2+C,E1,E2	0	0	0	1	1	0	0	0	0	1	0	0	0	0	0	0	0	0	0	6
W1,W2+C+E1,E2	1	0	0	0	1	0	0	0	0	0	1	0	0	0	0	0	0	0	0	7
W1,W2,C+E1+E2	1	1	0	0	0	0	0	0	0	0	0	1	0	0	0	0	0	0	0	8
W1+W2+C+E1,E2	0	0	0	0	1	0	0	0	0	0	0	0	1	0	0	0	0	0	0	9
W1,W2+C+E1+E2	1	0	0	0	0	0	0	0	0	0	0	0	0	1	0	0	0	0	0	10
W1+W2,C+E1,E2	0	0	0	0	1	1	0	1	0	0	0	0	0	0	0	0	0	0	0	11
W1,W2+C,E1+E2	1	0	0	0	0	0	1	0	1	0	0	0	0	0	0	0	0	0	0	12
W1+W2+C,E1+E2	0	0	0	0	0	0	0	0	1	1	0	0	0	0	0	0	0	0	0	13
W1+W2,C+E1+E2	0	0	0	0	0	1	0	0	0	0	0	1	0	0	0	0	0	0	0	14
W1+W2,C,E1+E2	0	0	1	0	0	1	0	0	1	0	0	0	0	0	0	0	0	0	0	15
W1+W2+C+E1+E2	0	0	0	0	0	0	0	0	0	0	0	0	0	0	1	0	0	0	0	16
W1,W2,C,H	1	1	1	0	0	0	0	0	0	0	0	0	0	0	0	1	0	0	0	17
W1+W2,C,H	0	0	1	0	0	1	0	0	0	0	0	0	0	0	0	1	0	0	0	18
W1+W2,C+H	0	0	0	0	0	1	0	0	0	0	0	0	0	0	0	0	1	0	0	19
W1+W2+C,H	0	0	0	0	0	0	0	0	0	1	0	0	0	0	0	1	0	0	0	20
W1+W2+C+H	0	0	0	0	0	0	0	0	0	0	0	0	0	0	0	0	0	0	1	21
W1,W2+C+H	1	0	0	0	0	0	0	0	0	0	0	0	0	0	0	0	0	1	0	22
W1,W2,C+H	1	1	0	0	0	0	0	0	0	0	0	0	0	0	0	0	1	0	0	23
W1,W2+C,H	1	0	0	0	0	0	1	0	0	0	0	0	0	0	0	1	0	0	0	24
	1	2	3	4	5	6	7	8	9	10	11	12	13	14	15	16	17	18	19	

Table 3.2 Seismic Sources and Rupture Scenarios considered for NAF_N (Rows indicate rupture scenarios and columns show the seismic sources)

Details of fault segmentation of Düzce Fault and North Anatolian Fault Southern Strand (NAF_S) are provided by Cambazoğlu (2011). Two segments are defined for both fault zones. For Düzce Fault, the segmentation point is determined using the available information in the literature and satellite images. For NAF_S, the rupture zones of the two previous earthquakes (1957 Abant and 1967 Mudurnu Earthquakes) are considered as two separate segments. 80 km long Mudurnu segment starts from Sapanca Lake and extends up to Mudurnu. Abant segment, starts from Abant Lake and extents 40 km to Arpaseki (Barka, 1996). The rupture zones of these two earthquakes have an overlapping 20 kilometers (Ambraseys, 1970). The width of both sources are back calculated using Wells and Coppersmith (1994) relations and checked by the depths of previous earthquakes occurred on the fault. Geometry of the Düzce Fault and NAF_S along with the characteristic magnitudes are given in Table 3.3 and Table 3.4, respectively. The seismic sources and rupture scenarios for Duzce Fault and NAF_S considered in this study are provided in Table 3.5 and Table 3.6. (RL, RW and SR stand for rupture length, rupture width and slip rate, respectively.)

Geyve – İznik Fault Zones' activity is less compared to the other seismic sources in the region. Lack of large earthquakes on the fault zone in this century makes it harder to determine the exact location of segmentation points.

Table 3.3 Geometry of Düzce Fault

SEGMENTS	RL(km)	RW(km)	SR(mm/yr)	Mchar
D1	10.7	35.8	10	6.6
D2	29.4	35.8	10	7.1

Table 3.4 Geometry of NAF_S

SEGMENTS		RL(km)	RW(km)	SR(mm/yr)	Mchar
M	Mudurnu segment	64	12	12	6.9
A	Abant segment	40	12	15	6.7

The source geometry proposed by Cambazoglu (2011) was simplified as given in Table 3.7. The seismic sources and rupture scenarios for Geyve-İznik fault zone is given in Table 3.8.

Table 3.5 Sources and Scenarios generated for Duzce Fault

DUZCE	D1	D2	D1+D2
D1 , D2	1	1	0
D1 + D2	0	0	1

Table 3.6 Sources and Scenarios generated for NAF_S

NAFS	M	A	M+A
M,A	1	1	0
M+A	0	0	1

Table 3.7 Geometry of Geyve and Iznik Fault

SEGMENTS		RL(km)	RW(km)	SR(mm/yr)	Mchar
I	Iznik segment	111.6	12	6	7.2
G	Geyve segment	34.5	12	3	6.7

Table 3.8 Sources and Scenarios generated for Geyve & Iznik Fault

Geyve & Iznik	I	G	I+G
I , G	1	1	0
I+G	0	0	1

3.3.2 Magnitude Distribution Models for the Sources in the Region

Youngs and Coppersmith (1985) composite model is used to represent the relative rates of different size magnitude events for North Anatolian Fault Northern Strand, North Anatolian Fault Southern Strand, and Duzce Fault. As indicated, composite models works better for large fault segments which tends to rupture creating characteristic size earthquakes. For Geyve-Iznik fault, the composite model is modified to represent the weak seismicity of the source. Since the events attributed to Geyve-Iznik fault are smaller in size and magnitude, the moment released by the exponential tail of the composite model is increased by modifying the model parameter ΔM1.

The magnitude distribution function for each source is bounded with a minimum magnitude considering the engineering interest. Except for the Geyve – Iznik fault, the minimum magnitude is set to magnitude 5 for all sources. For Geyve – Iznik fault the minimum magnitude is lowered to magnitude 4 considering the historical seismicity of the source. The upper bound for the magnitude distribution functions is calculated by adding 0.25 to the characteristic magnitude for each source (Youngs and Coppersmith, 1985).

To estimate the b-value for the magnitude distribution functions, the results of the study by Cambazoglu (2011) was used. Cambazoglu (2011) used the Integrated Homogeneous Turkey Earthquake Catalog provided by Kandilli Observatory and Earthquake Research Center (Boğaziçi University) after filtrating the foreshocks and aftershocks to represent the seismicity of the

region. The remaining database after filtration is composed of 167 events with moment magnitudes between 4.0 and 7.5 (Table 3.9)

Table 3.9 Distribution of magnitudes of the earthquakes within the catalog in the region (After Cambazoglu, 2011)

MAGNITUDE BIN	**# OF EARTHQUAKES**
4 - 4.5	75
4.5 - 5.0	52
5.0 - 5.5	19
5.5 - 6.0	10
6.0 - 6.5	7
6.5 - 7.0	2
≥ 7.0	2
TOTAL	167

Having a catalogue with complete earthquake data is essential for accurate calculation of b-value. The cumulative rates of earthquakes bigger than different magnitude levels are plotted vs. years to examine the completeness of the catalogue (Figure 3.6). The breaking points for the linear trends in the rates are examined. For smaller magnitude events, two breaking points are observed, 1967 (increase in the digital accelerometers) and 1999 (densification of the seismic networks after the earthquakes). The 1999 break is weaker than the other and diminishes for magnitudes greater than 4.5, therefore the catalogue is assumed to be complete for 38 years for earthquakes with magnitudes between 4 and 5. For greater magnitudes, the catalogue is assumed to be complete for 100 years. The results presented in Table 3.10 show the time intervals in which the earthquake database is assumed to be complete.

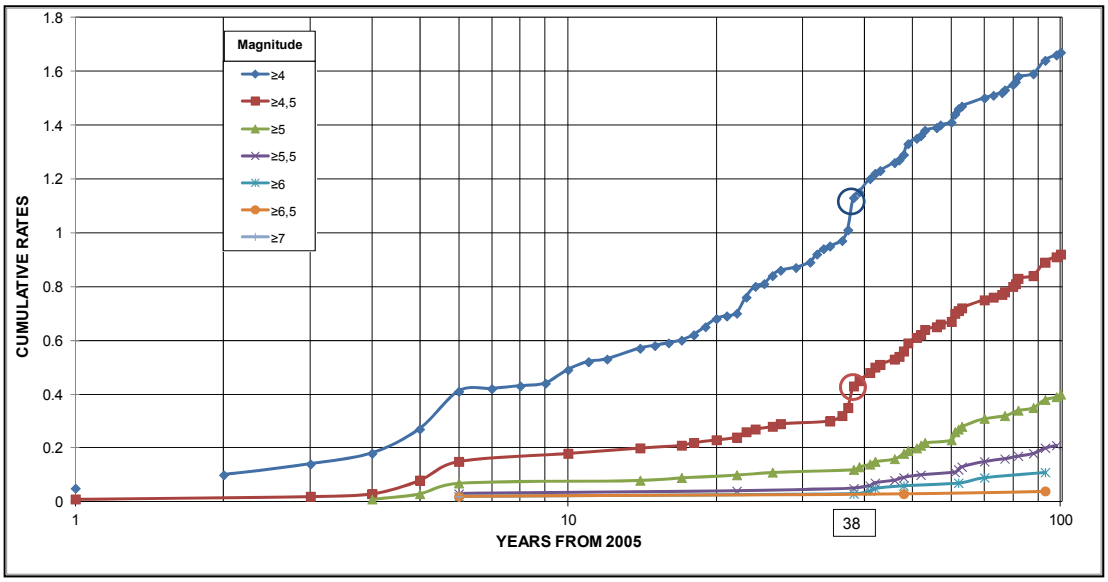

Figure 3.6 Catalogue completeness check (The circles imply the break points of the linear trend)

Table 3.10 Complete database intervals for different magnitude bins

MAGNITUDE BIN	COMPLETE CATALOG LENGTH (YEARS)
4 - 4.5	38
4.5 - 5.0	38
5.0 - 5.5	100
5.5 - 6.0	100
6.0 - 6.5	100
6.5 - 7.0	100
≥ 7.0	100

The basic maximum likelihood method to estimate the b-value is proposed by Aki (1965) as given in Equation 3.19:

$$\frac{1}{\beta} = \bar{M} - M_o \qquad 3.19$$

Where $\bar{M}$ is the average magnitude and M_o is the lowest magnitude at which the catalog is complete. In this study, the modified maximum likelihood method which takes into account the variable completeness at the catalog for the different magnitude bins is used (Weichert, 1980). The average magnitude ($\bar{M}$) is found by considering the rates for the magnitude bins:

$$\bar{M} = \frac{\Sigma M_i R_i}{\Sigma R_i} \qquad 3.20$$

$$R_i = \frac{N_i}{T_i} \qquad 3.21$$

Where M_i is the average magnitude of each magnitude bin (eg. 4-4.5, 4.5–5.0 …), R_i is the rate for each interval, N_i is the number of events within each magnitude bin and T_i is the time interval for each magnitude bin which the catalogue is assumed to be complete. The results of the maximum likelihood method analysis are summarized in a tabular form in Table 3.11 and Figure 3.7. By this study the β parameter is found to be 1.74 which makes the value of the recurrence parameter b as 0.75. The b-value used by the previous studies in the literature are in good agreement with the value estimated in this study, the b-value used by Erdik et al., 2004, Kalkan et al., 2009, and Crowley and Bommer (2006) were 0.80, 0.72, and 0.69, respectively.

Table 3.11 Maximum likelihood estimation of the recurrence parameter b

M1	**M2**	**M_i**	**N_i**	**Time Interval (years)**	**R_i**	**$M_i * R_i$**
4.0	4.5	4.25	70	38	1.8	7.8
4.5	5.0	4.75	31	38	0.8	3.9
5.0	5.5	5.25	19	100	0.2	1.0
5.5	6.0	5.75	10	100	0.1	0.6
6	6.5	6.25	7	100	0.1	0.4
6.5	7.0	6.75	2	100	0.0	0.1
7.0	7.5	7.25	2	100	0.0	0.1
				SUM =	3.1	14.0
				$\bar{M} =$	4.6	

3.3.3 Activity Rates and Recurrence Relations for the Seismic Sources in the Region

For estimating the activity rates the annual slip (slip rate) of each source should be defined. Past studies based on GPS measurements and field research performed for the region (McClusky et al., 2000, Reilinger et al., 2000) showed that the total slip rate of North Anatolian Fault is around 25 mm/year. However, the seismic moment accumulated due to this annual slip on the fault is shared by the parallel fault segments.

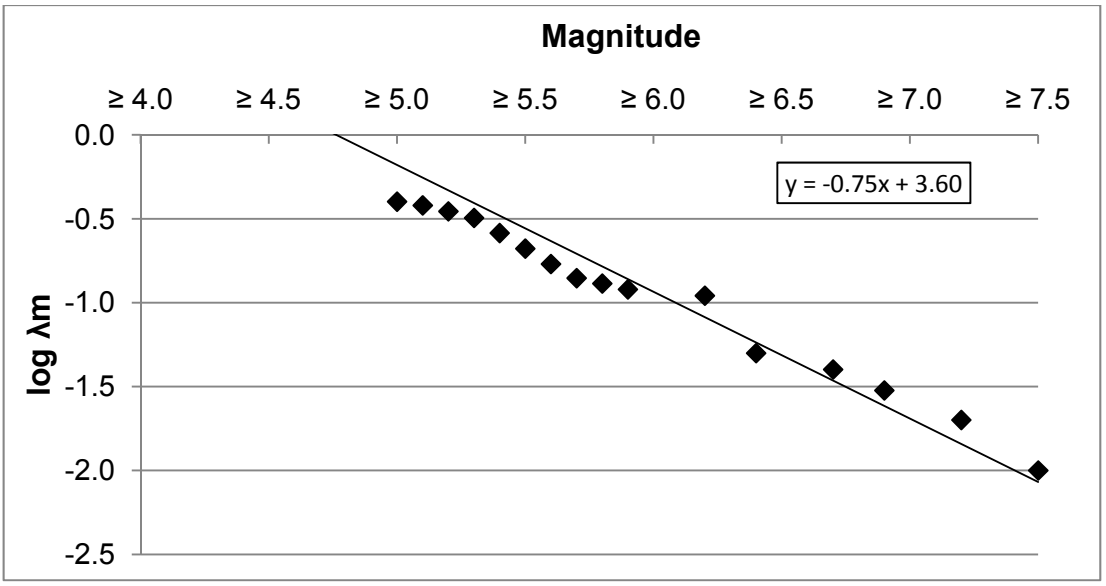

Figure 3.7 Maximum likelihood model

For the segments that forms the west and center parts of NAF_N (Çınarcık, Hersek and Gölcük-Karamürsel-İzmit segments), the total slip rate of 25 mm/year is shared with Geyve & Iznik Fault. The slip rate of 19 mm/year is assigned to these segments of NAF_N and slip rate of 6 mm/year is assigned to Iznik fault. The total slip rate of 25 mm/year is shared by the eastern segment of NAF_S (Abant) and Duzce fault. Since contribution of Duzce Fault to the total slip is around 33% to 50% (Ayhan et al., 2001), a slip rate of 15 mm/year is assigned to NAF_S Abant Segment and 10 mm/year is assigned to Duzce Fault. Same slip rate of (10 mm/year) is assigned to the segments of NAF_N that are connected to the Duzce fault (Sapanca-Akyazı, Karadere and Hendek segments) for consistency. The slip rate of 3 km/year is assigned to the Geyve segment of the Geyve-Iznik Fault since this segment meets with the Mudurnu segment (12 mm/year) and joins to the Abant fault (15 mm/year) to form the Southern Strand (see Figure 3.5).

The slip rates and the weights assigned to different rupture scenarios are validated with the historical seismicity of the sources. The epicenter-source matching for the study area is performed by Cambazoglu, 2011. The

cumulative rates of earthquakes for each source are calculated considering the catalogue completeness intervals and plotted in Figures 3.8 to 3.11 for NAF_N, NAF_S, Duzce and Geyve-Iznik faults, respectively. The uncertainty in the rates is represented by the error bars calculated by Weichert (1980) equations. The rupture scenarios presented in Tables 3.4, 3.5, 3.6 and 3.8 are plotted on the same graphs (gray lines in Figures 3.8 to 3.11) along with the weighted average of these scenarios (bold broken lines in Figures 3.8 to 3.11). The best fit between the cumulative rates of historic earthquakes and weighted average lines are established by modifying the weights of individual scenarios. Please note that, only 2 scenarios are generated for NAF_S, Duzce and Geyve-Iznik faults therefore, the weights of these scenarios were easier to establish. 24 scenarios are generated for NAF_N and the weights of individual scenarios cannot be determined by these constraints. We grouped the scenarios by the number of segments included and assigned the same weight to the scenarios in one group. The highest weights are assigned to the scenarios modeling the rupture of individual segments and full rupture of the fault, represented by the upper and lower distributions in Figure 3.8.

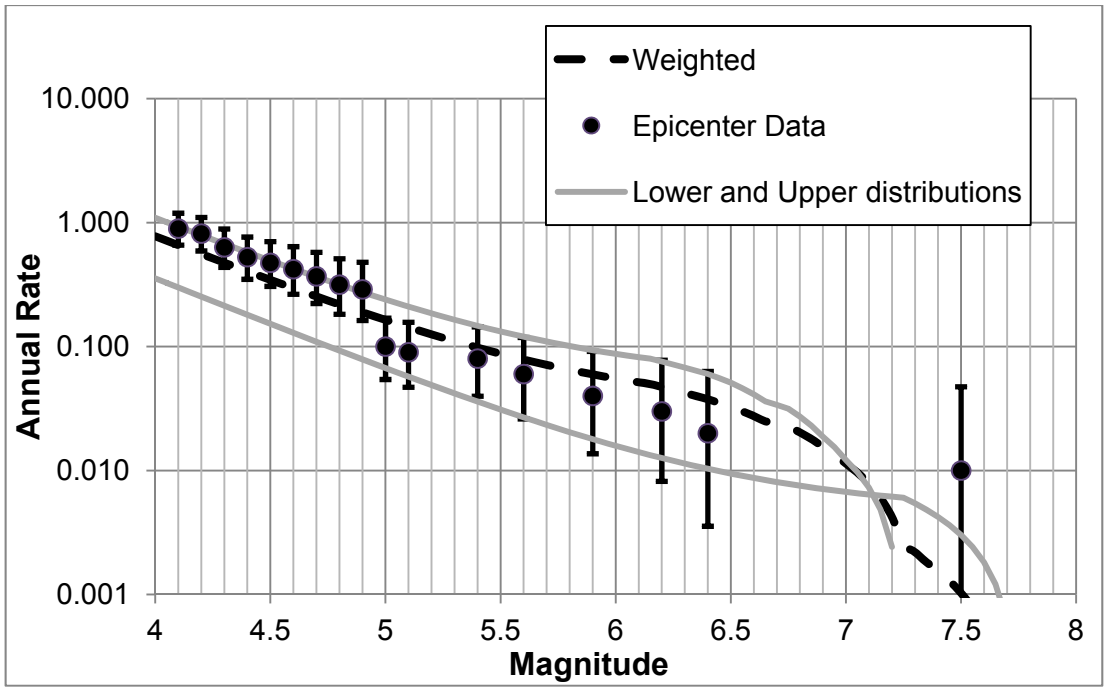

Figure 3.8 Comparison of recurrence relation and epicenter data for NAF_N

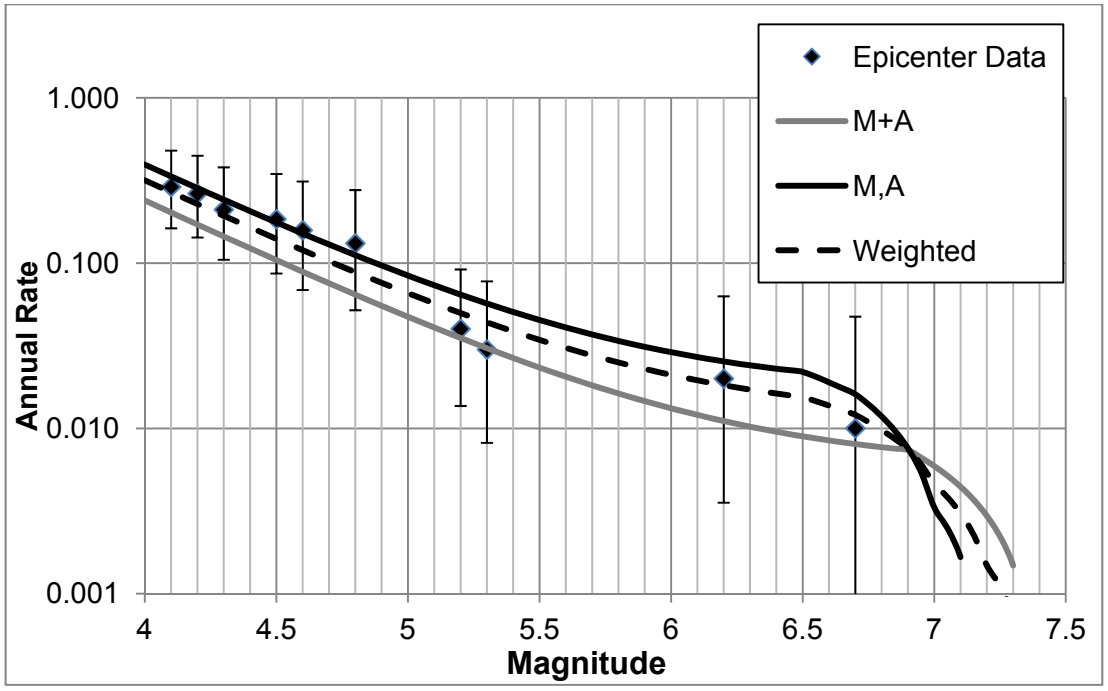

Figure 3.9 Comparison of recurrence relation and epicenter data for NAF_S

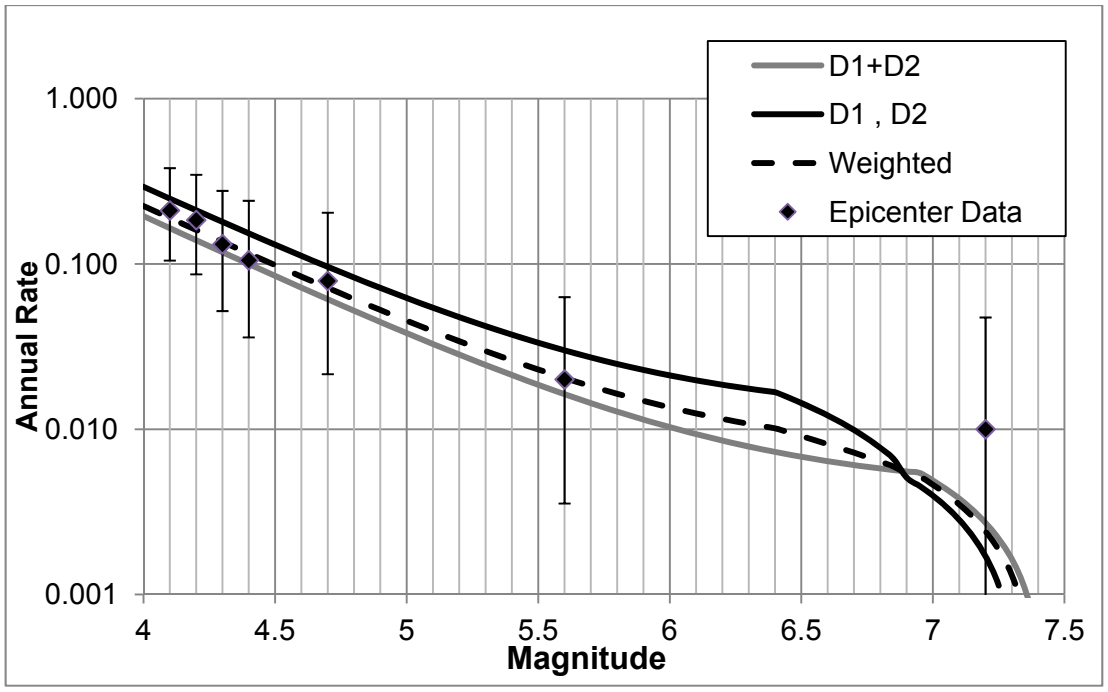

Figure 3.7 Comparison of recurrence relation and epicenter data for Duzce Fault

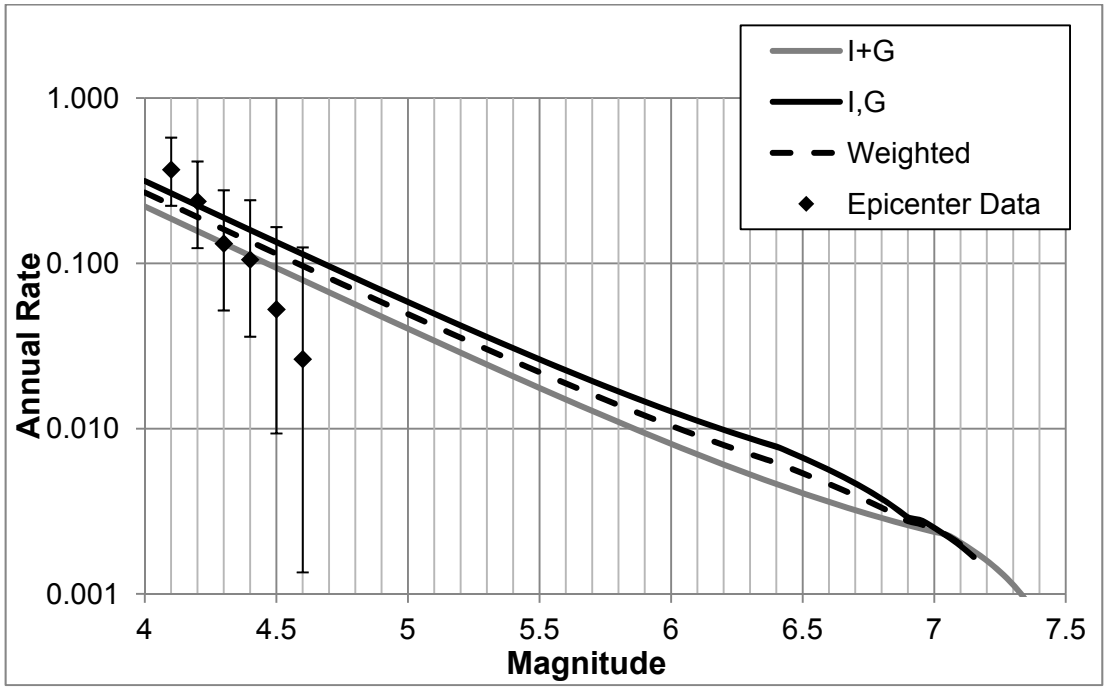

Figure 3.8 Comparison of recurrence relation and epicenter data for Geyve & Iznik Fault

CHAPTER 4

SELECTION OF GROUND MOTION PREDICTION MODELS

In probabilistic seismic hazard assessment, the ground motion prediction equations (GMPEs) are used to estimate the strong ground motion due to the earthquake scenarios from each source. These equations use physical-based statistical models to predict the ground motion intensities in terms of source (magnitude, depth, style-of faulting, etc.), path (distance, etc.) and site (site conditions, basin effects, etc.) parameters. Ground motion prediction models introduce the largest uncertainty in the hazard calculations therefore they have a significant effect on the total hazard at the site.

Many GMPEs are available in the literature, global ground motion models representing the shallow crustal regions and local ground motion models developed for Turkey (Özbey et al., 2003, Kalkan and Gulkan, 2004, Akkar and Cagnan, 2010). Choosing the ground motion model from one of these groups is a controversial topic since both has its own advantages and disadvantages. The local ground motion prediction equations are developed from the regional databases therefore they reflect the regional differences better then the global models. However, since they are based on a limited small database, the uncertainties in these models are higher than the global models. Despite the local models, the global models are based on large databases which decrease the epistemic uncertainty in the models.

Since the total hazard is significantly affected by the epistemic uncertainty in the ground motion models, global ground motion models are used in this study. The Next Generation Attenuation (NGA) models published in 2008 are selected among many available global models. This chapter presents the results of a preliminary and complementary study to examine the applicability of the NGA models to the region by simply comparing the strong ground motions of the events occurred in the region to the NGA model predictions. Within the contents of this chapter, general information on the parameters and limitations of the NGA models is provided. Results of the preliminary study comparing the spectral acceleration values from actual ground motions and ground motion model predictions are presented. Detailed discussion on the effect of NGA models to the total hazard for the region is provided in Chapter 6. To cope with the uncertainty in ground motion predictions, ±3σ value proposed by each model is included in the analysis.

4.1 Next Generation Attenuation Models

For predicting the ground motion for shallow crustal earthquakes in western USA and the regions with similar tectonic activity, a comprehensive study was performed between 2004 and 2008, and Next Generation Ground Motion Attenuation (NGA) Relations were published in 2008 (Table 4.1). The models were developed based on the updated PEER (Pacific Earthquake Engineering Research Center) strong ground motion database. The PEER database includes 3551 recordings from 173 earthquakes occurred between 1952 and 2003. Each developing team listed on Table 4.1 used a subset of this database based on the selection criteria given by Chiou et al., 2008. The number of earthquakes and recordings obtained from the events occurred in Turkey included to the datasets of each NGA model is summarized in Table 4.2.

The NGA models predict 5% damped spectral accelerations for the spectral periods of 0 seconds to 10 seconds. The models can be used for strike – slip, reverse and normal faulting styles. The applicable magnitude ranges of the

model are 5.0-8.5 for strike – slip earthquakes and 5.0-8.0 for reverse and normal earthquakes. The models are applicable for distances up to 200 kilometers away from the fault. The site effects were modeled using continuous functions and Vs30 was selected as the site response parameter. For the model proposed by Idriss (2008), the applicability is restricted by Vs30 > 450 m/s. Effects of some physical properties of rupture on the ground motion were included into models. In all of the models, moderate to large magnitude scaling, distance scaling at both close and far distances, style of faulting and site amplification effects were included. For most of the models, footwall and hanging wall effects, depth to faulting and basin amplification/depth to bedrock are also considered. (Power et al., 2008) The functional forms of the models are available in Earthquake Spectra Special Issue (Volume 24, No. 1, 2008).

Table 4.1 Global Ground Motion Prediction Equations

GLOBAL GROUND MOTION MODELS	
1.	Abrahamson & Silva NGA Model (2008)
2.	Boore & Atkinson NGA Model (2008)
3.	Campbell & Bozorgnia NGA Model (2008)
4.	Chiou & Youngs NGA Model (2008)
5.	Idriss NGA Model (2008)

Table 4.2 The number of earthquakes and recordings obtained from the events occurred in Turkey included to the databases of each NGA model

MODEL	**# of recordings**	**# of earthquakes**
A & S (2008)	35	6
B & A (2008)	52	3
C & B (2008)	40	5
C & Y (2008)	35	7
I (2008)	14	3

4.2 Available Strong Ground motion Recording in the Region and Preliminary Comparison

For testing the applicability of the NGA models in the hazard assessment studies performed in the region, a complementary study assessing the differences between the spectral acceleration values obtained from the available ground motion recordings from the region and the prediction models is performed.

The ground motion recordings were compiled from the DAPHNE database created by collaboration of Middle East Technical University Earthquake Engineering Research Center and General Directorate of Disaster Affairs. This database consists of 4607 strong ground motion recordings from the earthquakes occurred between the years 1976 and 2007 in Turkey. 357 strong ground motions that were recorded by the stations in the area during the events occurred in the region were selected and included in the dataset.

The rotation-independent geometric mean response spectrum for each recording is calculated using the methodology proposed by Boore et al., 2006 since the NGA models used this definition to calculate the response spectra of the recording in the PEER database. For some the filtered records in the dataset, different high-cut and low-cut filters were used for the two horizontal component of the same recording. Different filters created a discrepancy in the time domain and the start times of the strong ground motion for horizontal components were shifted (Akkar, personal communication, November 2011) as shown in Figure 4.1(a). This shift introduces significant uncertainty in the rotation-independent geometric mean calculations therefore; the records having these shifts were modified before taking the resultant (Figure 4.1(b)). An example response spectrum for the two individual horizontal components and the resultants obtained by using the geometric mean and GMRotI50 is provided in Figure 4.2.

4.3 Preliminary Comparison of the NGA (2008) Models with the Strong Ground Motions of the Region

The magnitude scaling, distance scaling and site effects scaling of the NGA (2008) models implied by the dataset of recordings from the study region is evaluated using the residuals as given in Equation 4.1:

$$RESIDUAL = \ln(actual) - \ln(predicted) \quad (4.1)$$

where the actual represents the peak ground acceleration or spectral acceleration of the actual recording and predicted represents the NGA model predictions. Since the ground motion prediction models are log-normally distributed, the natural logarithms of the actual ground motions are considered. The distribution of the residuals with respect to magnitude, distance and Vs30 for PGA, spectral accelerations at the spectral periods of T=0.3 second and T = 1.0 second are presented; from Figure 4.3 to Figure 4.5 for Abrahamson and Silva (2008) Model, from Figure 4.6 to Figure 4.8 for Boore and Atkinson (2008) Model, from Figure 4.9 to Figure 4.11 for Campbell & Bozorgnia Model (2008), from Figure 4.12 to Figure 4.14 for Chiou & Youngs Model (2008) and from Figure 4.15 to Figure 4.17 for Idriss (2008) Model.

The distribution of residuals is unbiased within the magnitude range at which the NGA models are considered to be available since no trend is observed along the zero line. However, the predictions are consistently higher than the actual values. Similarly, the distributions of residuals with respect to Vs30 are balanced along the zero line, again with small overestimate of the actual data by NGA models. Both of these problems may be solved easily by modifying the constant in each model using the Turkish Ground Motion Database. However, a trend is observed in the distribution of residuals with respect to distance (especially in short distances) in each model indicating the differences in regional attenuation characteristics. The variables in the distance scaling of each model should be modified to fix the trend; however,

it is out of the scope of this study. A comprehensive study on the database including all the ground motions recorded in Turkey is performed by Kargıoglu (2012) to check the applicability of NGA models to the seismic hazard assessment studies performed in Turkey.

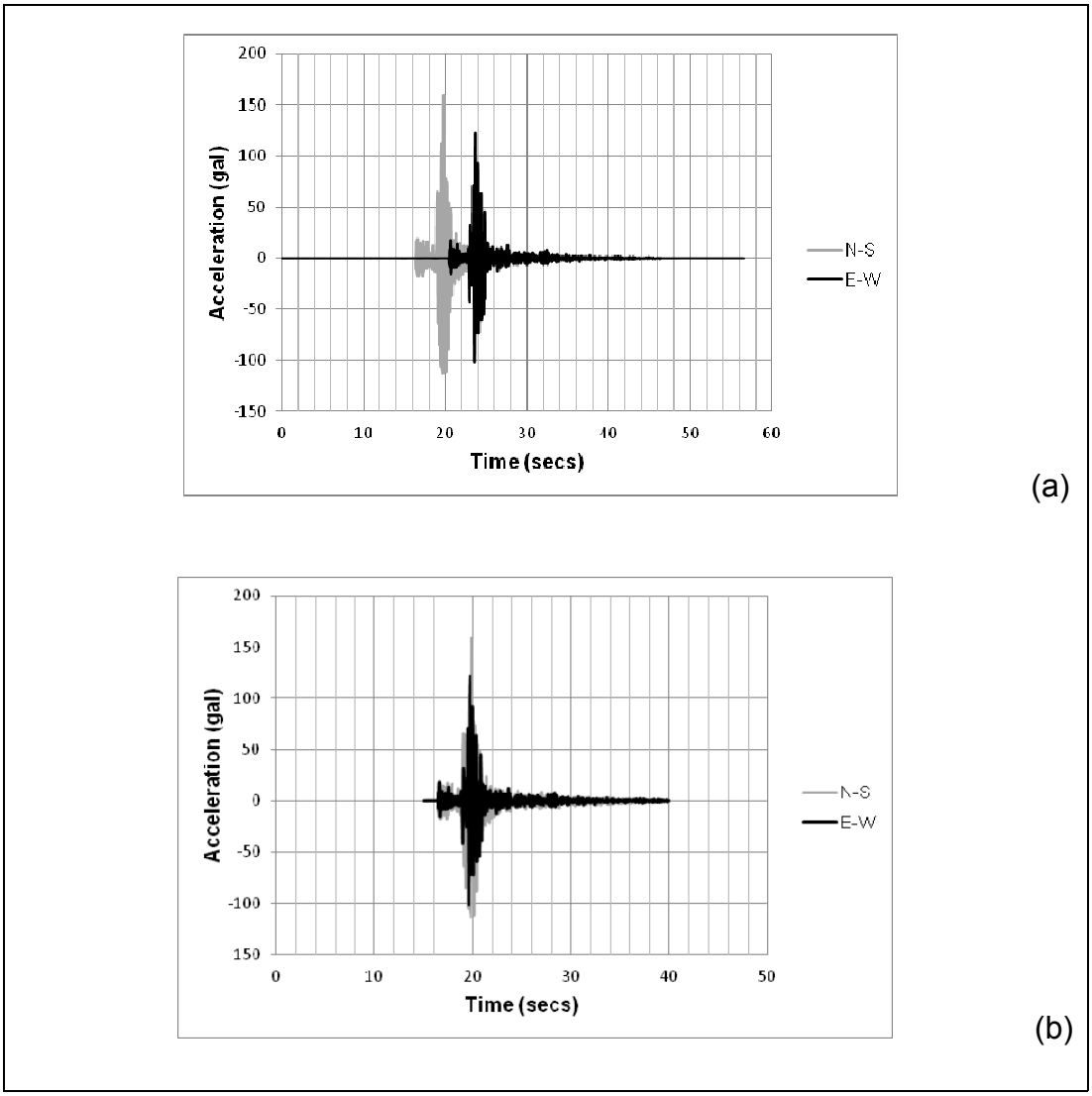

Figure 4.1 The original (a) and processed (b) accelerogram obtained from the recording 19991112171644_9904

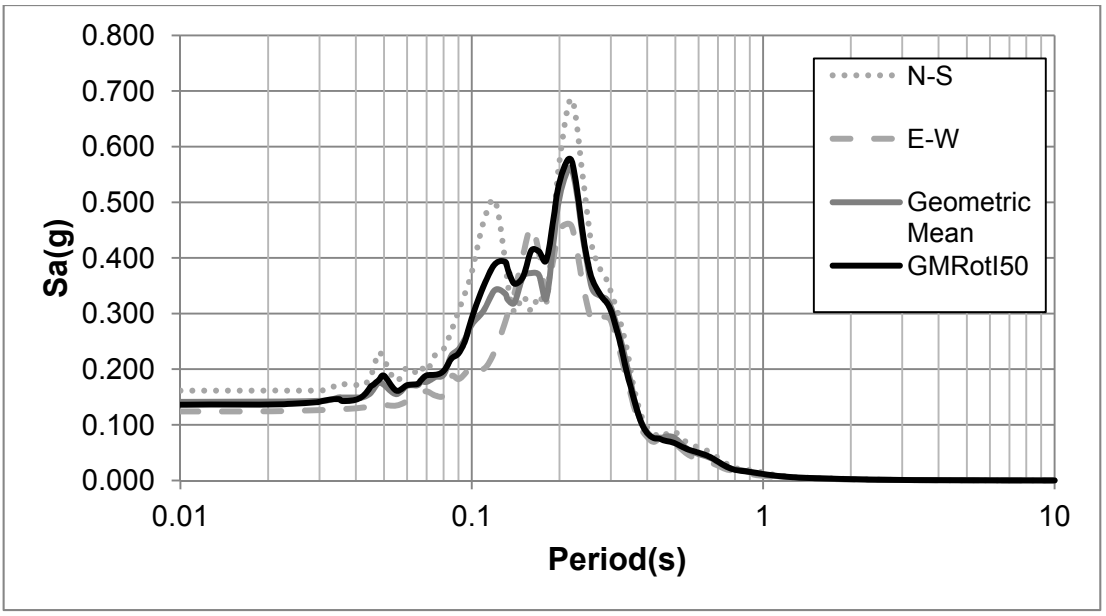

Figure 4.2 The response spectrum for the two horizontal components, geometric mean and GMRotI50 resultants obtained from the recording 19991112171644_9904

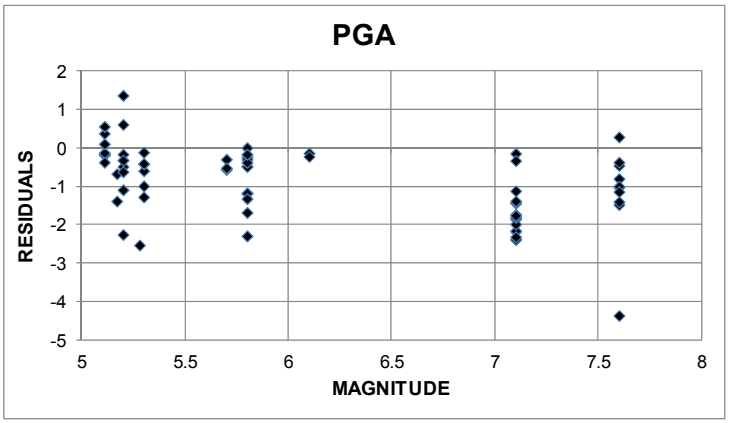

(a)

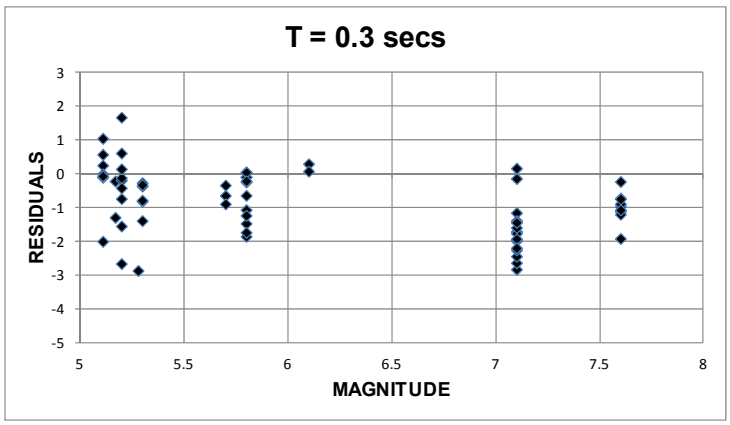

(b)

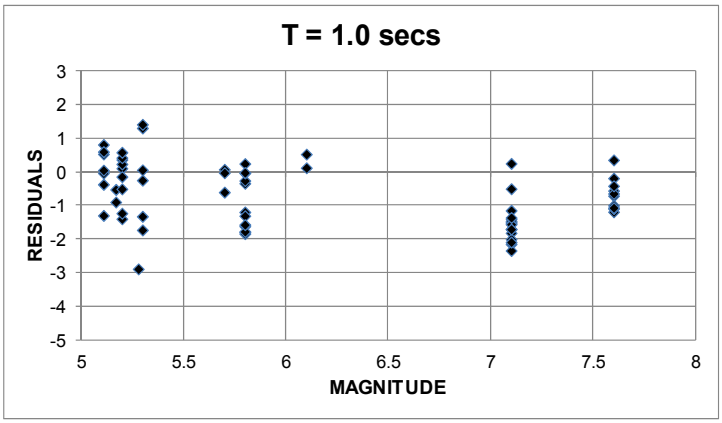

(c)

Figure 4.3 Residuals vs Magnitude at a)PGA, b) T =0.3 secs and c) T = 1.0 secs for A & S (2008)

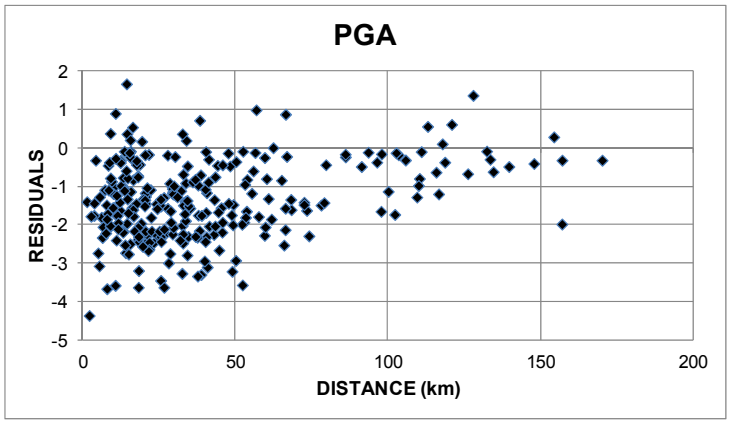

(a)

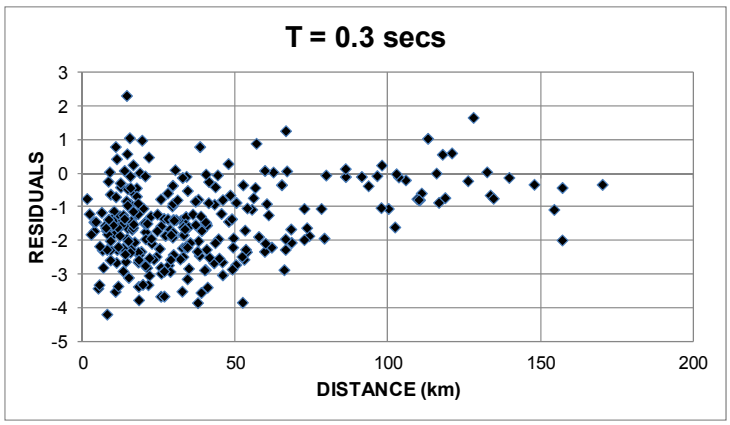

(b)

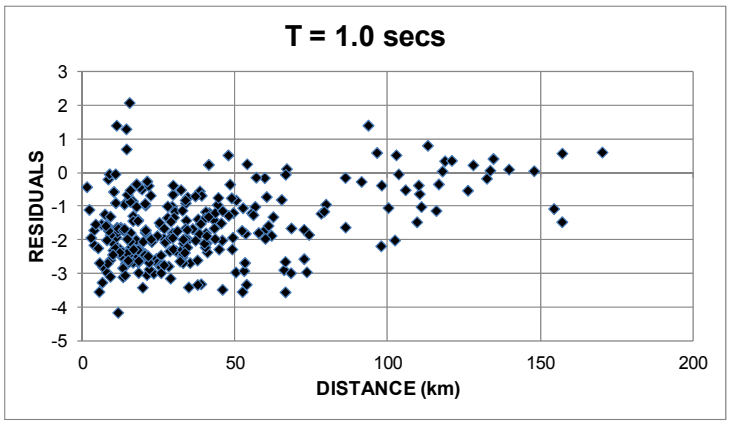

(c)

Figure 4.4 Residuals vs Distance at a)PGA, b) T =0.3 secs and c) T = 1.0 secs for A & S (2008)

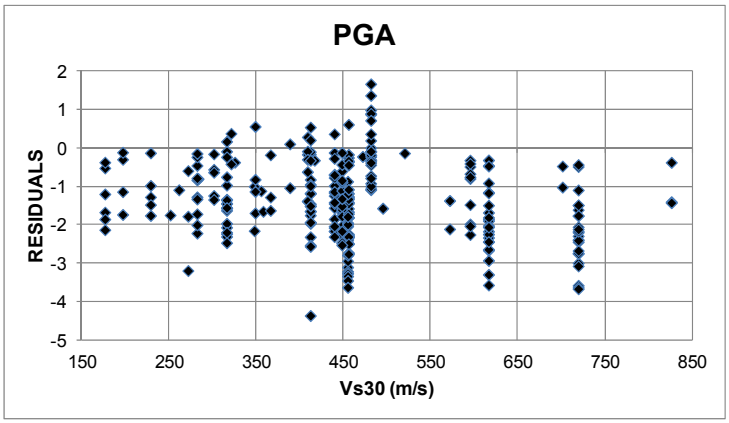

(a)

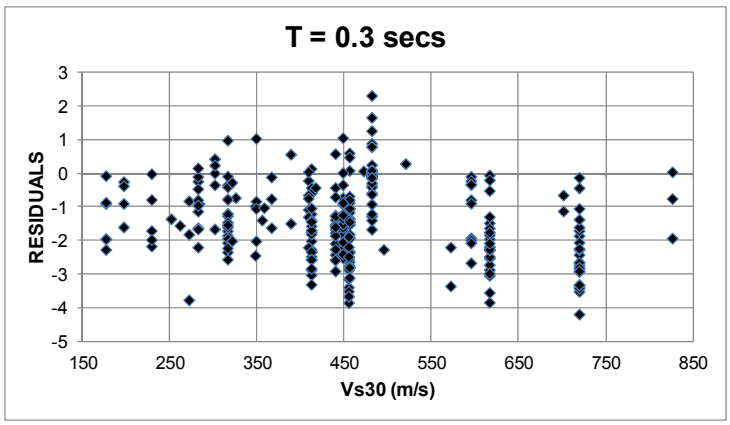

(b)

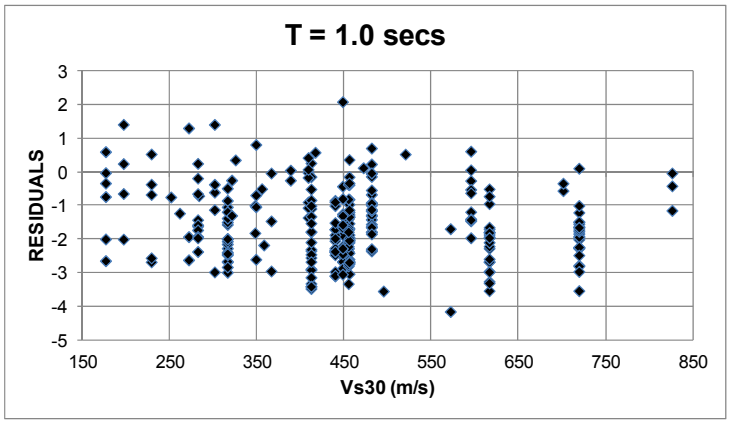

(c)

Figure 4.5 Residuals vs Vs30 at a)PGA, b) T =0.3 secs and c) T = 1.0 secs for A & S (2008)

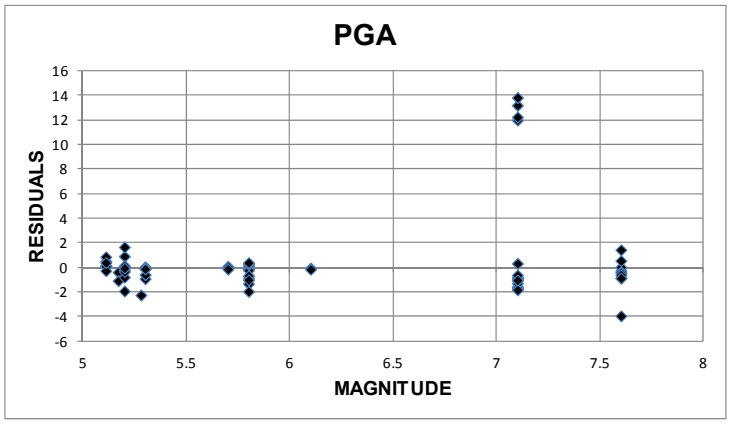

(a)

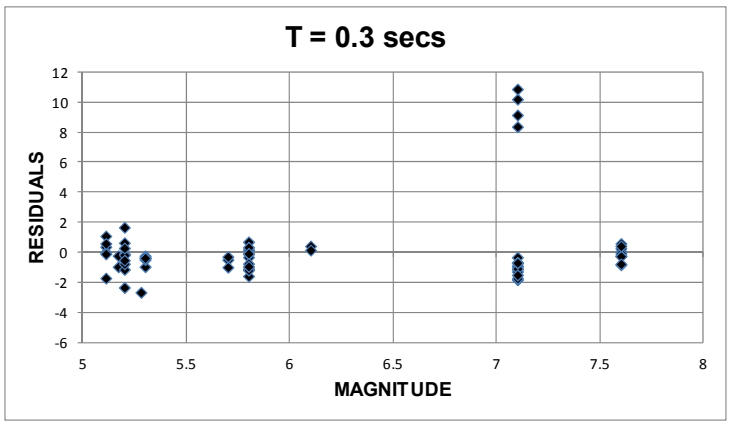

(b)

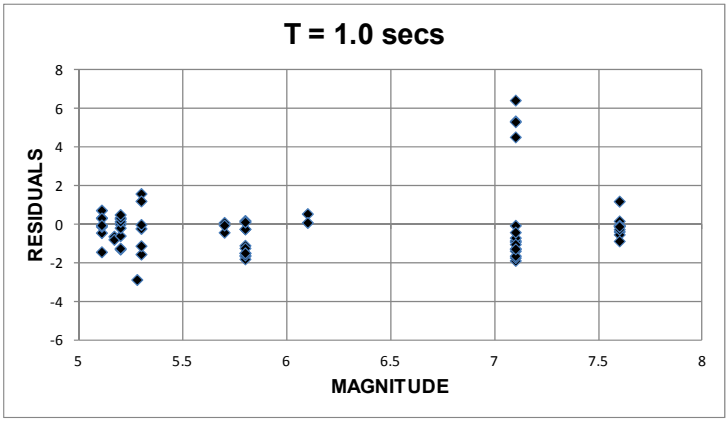

(c)

Figure 4.6 Residuals vs Magnitude at a)PGA, b) T =0.3 secs and c) T = 1.0 secs for B & A (2008)

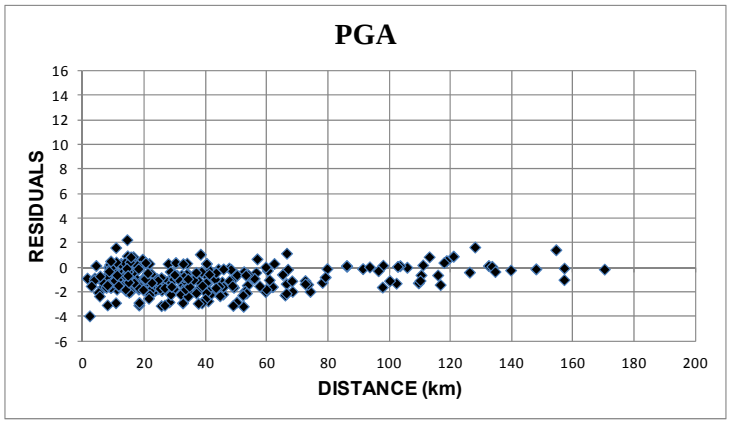

(a)

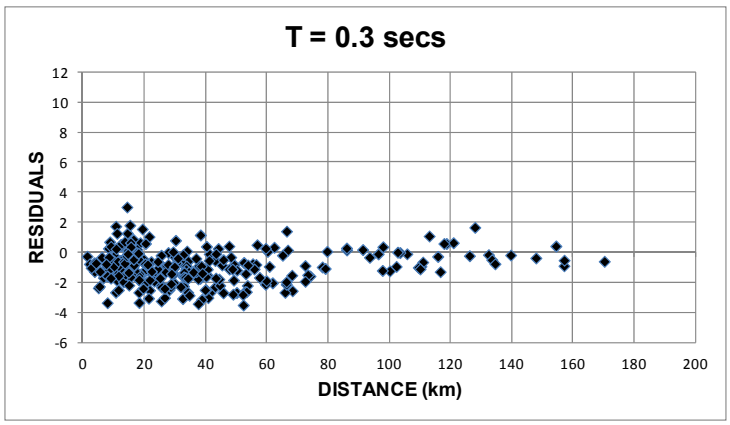

(b)

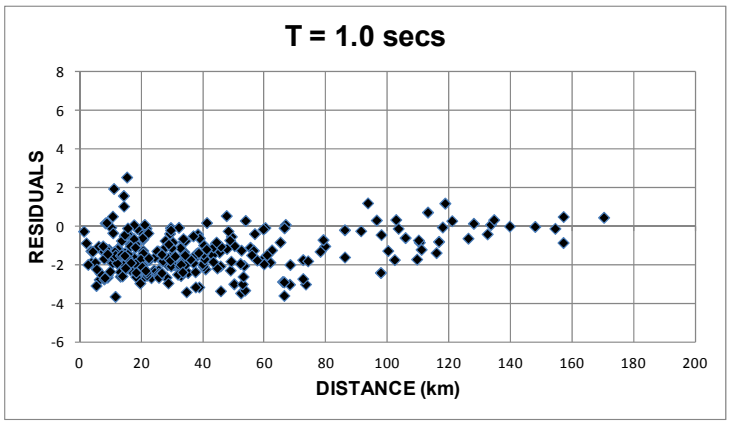

(c)

Figure 4.7 Residuals vs Distance at a)PGA, b) T =0.3 secs and c) T = 1.0 secs for B & A (2008)

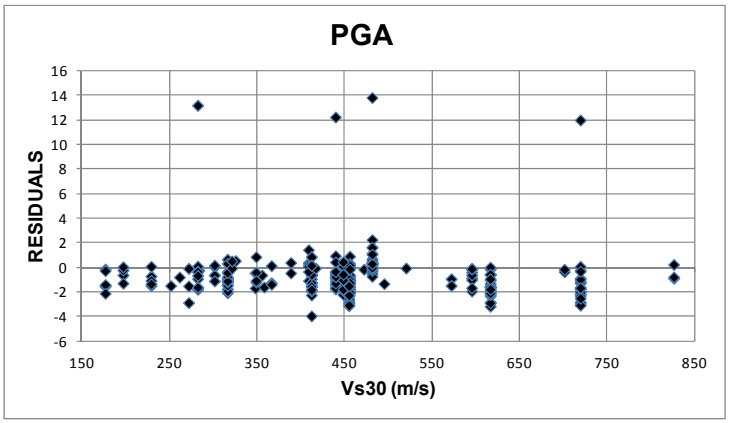

(a)

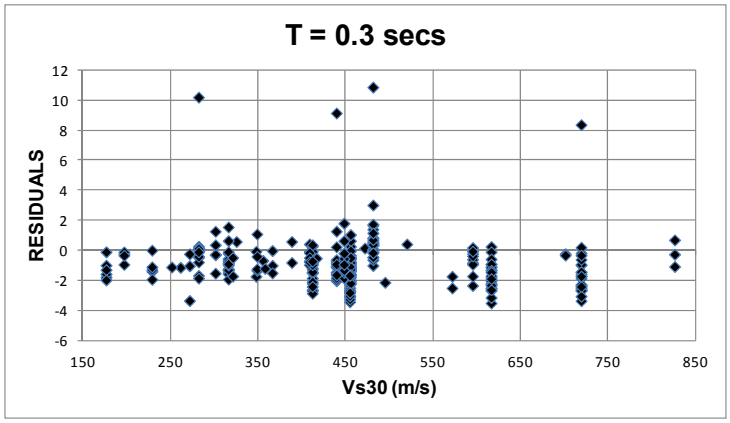

(b)

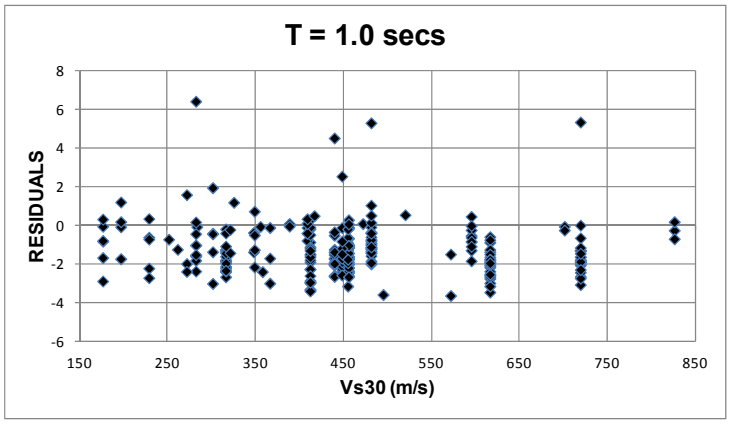

(c)

Figure 4.8 Residuals vs Vs30 at a)PGA, b) T =0.3 secs and c) T = 1.0 secs for B & A (2008)

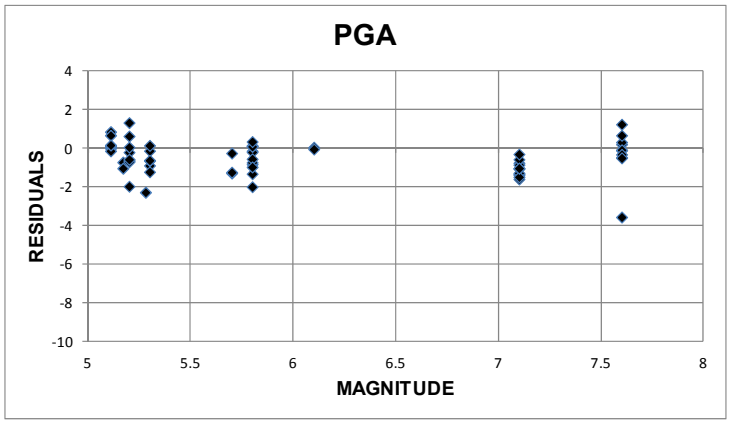

(a)

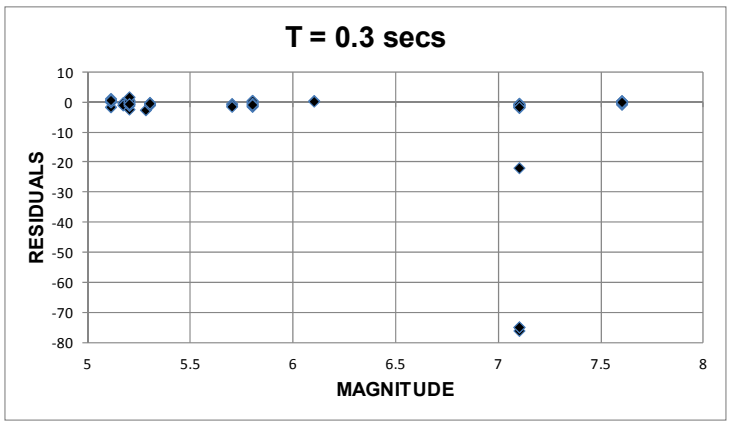

(b)

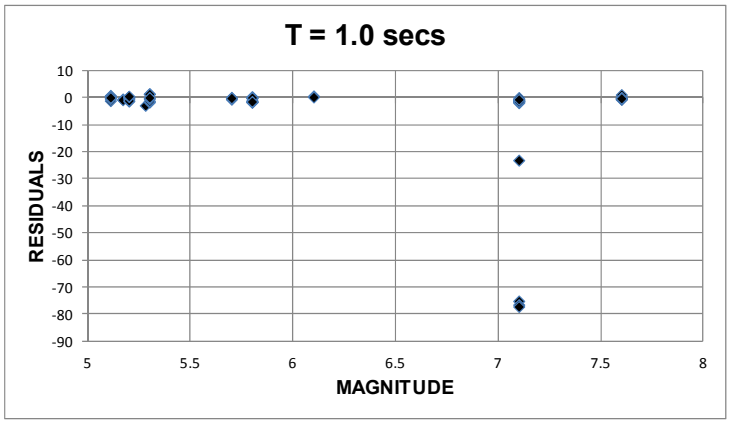

(c)

Figure 4.9 Residuals vs Magnitude at a)PGA, b) T =0.3 secs and c) T = 1.0 secs for C & B (2008)

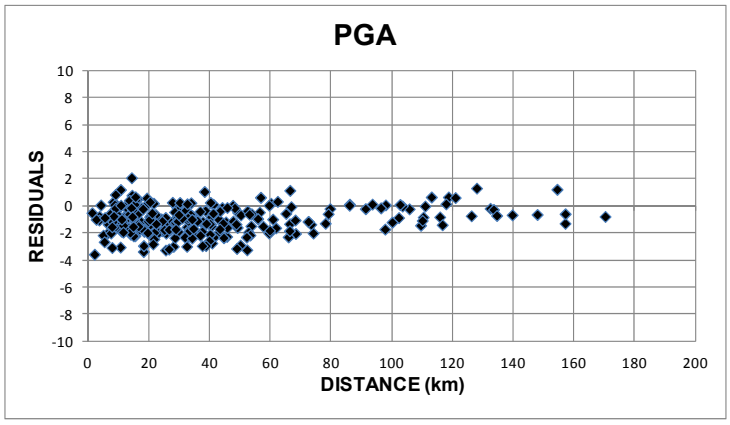

(a)

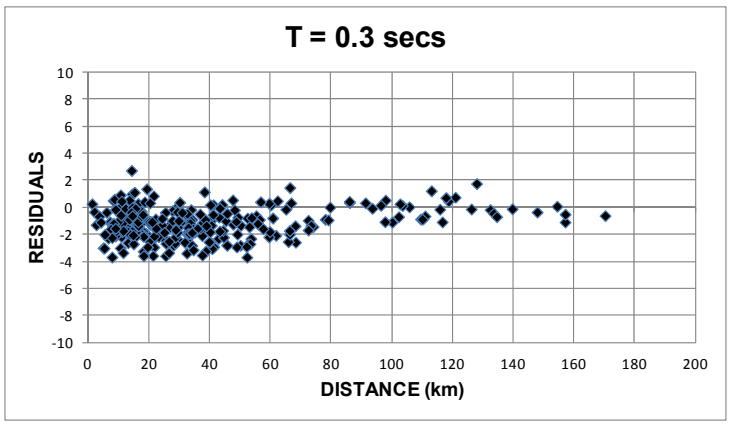

(b)

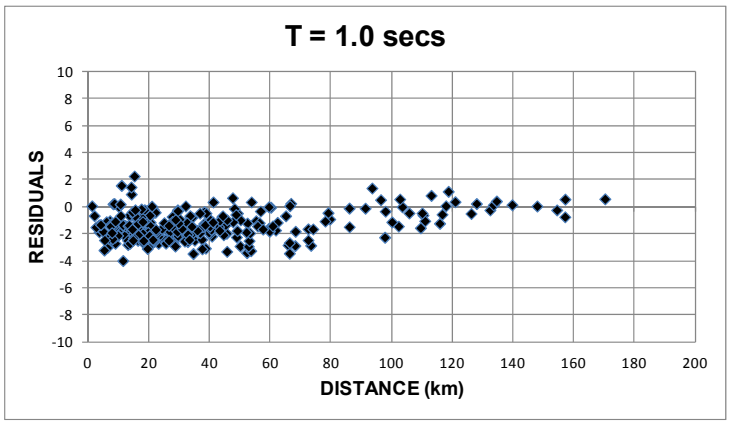

(c)

Figure 4.10 Residuals vs Distance at a)PGA, b) T =0.3 secs and c) T = 1.0 secs for C & B (2008)

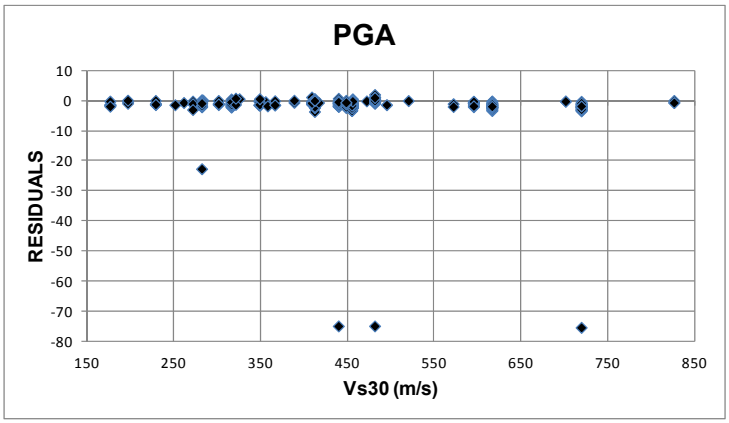

(a)

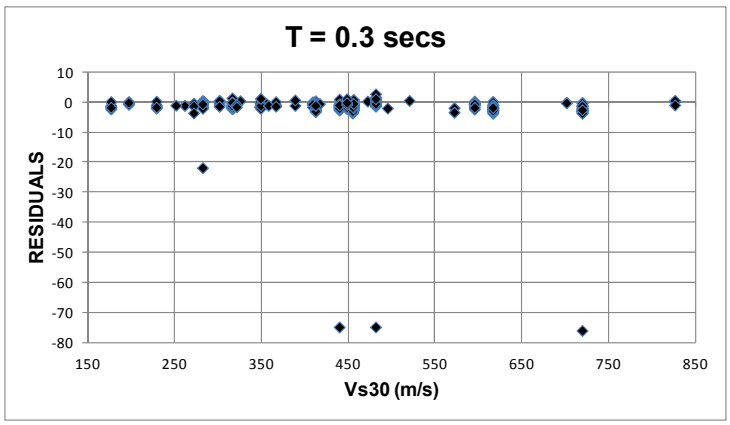

(b)

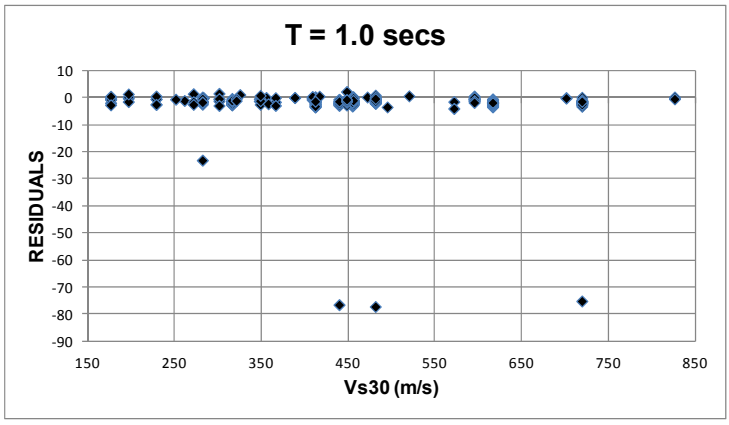

(c)

Figure 4.11 Residuals vs Vs30 at a)PGA, b) T =0.3 secs and c) T = 1.0 secs for C & B (2008)

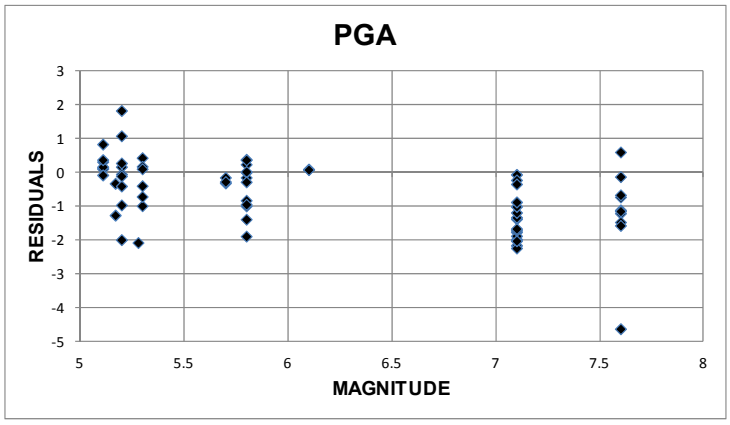

(a)

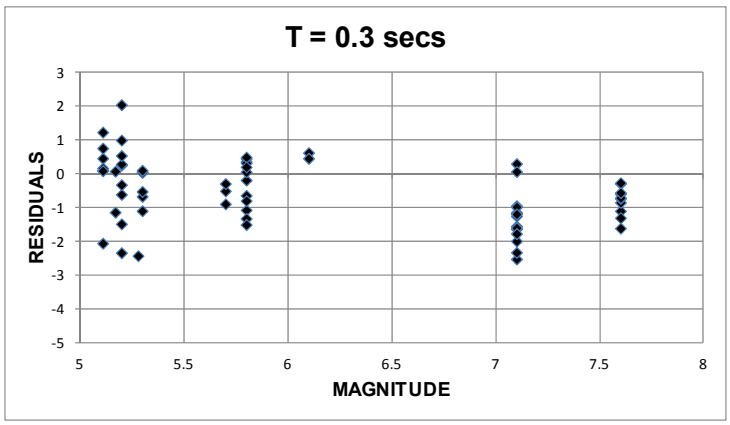

(b)

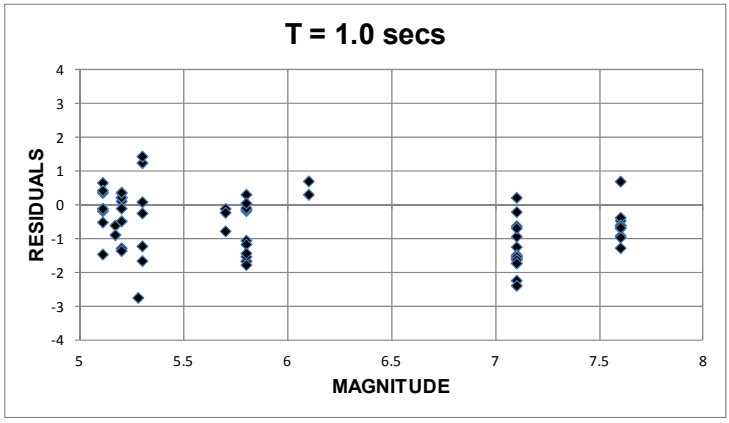

(c)

Figure 4.12 Residuals vs Magnitude at a)PGA, b) T =0.3 secs and c) T = 1.0 secs for C & Y (2008)

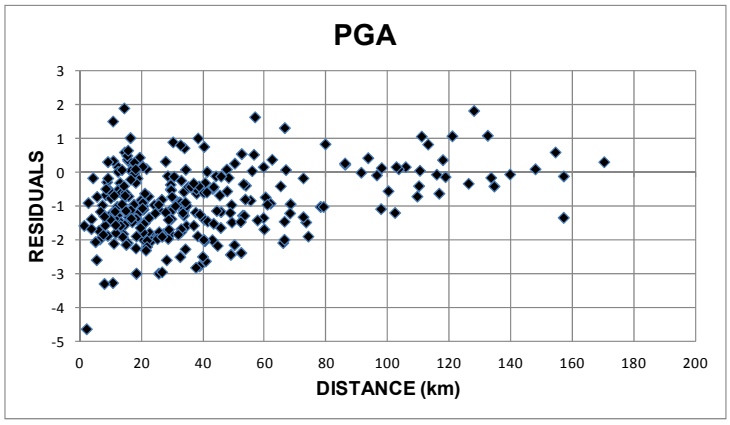

(a)

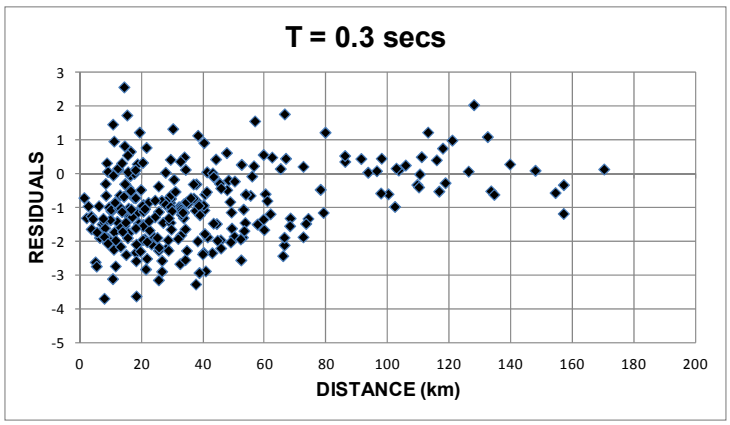

(b)

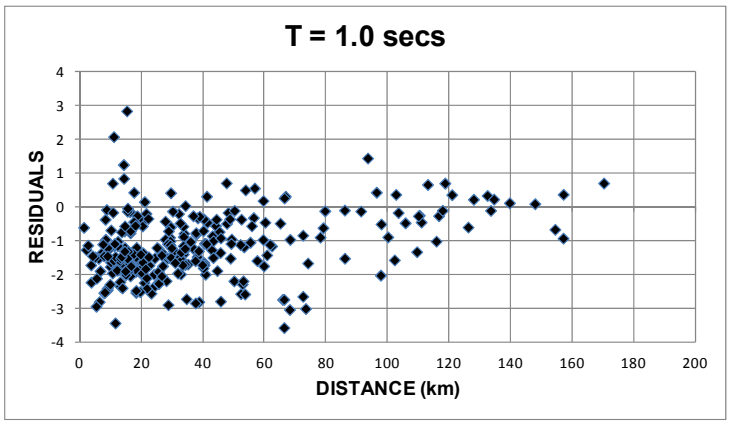

(c)

Figure 4.13 Residuals vs Distance at a)PGA, b) T =0.3 secs and c) T = 1.0 secs for C & Y (2008)

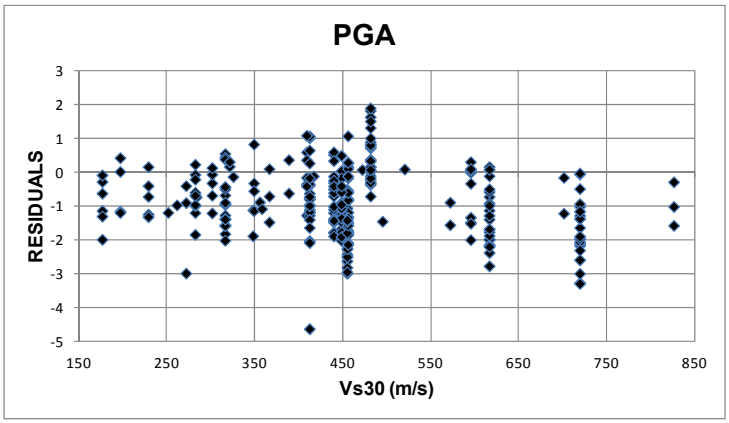

(a)

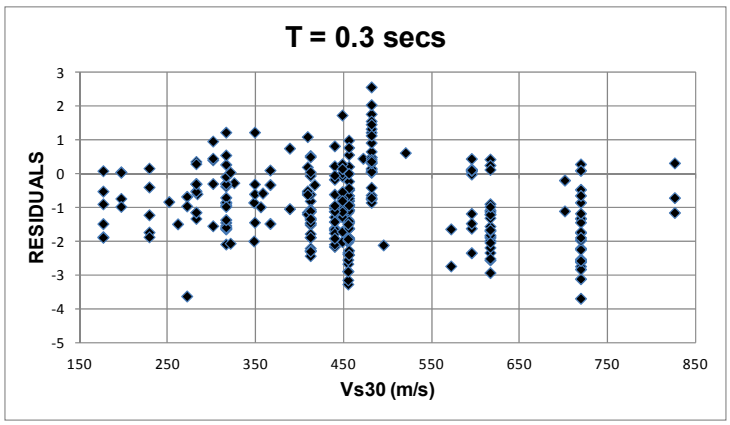

(b)

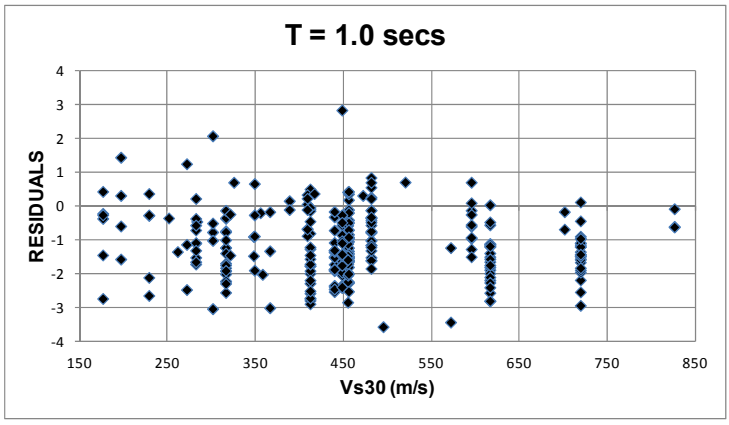

(c)

Figure 4.14 Residuals vs Vs30 at a)PGA, b) T =0.3 secs and c) T = 1.0 secs for C & Y (2008)

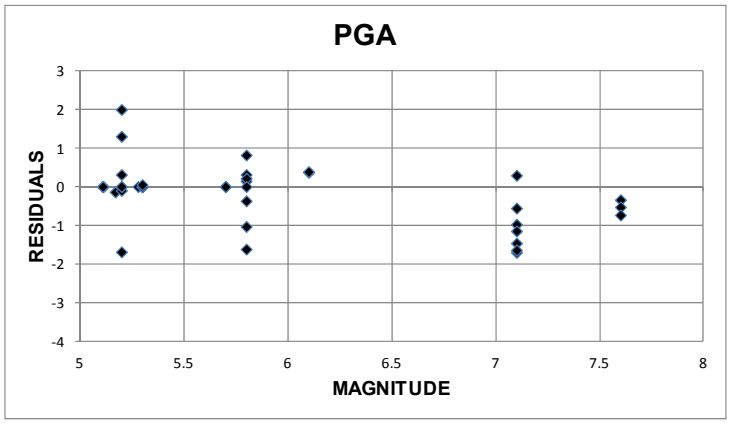

(a)

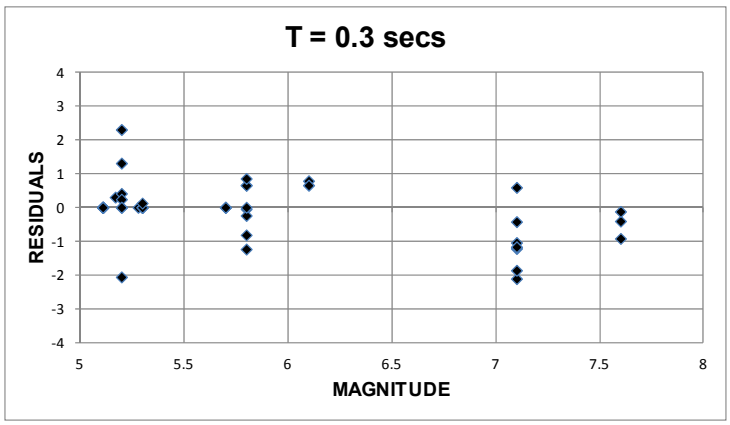

(b)

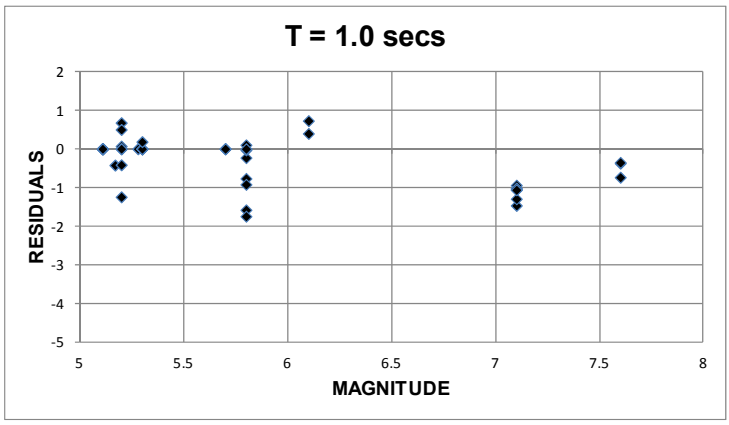

(c)

Figure 4.15 Residuals vs Magnitude at a)PGA, b) T =0.3 secs and c) T = 1.0 secs for Idriss (2008)

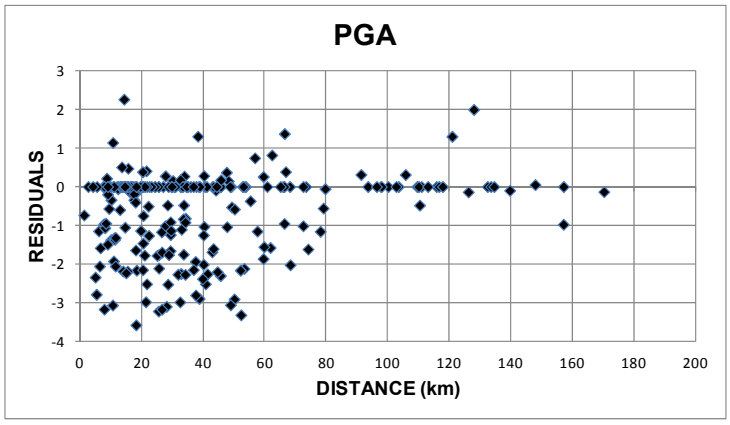

(a)

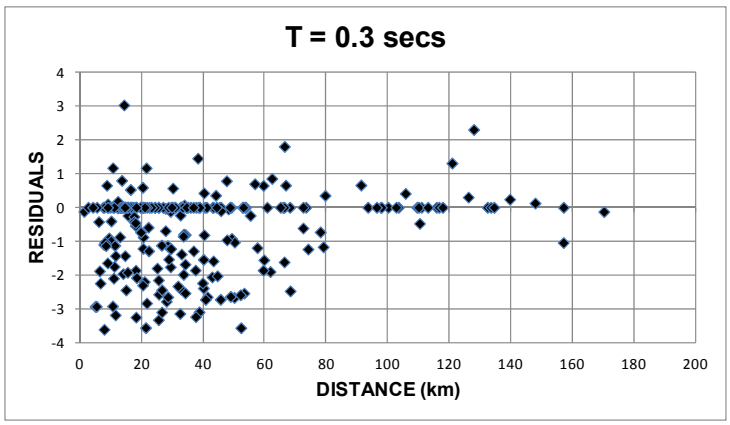

(b)

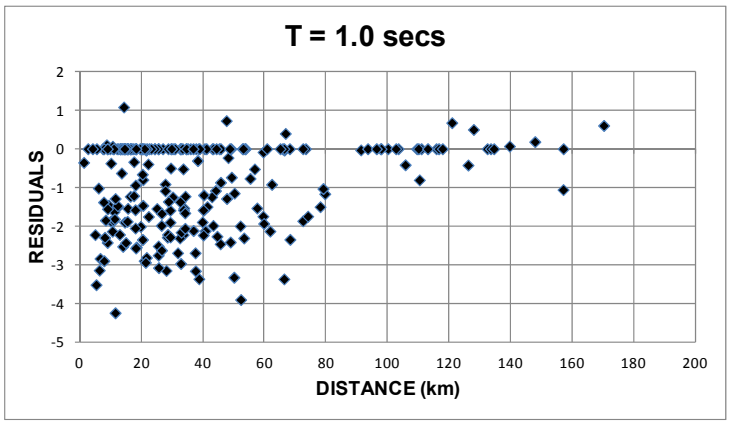

(c)

Figure 4.16 Residuals vs Distance at a)PGA, b) T =0.3 secs and c) T = 1.0 secs for Idriss (2008)

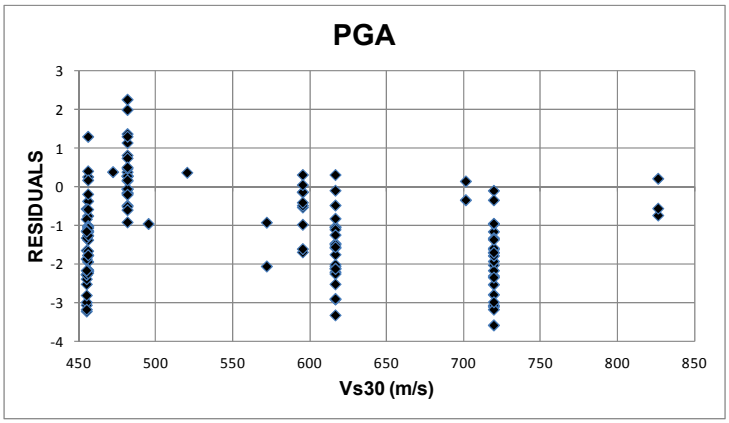

(a)

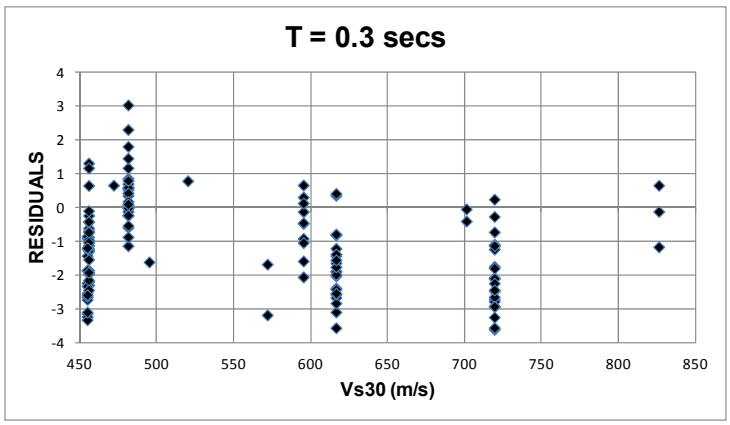

(b)

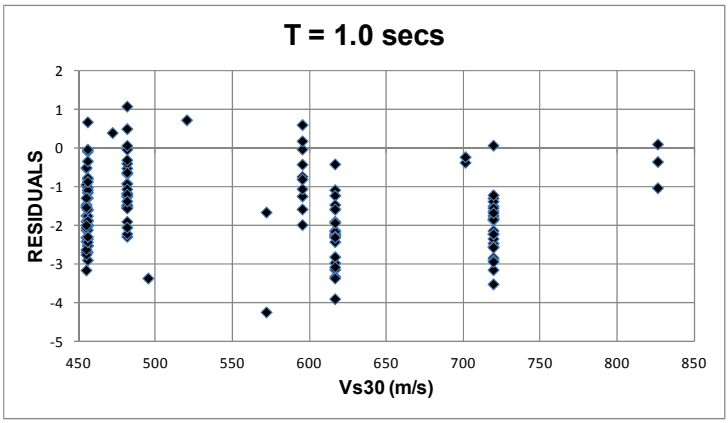

(c)

Figure 4.17 Residuals vs Vs30 at a)PGA, b) T =0.3 secs and c) T = 1.0 secs for Idriss (2008)

CHAPTER 5

PROBABILISTIC SEISMIC HAZARD ASSESSMENT FOR EASTERN MARMARA REGION

The probabilistic approach is used in this study to determine the seismic hazard in Eastern Marmara region for the accepted risk levels in Turkish Earthquake Code (2007). The seismic source models to be used in probabilistic seismic hazard assessment (PSHA) were developed for the fault zones in Eastern Marmara region and presented in Chapter 3. The activity rates, magnitude distribution functions, and reoccurrence models from the seismic source models were incorporated in hazard calculations. The most critical element of PSHA is the ground motion prediction models since the major part of aleatory variability and epistemic uncertainty included in PHSA comes from these models. Details on the selection of the suitable ground motion prediction models for this region were presented in Chapter 4.

Within the contents of this chapter, the probabilistic seismic hazard assessment methodology used in this study is summarized in terms of the hazard integral and its main components. The hazard curves, deaggregation of the hazard and uniform hazard spectrum for six selected sites in the region are presented. Acceptable risk levels in Turkish Earthquake Code (TEC-2007) are introduced and the uniform hazard spectra for example sites at rock and soil site conditions are compared to the TEC-2007 requirements. Hazard maps developed for rock site conditions for PGA, T=0.2 and T=1 second spectral accelerations are provided. Detailed discussion of the results presented in this chapter will be given Chapter 6

5.1 Probabilistic Seismic Hazard Assessment Methodology

The basic methodology of probabilistic seismic hazard analysis (PHSA) proposed by Cornell in 1968 requires the computation of how often a specific level of ground motion will be exceeded at the site. In other words, in a PSHA, the annual rate of events that produce a ground motion intensity measure, IM that exceeds a specified level, L, at the site is computed. This annual rate, ν, is also called the "annual rate of exceedence". Traditionally, the equation for a seismic hazard analysis due to a single source has been given by:

$$\nu(IM > L) = N_{\min} \cdot \int_M \int_R f_M(M) f_R(M,R) P(IM > L | M,R) \times dM \times dR \qquad (5.1)$$

where R is the distance from the source to site, M is the earthquake magnitude; N_{min} is the annual rate of earthquakes with magnitude greater than or equal to the minimum magnitude, $f_M(M)$ and $f_R(M,R)$ are the probability density functions for the magnitude and distance and $P(IM>L \mid M,R)$ is the probability of observing a ground motion greater than L for a given earthquake magnitude and distance.

The probabilistic seismic hazard analysis consists of defining a suite of earthquake scenarios, estimating the range of ground motions for each earthquake scenario, and computing the rate of each combination of earthquake scenario and ground motion (Gülerce and Abrahamson, 2010). Each scenario is defined by the size of the earthquake (magnitude, M) and the location which defines the distance, R, from the site. The ground motion variability is contained in the $P(IM>L \mid M,R)$ term such as:

$$P(IM > L \mid M,R) = \int_\varepsilon f_\varepsilon(\varepsilon) \times P(IM > L \mid M,R,\varepsilon) \times d\varepsilon \qquad (5.2)$$

where ε is the number of standard deviations above or below the median, $f_\varepsilon(\varepsilon)$ is the probability density function for the epsilon (given by a standard normal distribution) and $P(IM>L \mid M,R,\varepsilon)$ is either 0 or 1. In this formulation,

P(IM>L | M,R,ε) selects those scenarios and ground motion combinations that lead to ground motions greater than the test level L (Gülerce and Abrahamson, 2010). The final form of the hazard integral is given in Equation 5.3:

$$\nu(IM > L) = N_{\min} \cdot \int_{M}\int_{R}\int_{\varepsilon} f_M(M)\, f_R(M,R)\, f_\varepsilon(\varepsilon) P(IM > L | M,R,\varepsilon) \times dM \times dR \times d\varepsilon \quad (5.3)$$

For multiple seismic sources, the total annual rate of events with ground motions that exceed L at the site is the sum of the annual rate of events from the individual sources (assuming that the sources are independent).

$$\nu(IM > L) = \sum_{i}^{Sources} \nu_i(IM > L) \quad (5.4)$$

Seismic source characterization includes the definition of the location and geometry of seismic sources, estimation of the characteristic magnitude and activity rate for each seismic source, and selection of the proper magnitude distribution function along with the reoccurrence relation. Therefore, the probability density functions f(M) and f(M,R) in Equation 5.3, and the activity rates (denoted by N_{min} in Equation 5.3) for the seismic sources in the study area were defined in Chapter 3. Selection of ground motion prediction models suitable for the PSHA in the region were discussed in details in Chapter 4. The ground motion and ground motion variability denoted by P(IM>L | M,R,ε) and $f_\varepsilon(\varepsilon)$ were incorporated to the hazard integral using the selected ground motion prediction models.

To make the comparison of the hazard results to the defined risk levels in the Turkish Earthquake Code (TEC, 2007) possible, a Poisson process is assumed:

$$\nu(IM > L) = \frac{-\ln(1 - P(IM > L | T))}{T} \quad (5.4)$$

where T is the number of years and P(IM>L│T) is the chance of being exceeded. The inverse of this rate is called the return period. The acceptable risk levels in TEC-2007 are similar to the other design codes around the world. The acceptable risk levels in TEC-2007 and others were converted to the annual rate of exceedance and return period as presented in Table 5.1.

Table 5.1 Acceptable risk levels in TEC-2007 and other design codes

Code	Time	Prob. of Exceedance	Return Period	ν
TEC 2007	50 years	10%	475 years	0.0021
	50 years	50%	72 years	0.0139
	50 years	2%	2475 years	0.0004
ICOLD	50 years	10%	475 years	0.0021
	100 years	50%	144 years	0.0069
NEHRP (FEMA - 273)	50 years	10%	475 years	0.0021
	50 years	2%	2475 years	0.0004
CBC 2003	50 years	10%	475 years	0.0021

5.2 PSHA Results for Example Sites in the Study Area

The numerical integration of the PSHA integral is performed by the computer code HAZ38 (developed by N. Abrahamson). The results of the study is presented in terms of hazard curves, deaggregation of the hazard, and uniform hazard spectrum for 6 city centers in Eastern Marmara; Adapazarı, Düzce, Gemlik, İzmit, İznik and Sapanca (denoted by yellow stars in Figure 5.1).

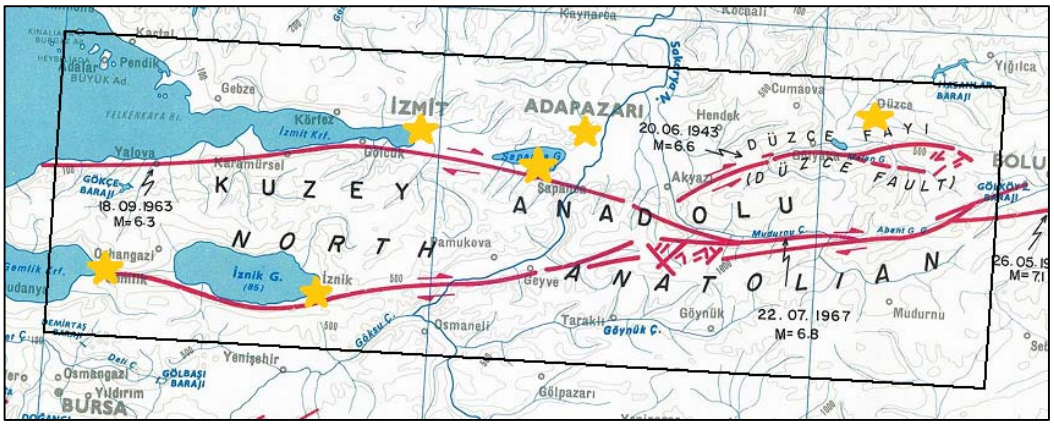

Figure 5.1 The six locations where the analysis are performed

The effect of all possible combinations of magnitude and distance on the probability of exceeding a selected ground motion level is illustrated in hazard curves (Abrahamson, 2006). The hazard curves for PGA and 14 spectral periods (T=0.01, T=0.03, T=0.05, T=0.075, T=0.1, T=0.2, T=0.5, T=1, T=2, T=3, T=4, T=5, T=7.5, and T=10 seconds) at six selected sites assuming rock site conditions (V_{s30} = 760 m/s) are presented in Figure 5.2 to Figure 5.16.

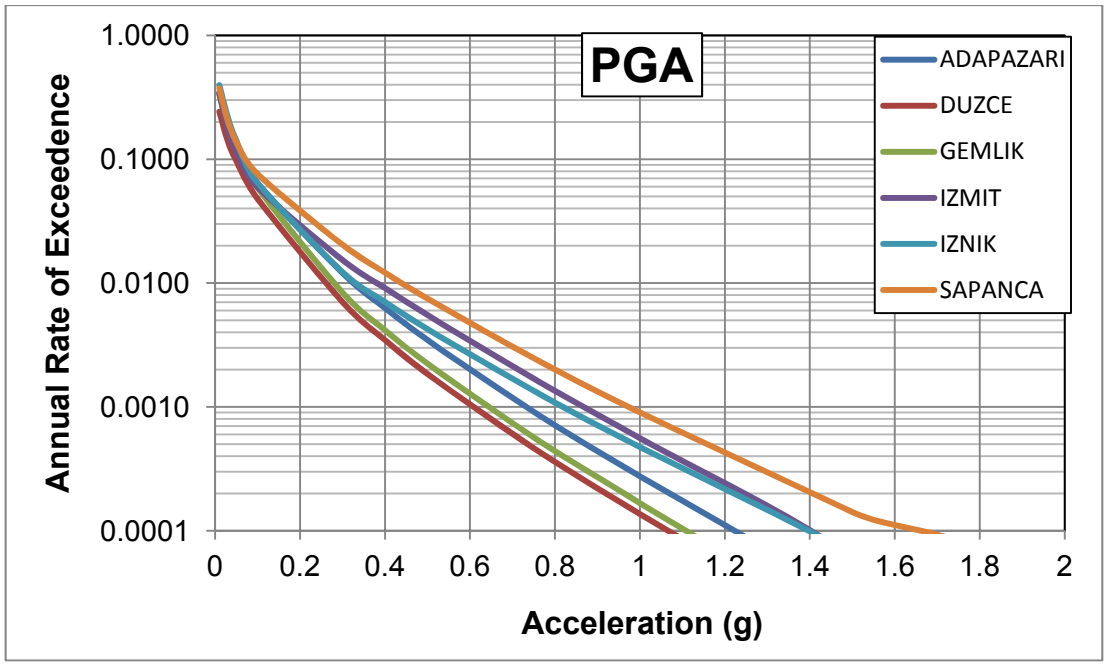

Figure 5.2 Hazard Curves for T = 0 secs

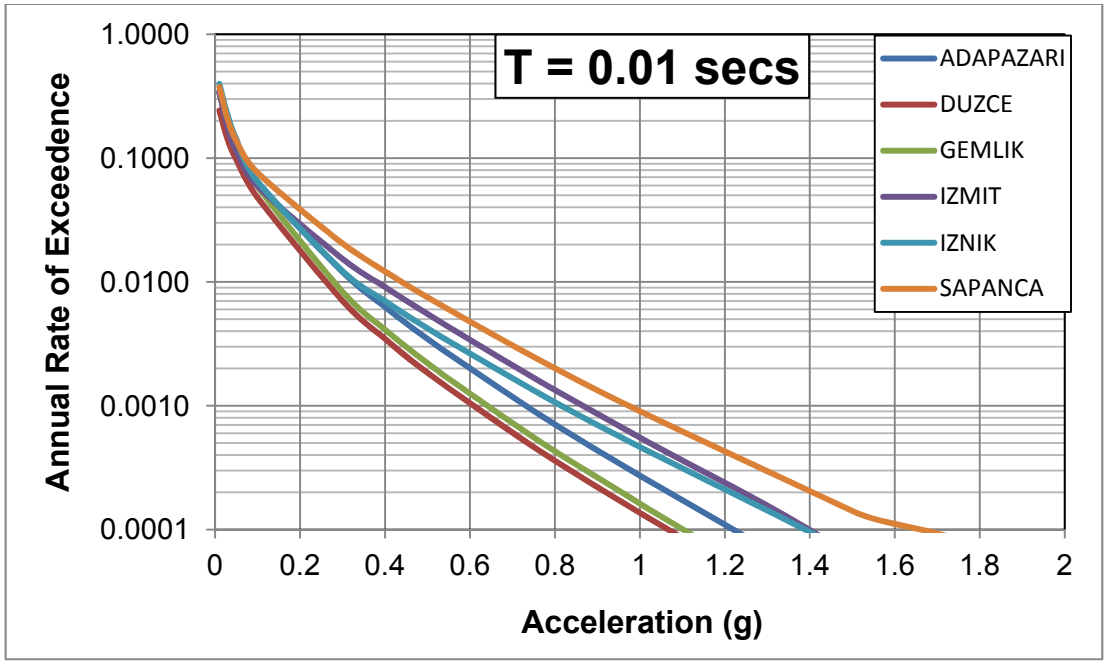

Figure 5.3 Hazard Curves for T = 0.01secs

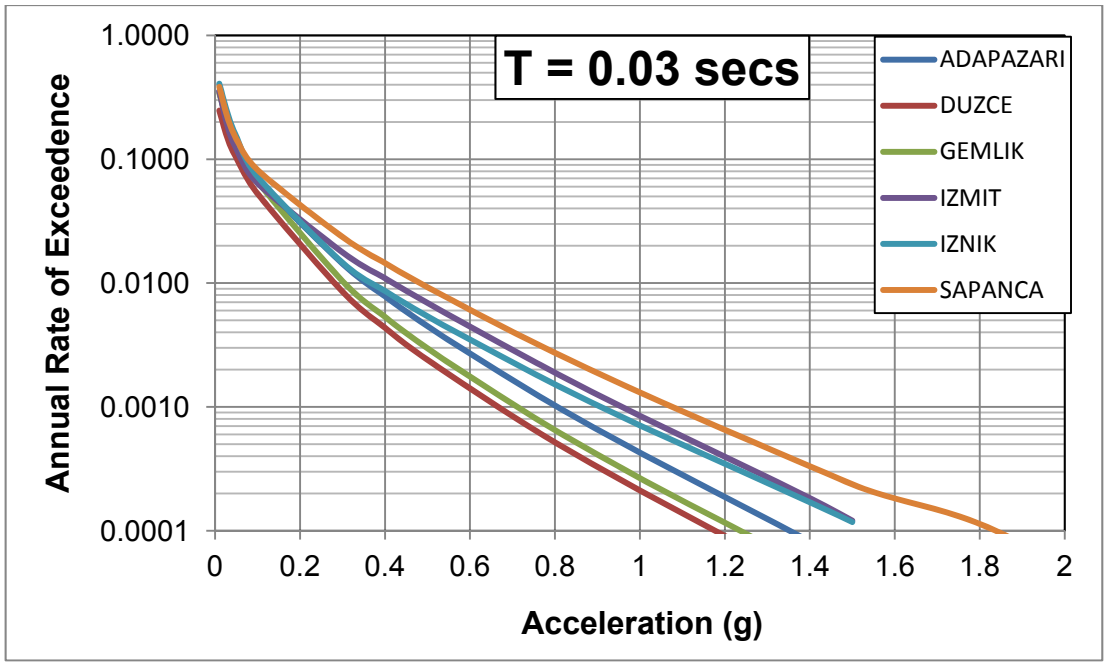

Figure 5.4 Hazard Curves for T = 0.03 secs

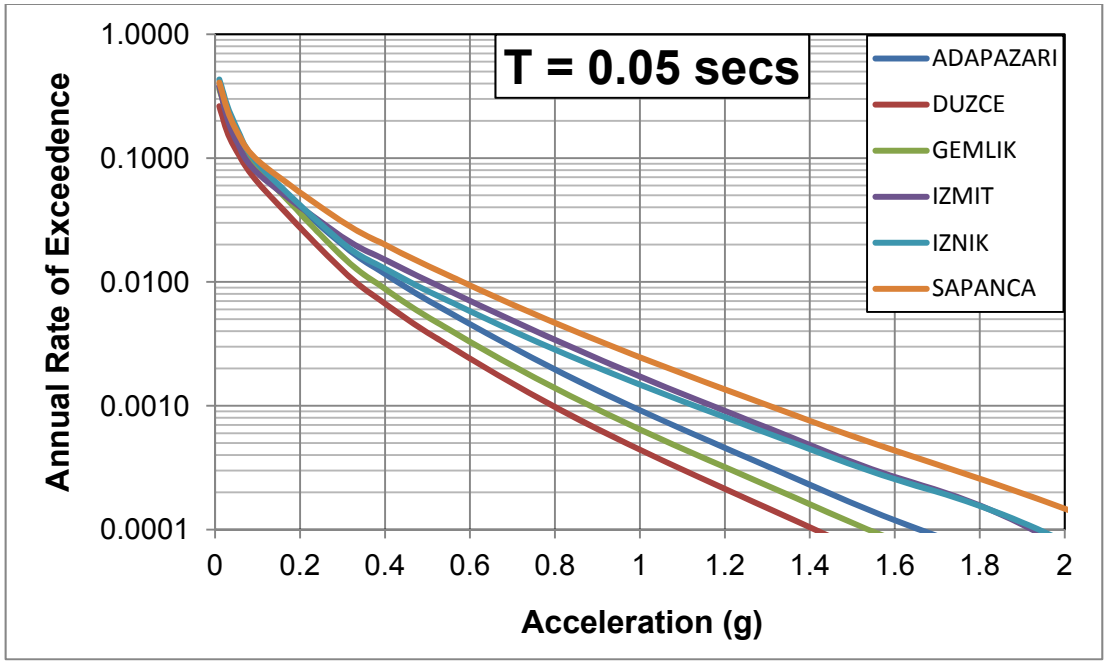

Figure 5.5 Hazard Curves for T = 0.05 secs

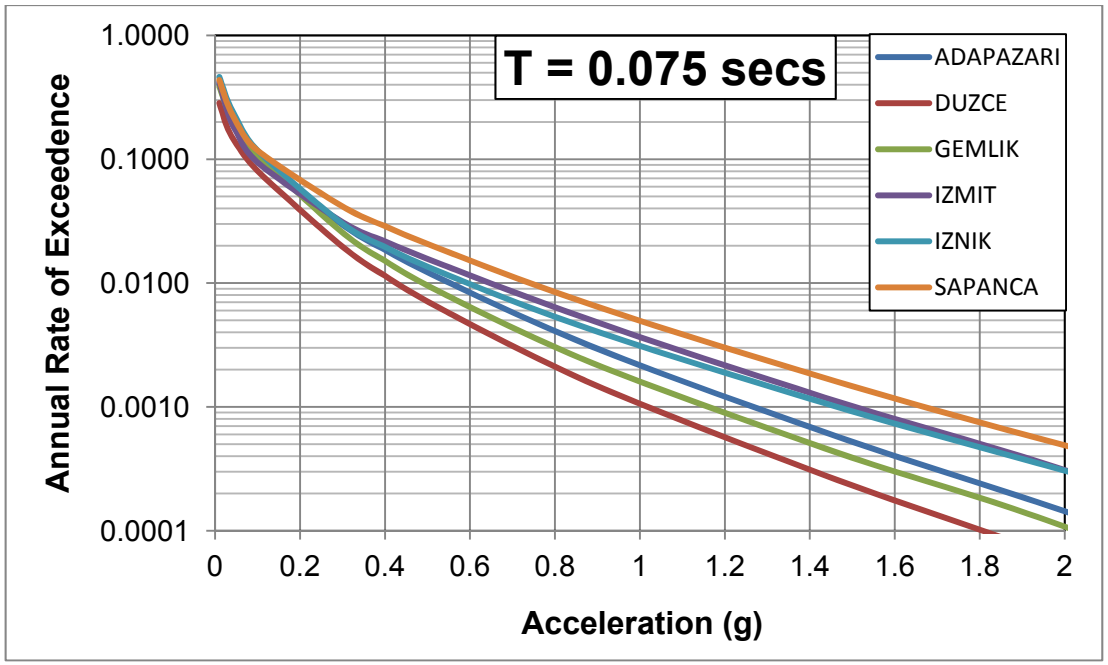

Figure 5.6 Hazard Curves for T = 0.075 secs

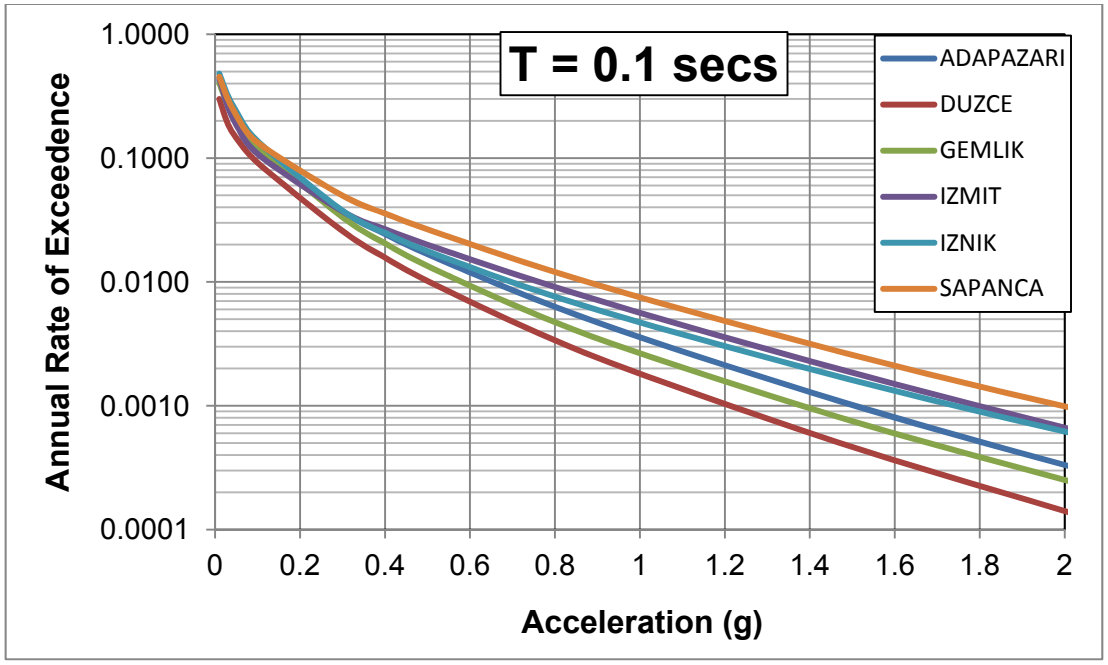

Figure 5.7 Hazard Curves for T = 0.10 secs

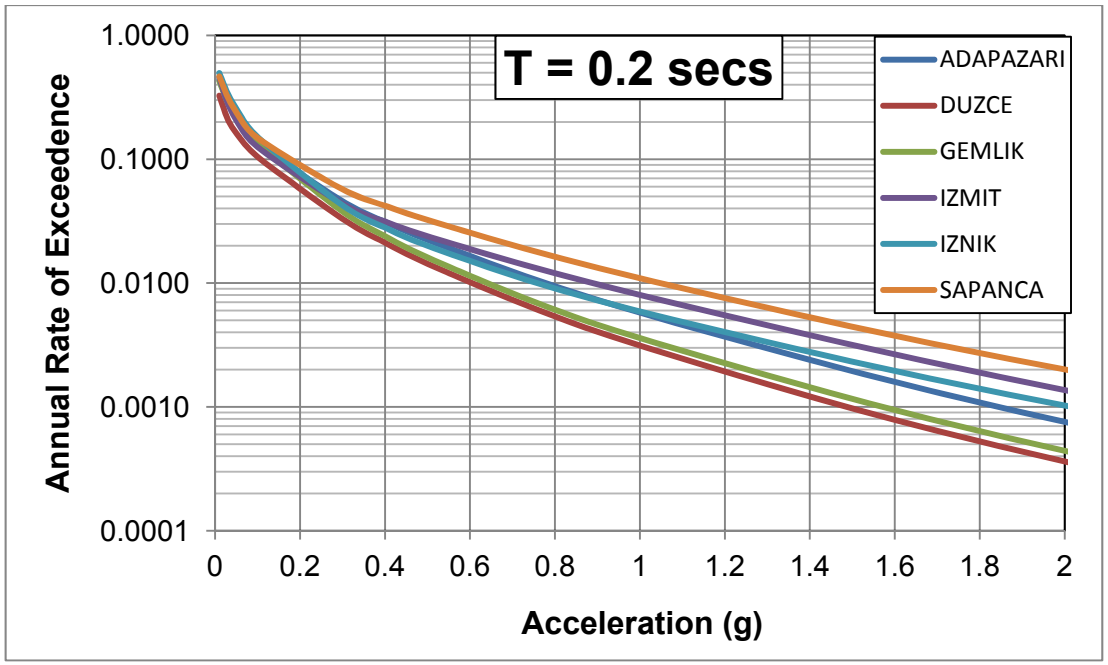

Figure 5.8 Hazard Curves for T = 0.20 secs

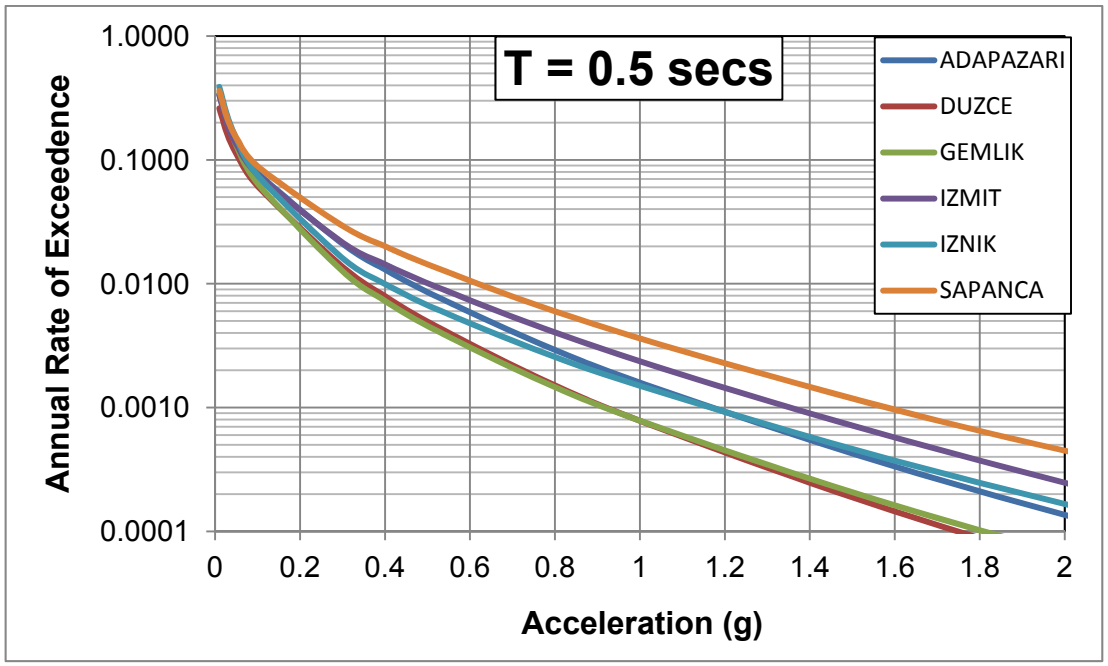

Figure 5.9 Hazard Curves for T = 0.50 secs

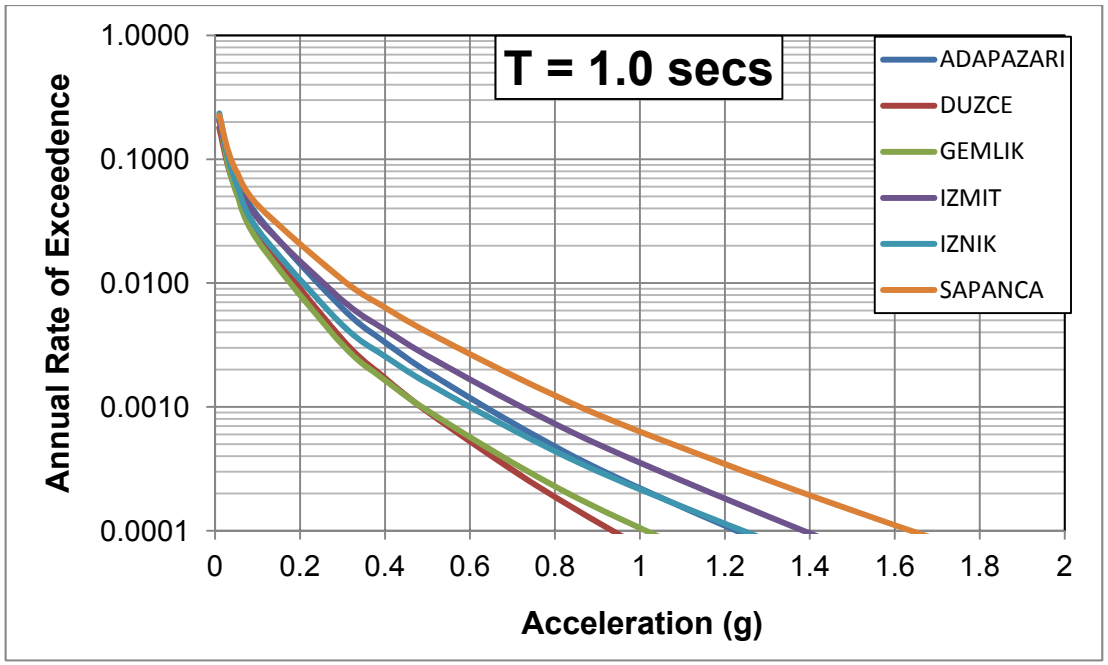

Figure 5.10 Hazard Curves for T = 1.00 secs

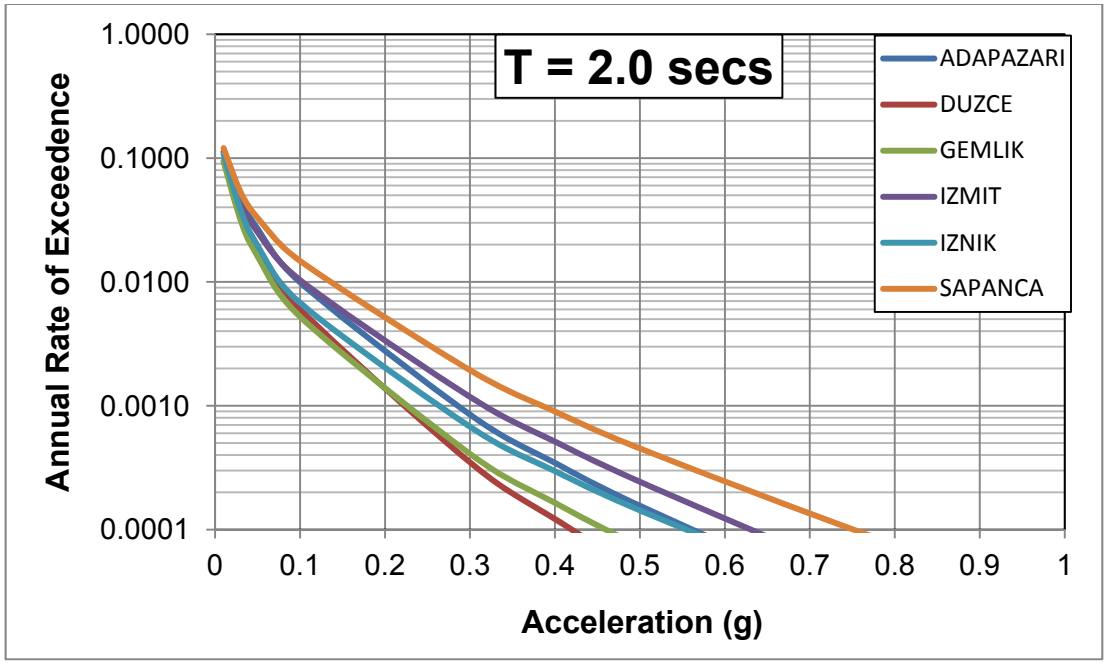

Figure 5.11 Hazard Curves for T = 2.00 secs

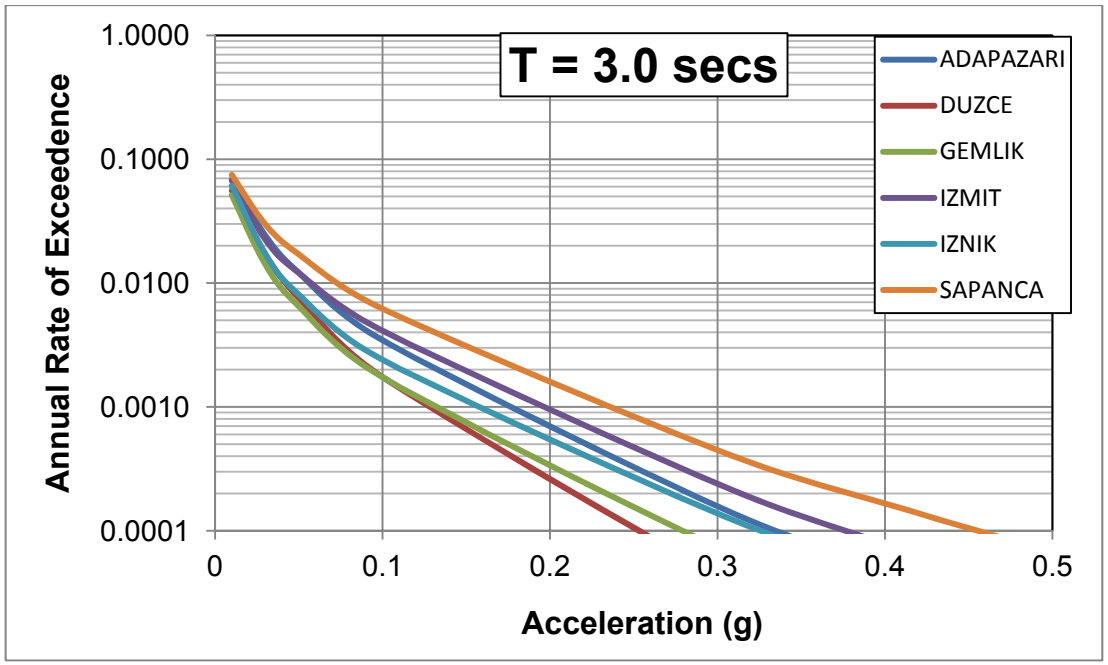

Figure 5.12 Hazard Curves for T = 3.00 secs

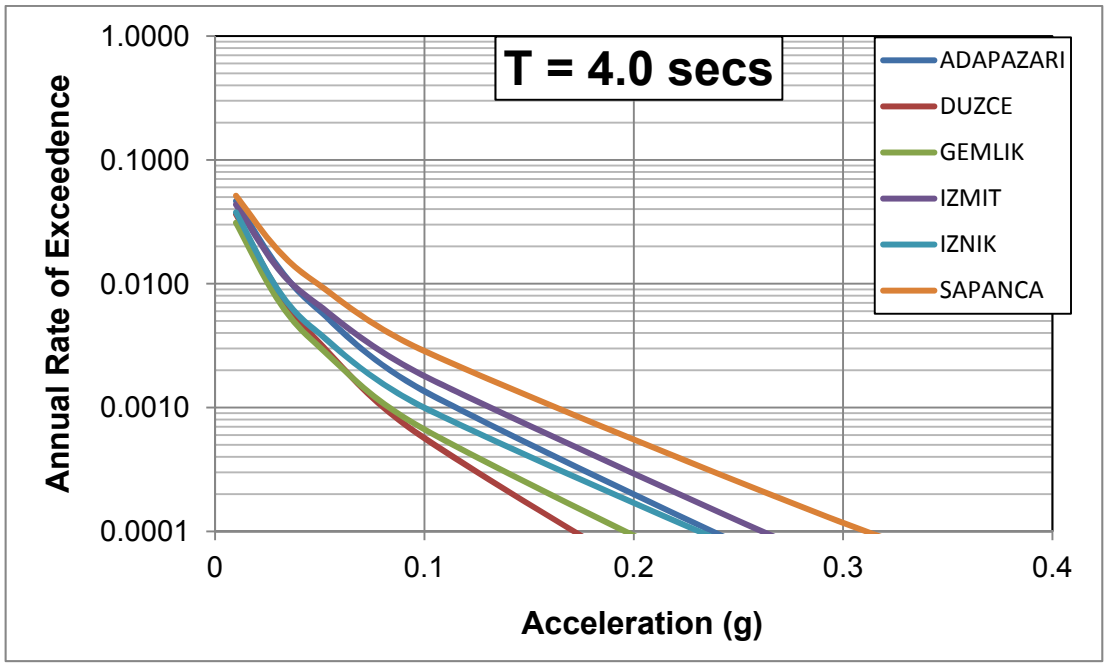

Figure 5.13 Hazard Curves for T = 4.00 secs

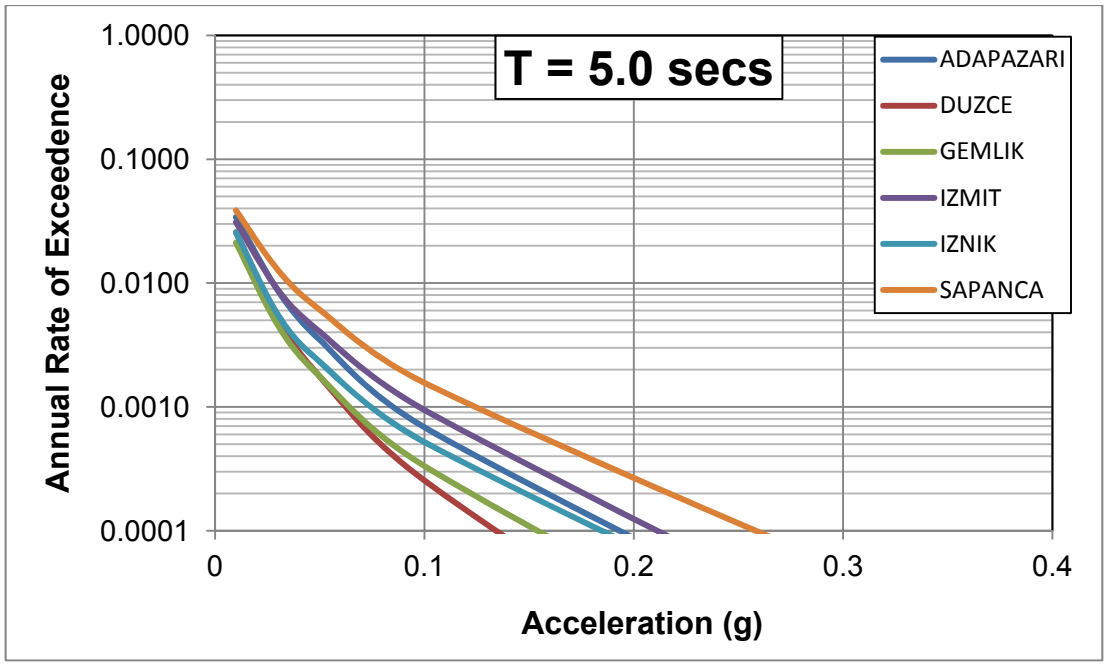

Figure 5.14 Hazard Curves for T = 5.00 secs

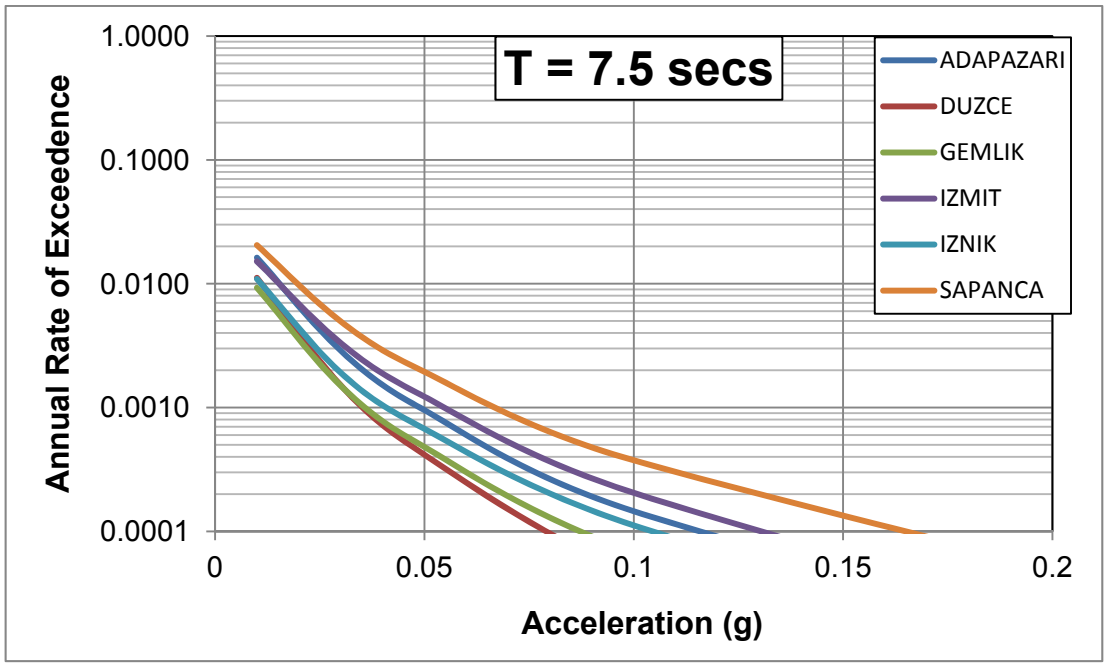

Figure 5.15 Hazard Curves for T = 7.50 secs

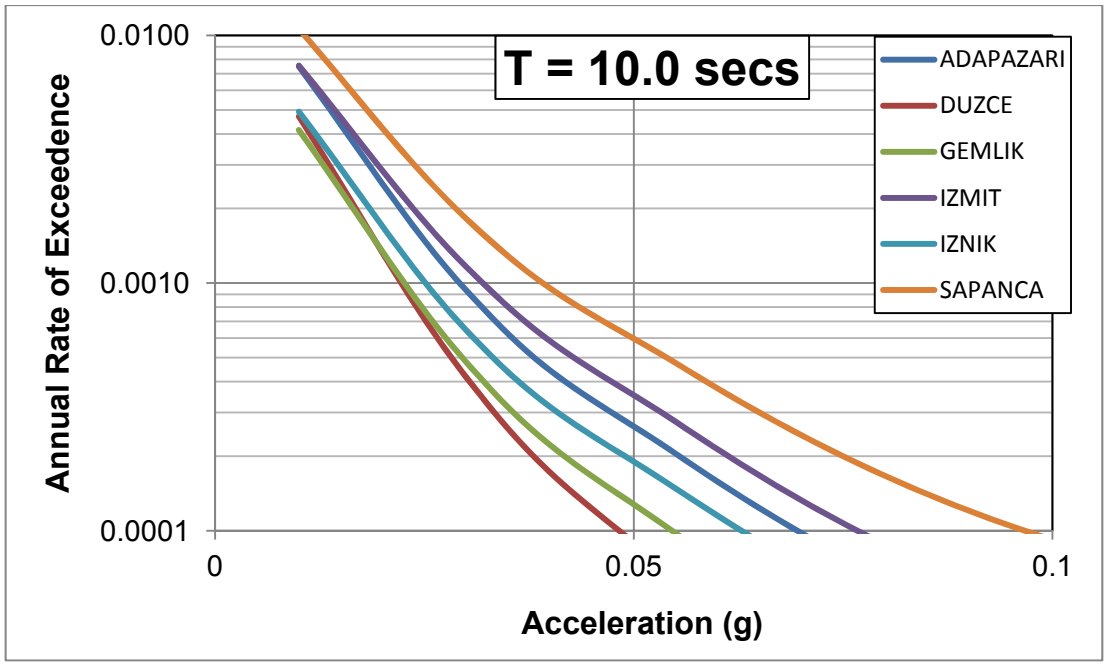

Figure 5.16 Hazard Curves for T = 10.00 secs

Highest level of seismic hazard is observed in Sapanca for all spectral periods as expected, since Sapanca is closer than the other sites to all of the seismic sources in the region (Figure 5.1). PSHA calculates probability of exceedance at the site contributed by all of the sources therefore the ground motion should be estimated from the total hazard curve rather than the hazard curves corresponding to individual sources. However, to demonstrate the contribution of seismic sources to the total hazard, hazard curves for individual sources for Sapanca is shown in Figure 5.17. The main contribution comes from the North Anatolian Fault Northern Strand (NAF_N) and North Anatolian Fault Southern Strand (NAF_S) due to the large seismic moment accumulation assigned to these sources with high slip rates.

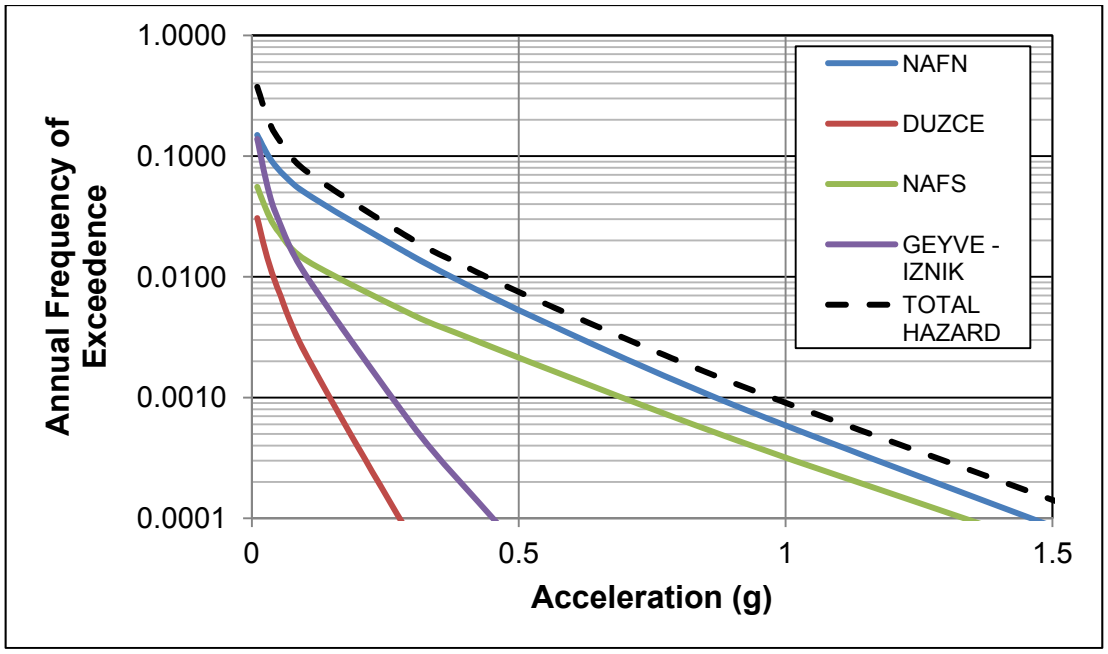

Figure 5.17 Contribution of the sources to total hazard at Sapanca

Hazard at Düzce is significantly lower than the other sites due to the fact that the hazard is underestimated for the sites in the eastern part of the region by ignoring the contribution of North Anatolian Fault Bolu-Gerede segment. This segment is out of the scope of this study so it is not included in the PSHA calculations. The peak ground accelerations for 10% probability of exceedance level in 50 years, 50% probability of exceedance level in 50 years, and 2% probability of exceedance level in 50 years at the selected sites are presented in Table 5.2.

Table 5.2 PGA for different exceedance levels at six locations

Risk Level	Adapazarı	Düzce	Gemlik	İzmit	İznik	Sapanca
2% in 50 years	0.92	0.78	0.82	1.08	1.04	1.22
10% in 50 years	0.60	0.48	0.51	0.70	0.66	0.80
50% in 50 years	0.26	0.22	0.24	0.30	0.28	0.36

The hazard curve gives the combined effect of all magnitudes and distances on the probability of exceeding the specified ground motion level. Since all of the sources, magnitudes, and distances are mixed together, it is difficult to understand what is controlling the hazard from the hazard curve by itself. To provide an insight into which events are most important for the hazard at a given ground motion level, the hazard curve is broken down into its contributions from different earthquake scenarios (Gülerce and Abrahamson, 2010). This process is called deaggregation (Bazzurro and Cornell, 1999). The deaggregation plots for 10% of exceedance in 50 years risk level for rock site conditions for PGA are presented in Figure 5.18 to Figure 5.23 for six locations; Adapazarı, Gemlik, İzmit, İznik, Sapanca and Düzce, respectively.

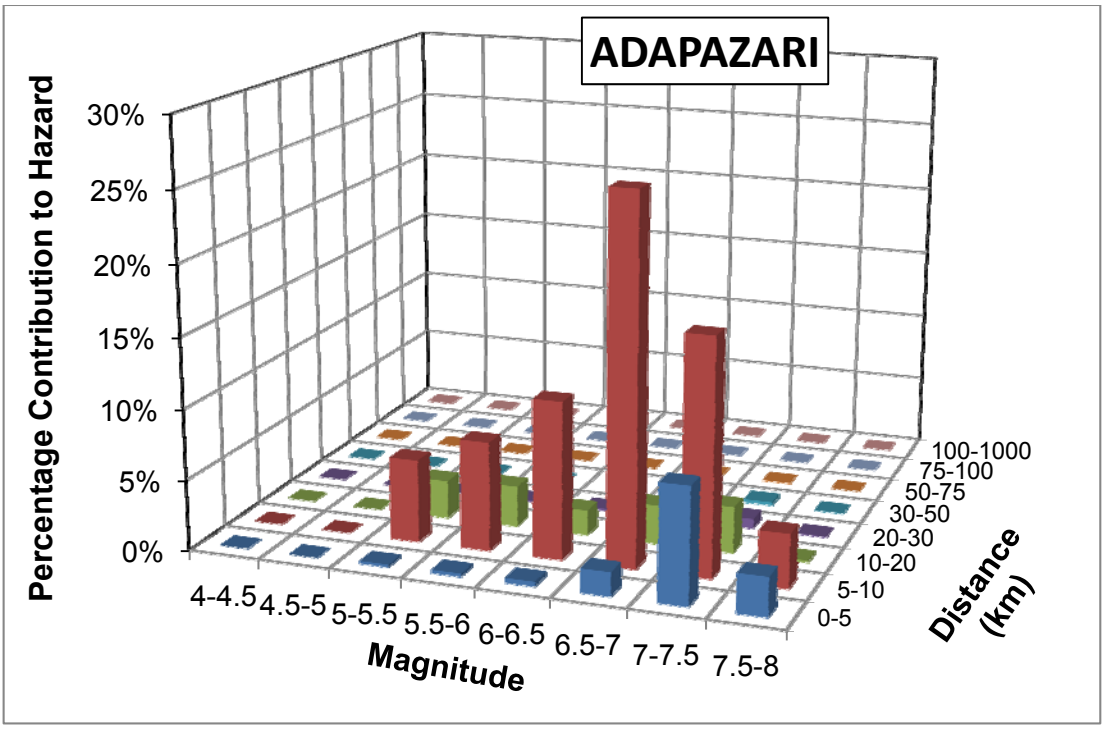

Figure 5.18 Deaggregation for Adapazari

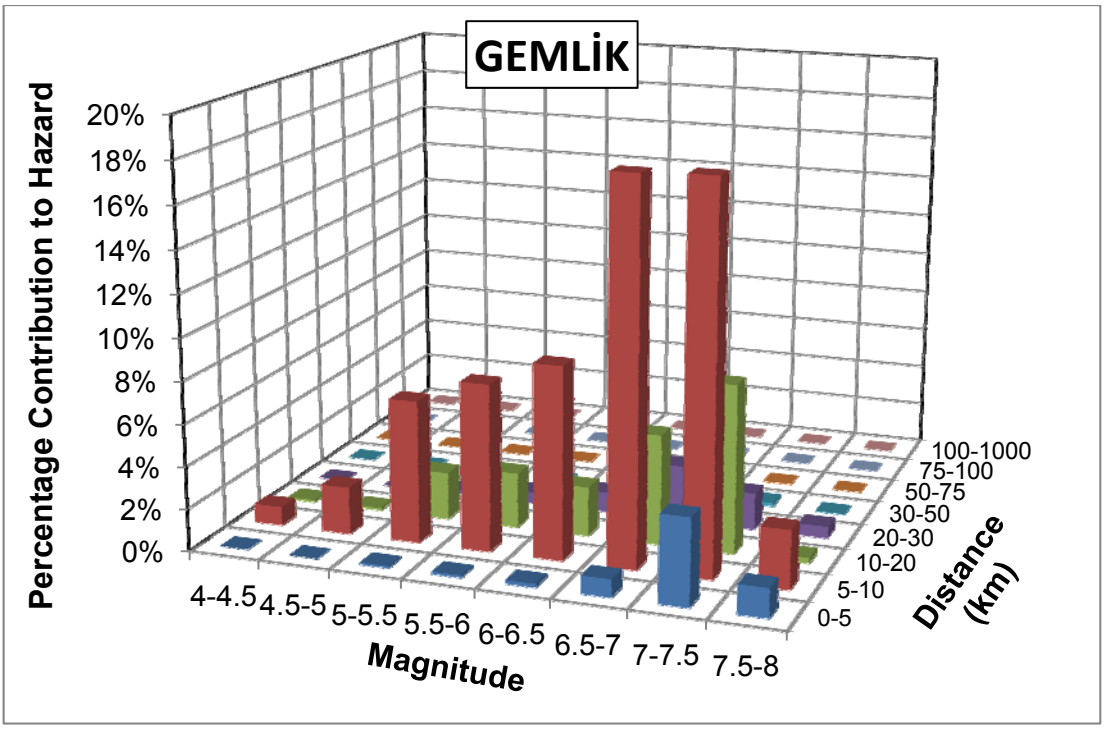

Figure 5.19 Deaggregation for Gemlik

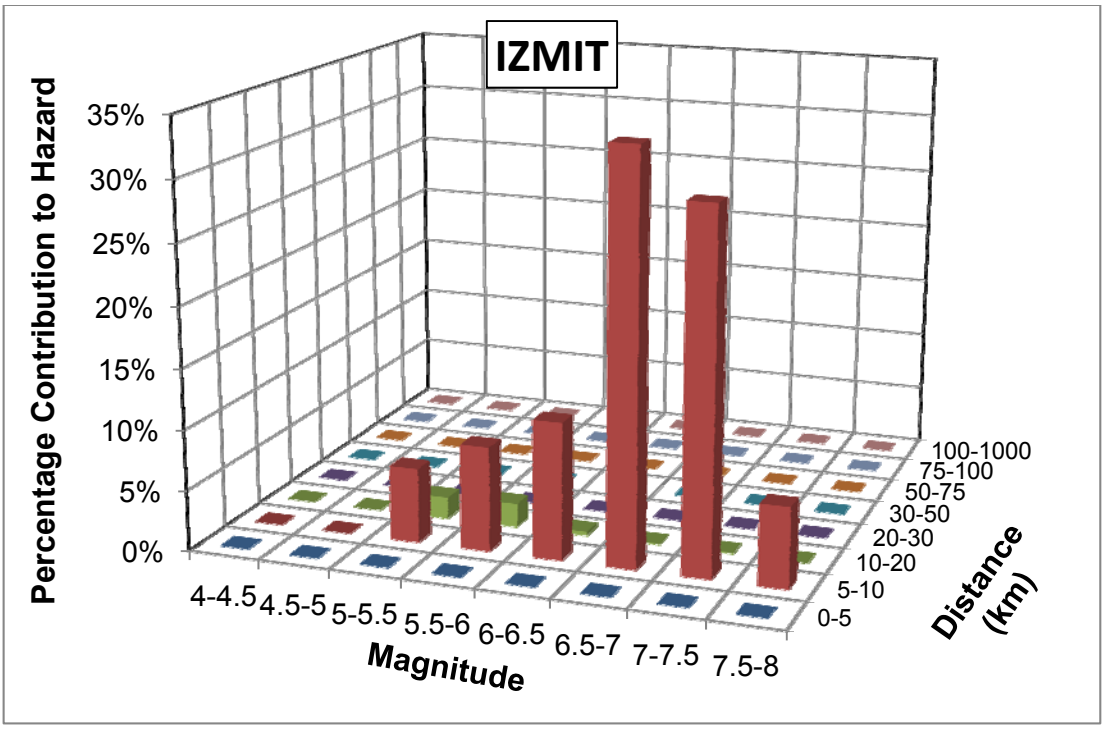

Figure 5.20 Deaggregation for İzmit

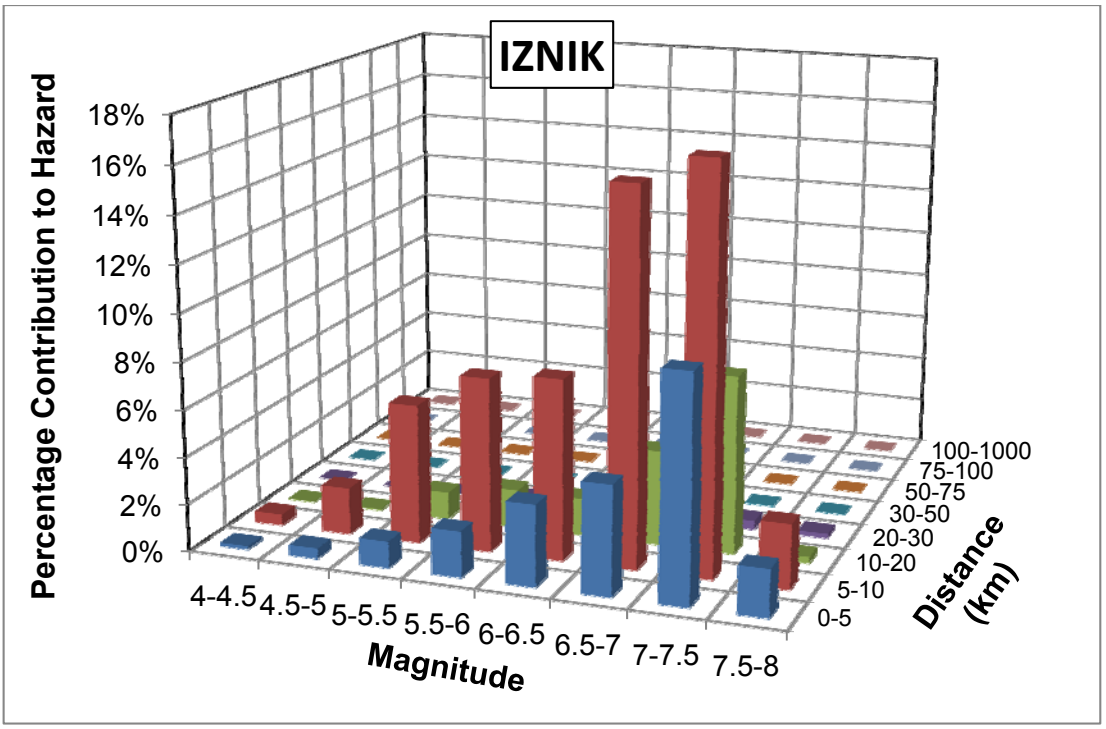

Figure 5.21 Deaggregation for İznik

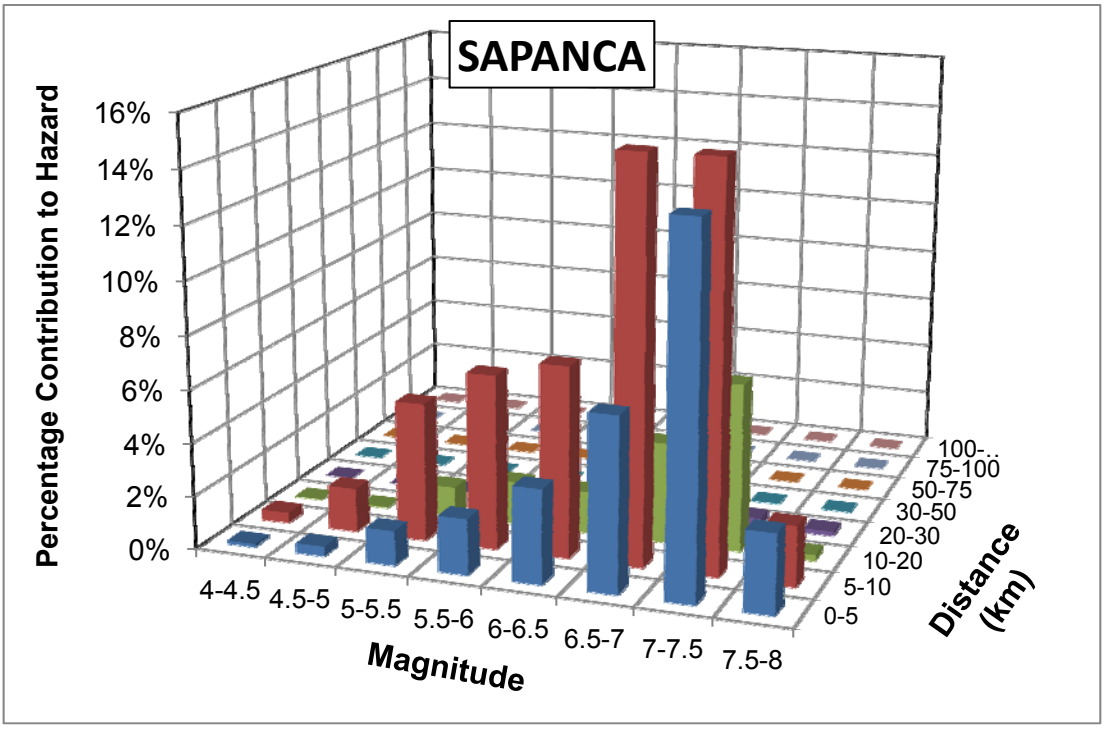

Figure 5.22 Deaggregation for Sapanca

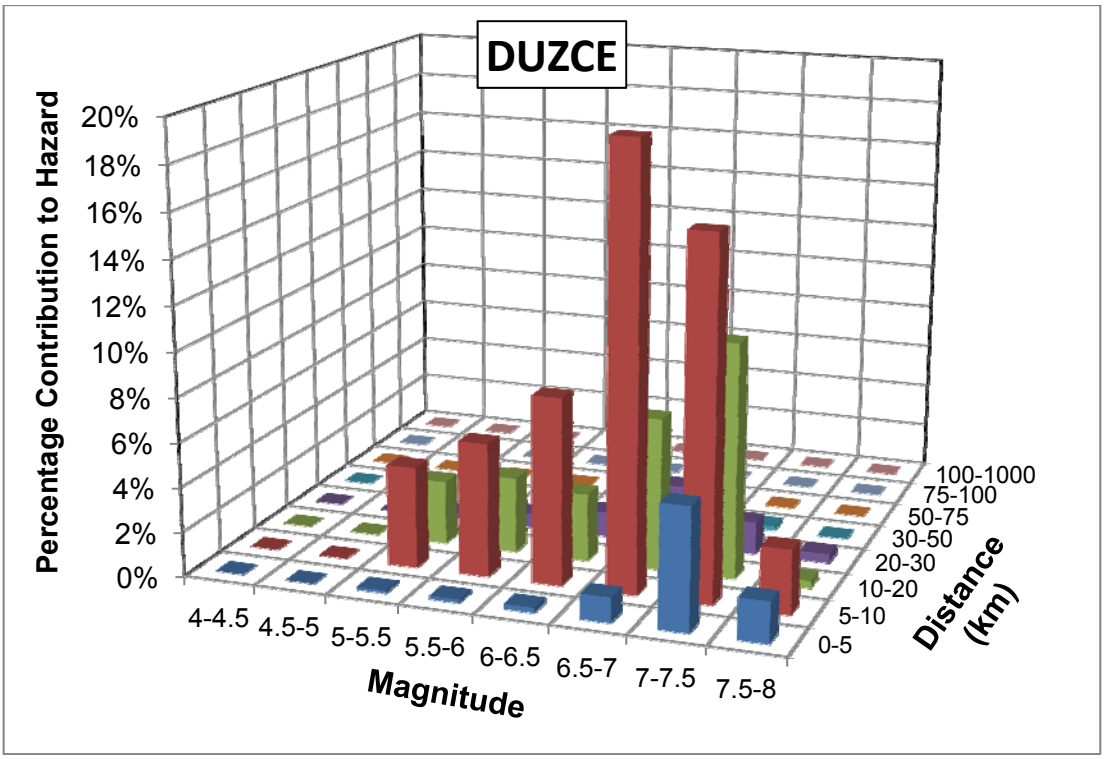

Figure 5.23 Deaggregation for Duzce

For sites close to the NAF_N strand, the hazard is dominated by this source as Figure 5.18 and Figure 5.20 indicate for Adapazarı and İzmit. For both of these sites, the dominating scenario has the magnitude between 6.5 and 7.5 at 5-10 kilometers distance. For Gemlik and İznik, the dominating source becomes Geyve-İznik Fault (red bars in Figure 5.19 and Figure 5.21), however the effect of NAF_N is still present (green bars in Figure 5.19 and Figure 5.21). Similarly, the main contributor to the hazard is Düzce Fault for Düzce (Figure 5.23) but the effect of sources within 10-20 km distance from the site (NAF_N and NAF_S) is also significant. It is difficult to obtain the main contributing source to the hazard from Figure 5.22 for Sapanca but the dominating scenario for Sapanca has a magnitude range of 6.5-7.5 and distance range of 0-10 kilometers.

The hazard curves for Adapazarı are developed using different NGA ground motion models (Abrahamson and Silva (2008), Boore and Atkinson (2008), Chiou and Youngs (2008), Campbell and Bozorgnia (2008), Idriss (2008)) and given in Figure 5.24. Using different attenuation models leads to less than 0.04 g difference in the ground motion for high annual probability of exceedance (0.01 or less) levels, however, the effect of ground motion prediction models increase as the level of annual probability of exceedance decreased. Equal weights are given to each ground motion model in the logic tree to calculate the hazard for all sites.

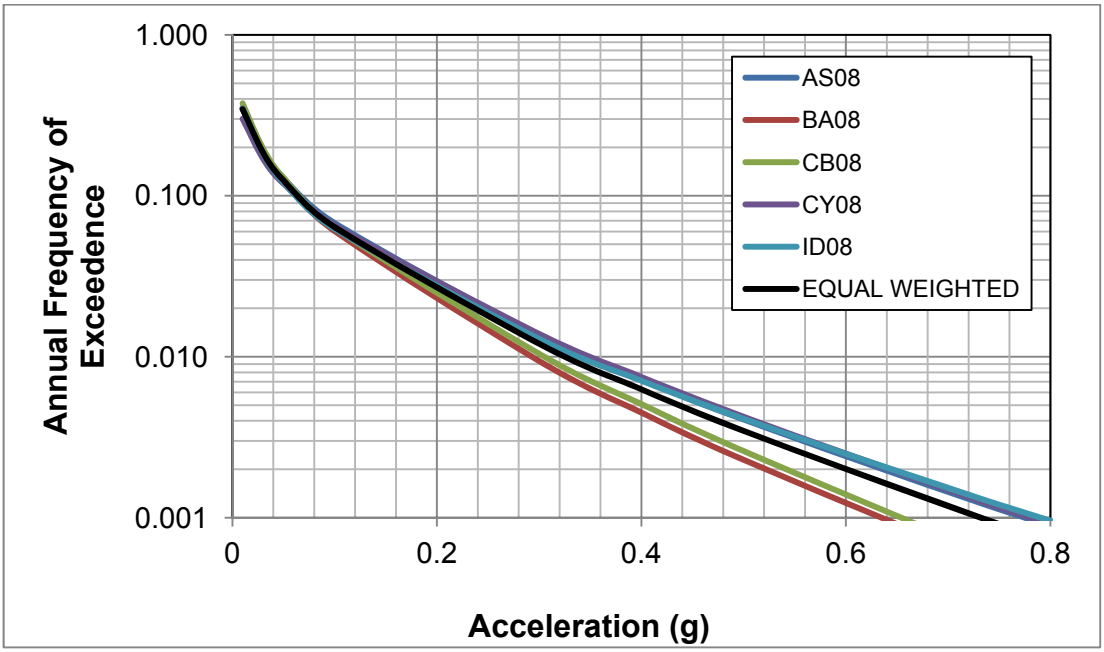

Figure 5.24 Hazard Curves for different Ground Motion Prediction Models for the source of Adapazarı

A common method for developing design spectra based on the probabilistic approach is to use the Uniform Hazard Spectrum (UHS). The UHS is developed by computing the hazard independently at a set of spectral periods and then computing the ground motion for a specified probability

level at each spectral period. The term “uniform hazard spectrum” is used because the spectral acceleration value at each period has an equal chance of being exceeded (Gülerce and Abrahamson, 2011).

The uniform hazard spectra of the selected sites (Adapazarı, Düzce, Gemlik, İzmit, İznik and Sapanca) for rock site conditions (V_{s30}=760 m/s) at 10% probability of exceedance risk level are presented in Figure 5.25 to Figure 5.30. Similarly, the uniform hazard spectra of the selected sites for soil site conditions (V_{s30}=270 m/s) are provided in Figure 5.31 to Figure 5.36. The TEC-2007 design spectrum for rock or soil site condition is plotted with the UHS to allow the comparison of the results with the code specifications. Soil class is selected as Z1 to represent rock site conditions (V_{s30} = 760 m/s) and Z3 to represent the soil site conditions (V_{s30} = 270 m/s) for TEC 2007 design spectrum.

The UHS developed for rock site conditions for all sites, except for Düzce, is significantly higher than the design spectrum between the 0.2-1 second spectral periods (Figure 5.25 to Figure 5.30). Higher ground motion levels would be also observed in Düzce if the Bolu-Gerede segment was added to the hazard calculations. The UHS and the design spectrum are in good agreement for long spectral periods (longer than 1.5 seconds). Similar trends are observed for soil site condition curves however, the differences between the 0.2-1 seconds plateau of the design spectrum and the UHS are smaller compared to the rock site curves for all sites.

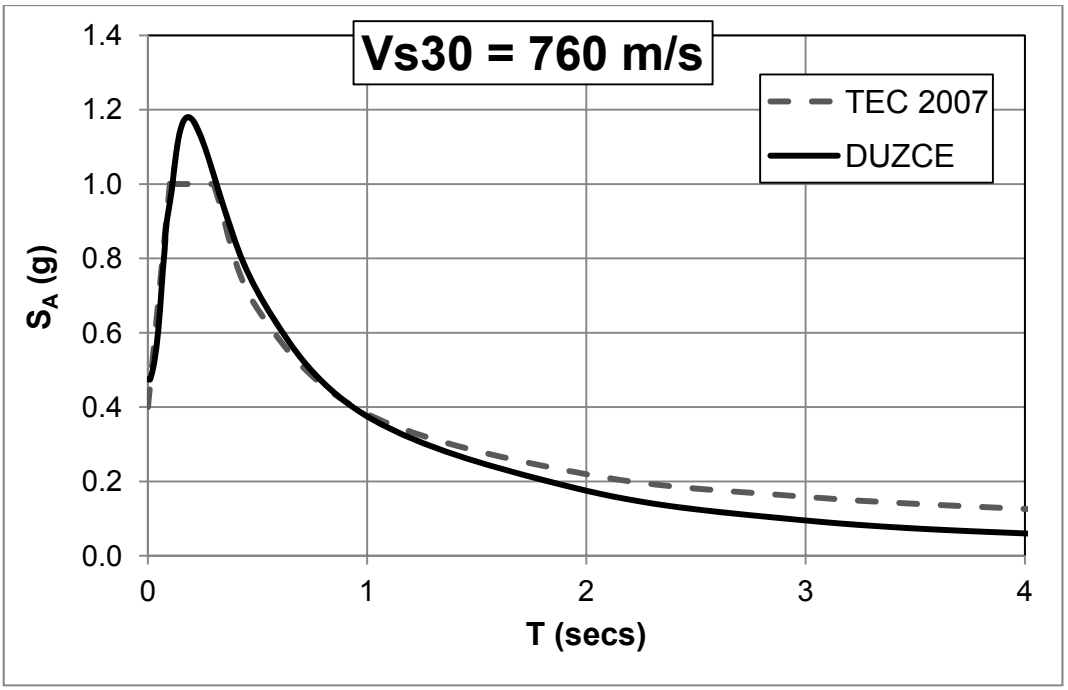

Figure 5.25 Uniform Hazard Spectra for Duzce

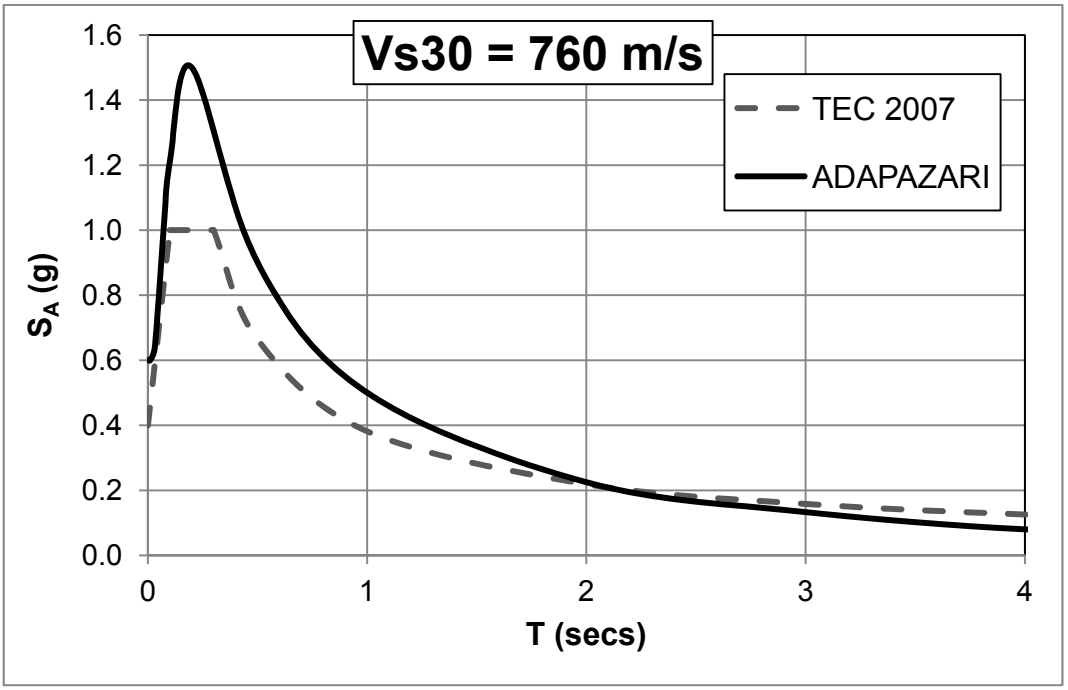

Figure 5.26 Uniform Hazard Spectra for Adapazarı

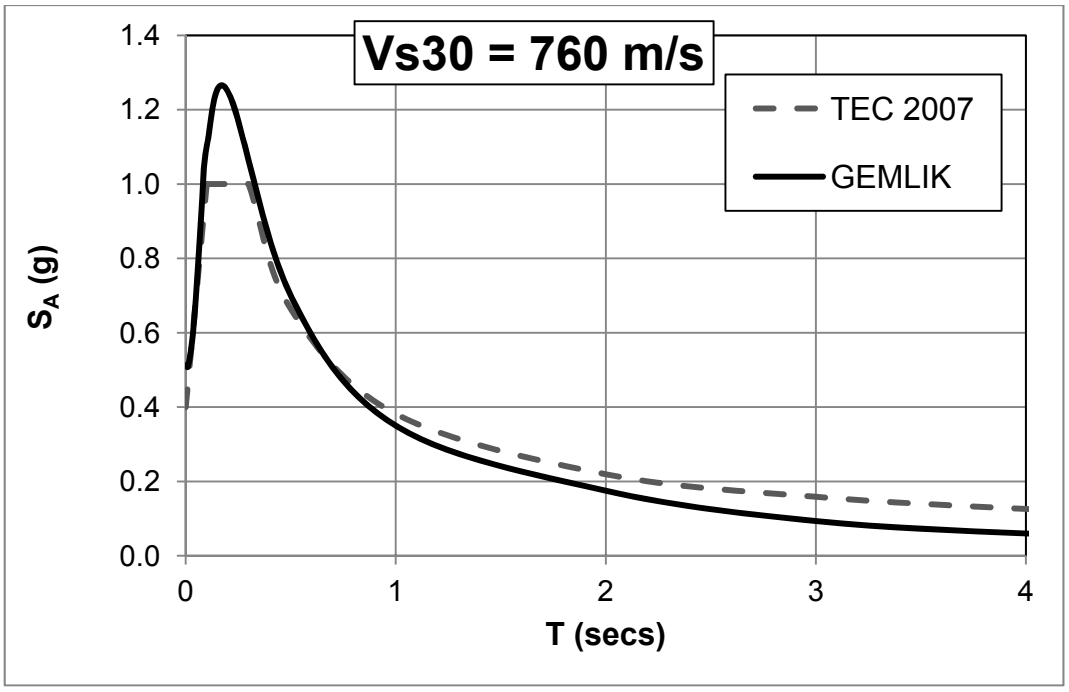

Figure 5.27 Uniform Hazard Spectra for Gemlik

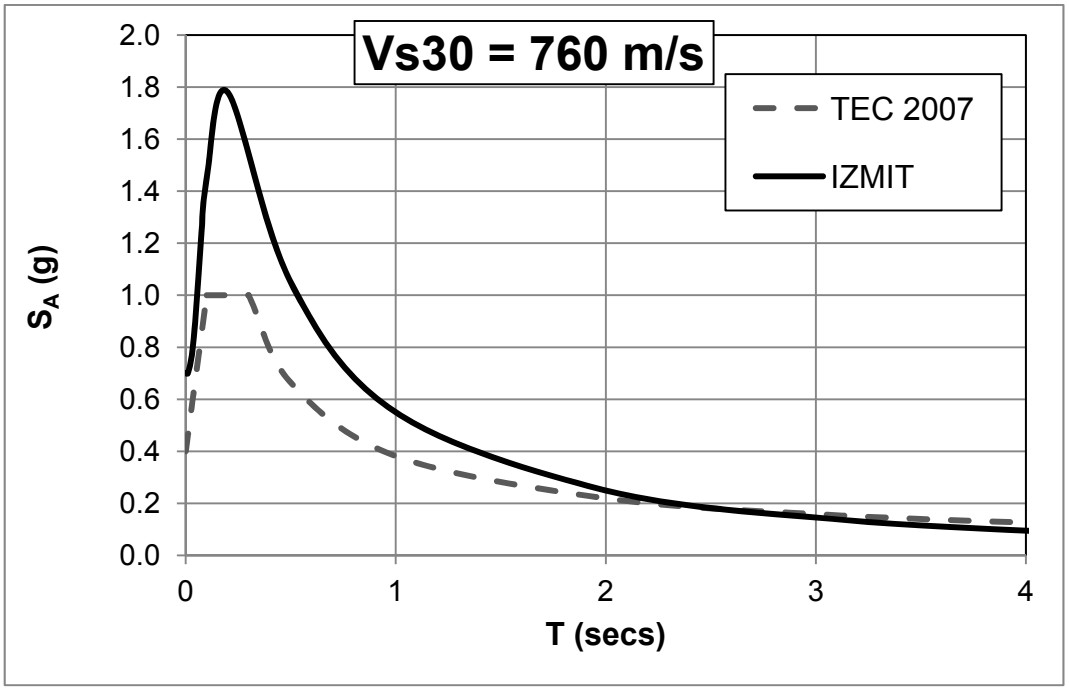

Figure 5.28 Uniform Hazard Spectra for İzmit

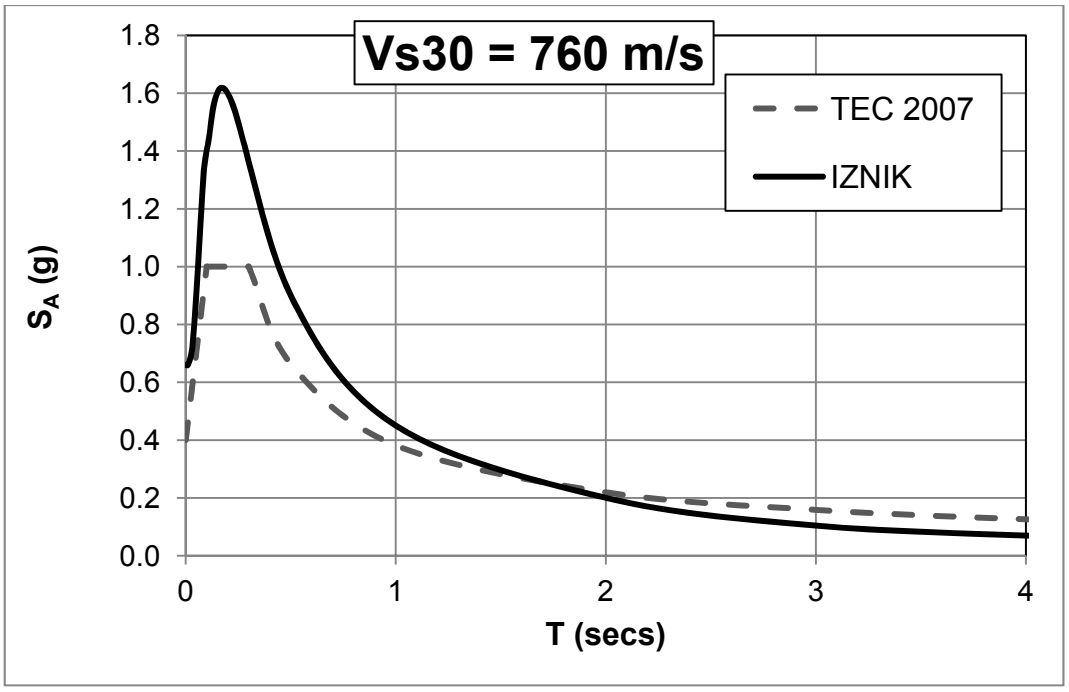

Figure 5.29 Uniform Hazard Spectra for İznik

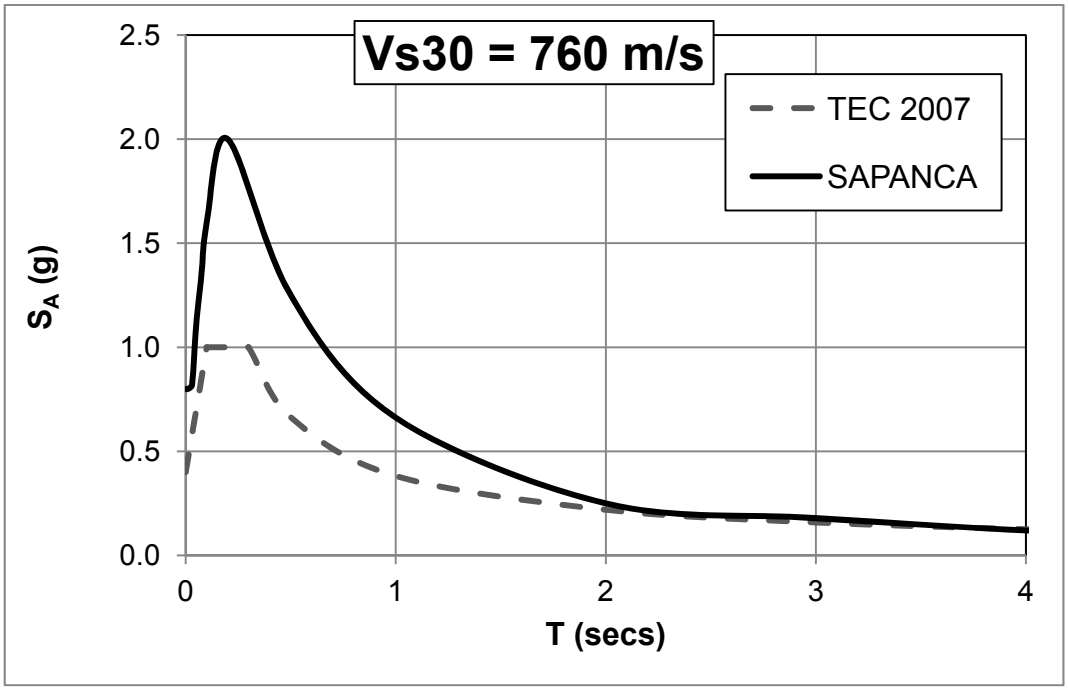

Figure 5.30 Uniform Hazard Spectra for Sapanca

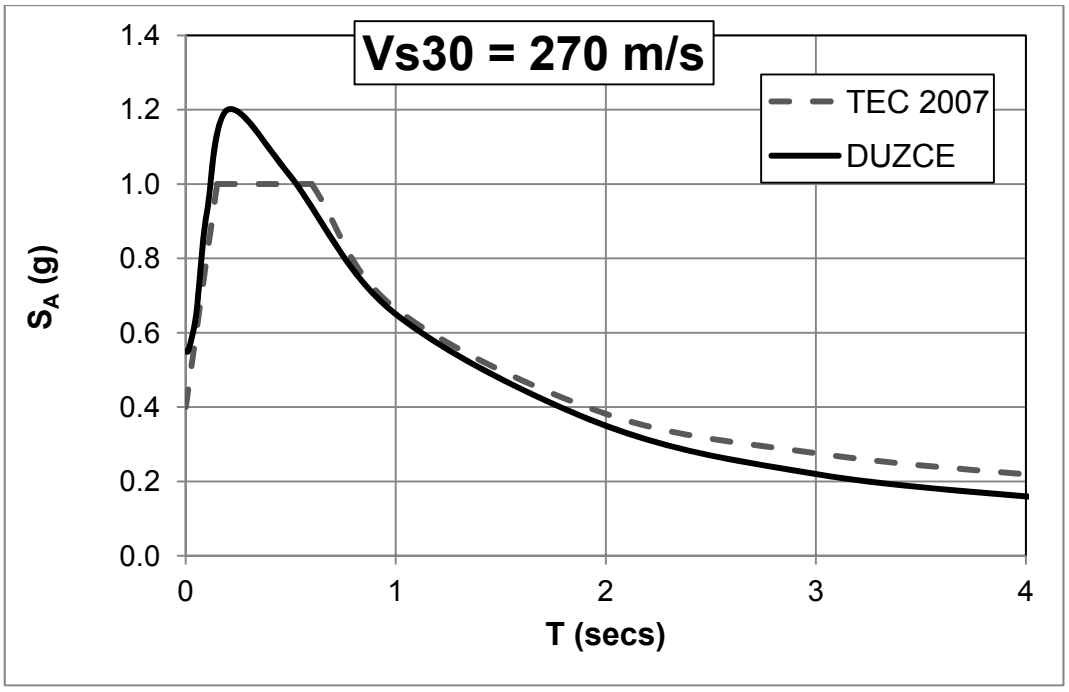

Figure 5.31 Uniform Hazard Spectra for Düzce

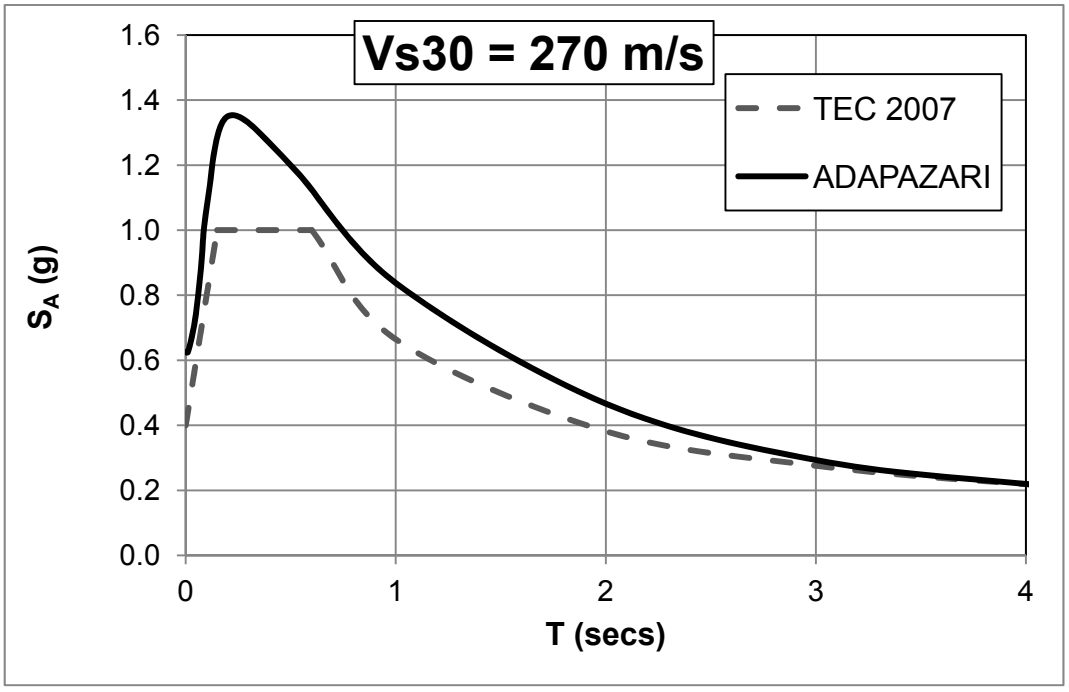

Figure 5.32 Uniform Hazard Spectra for Adapazarı

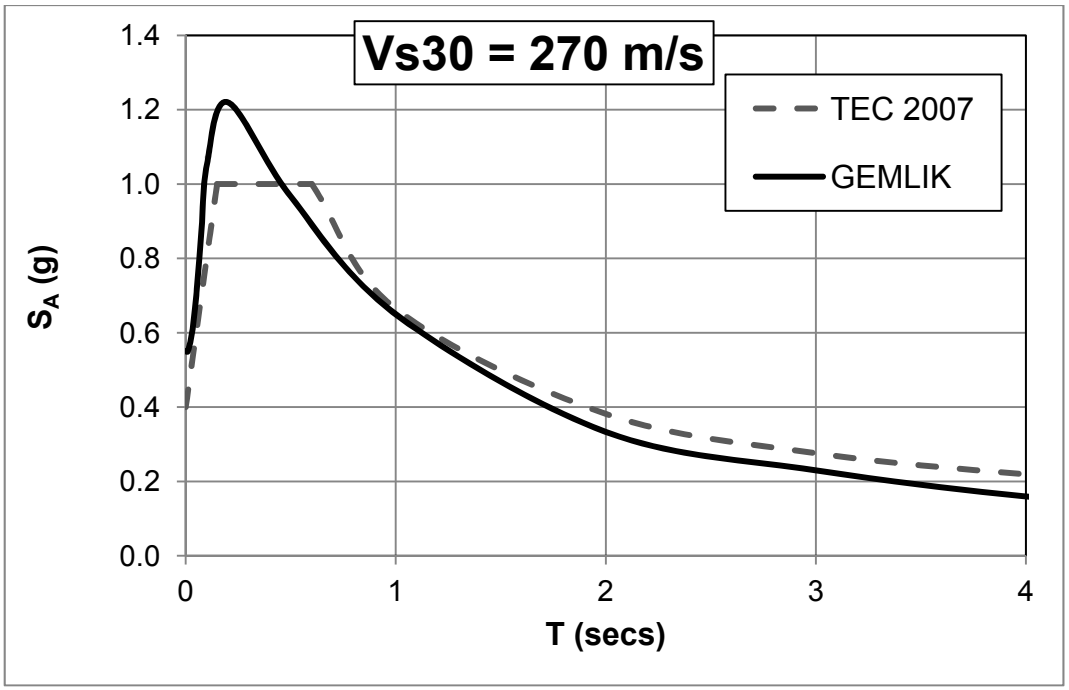

Figure 5.33 Uniform Hazard Spectra for Gemlik

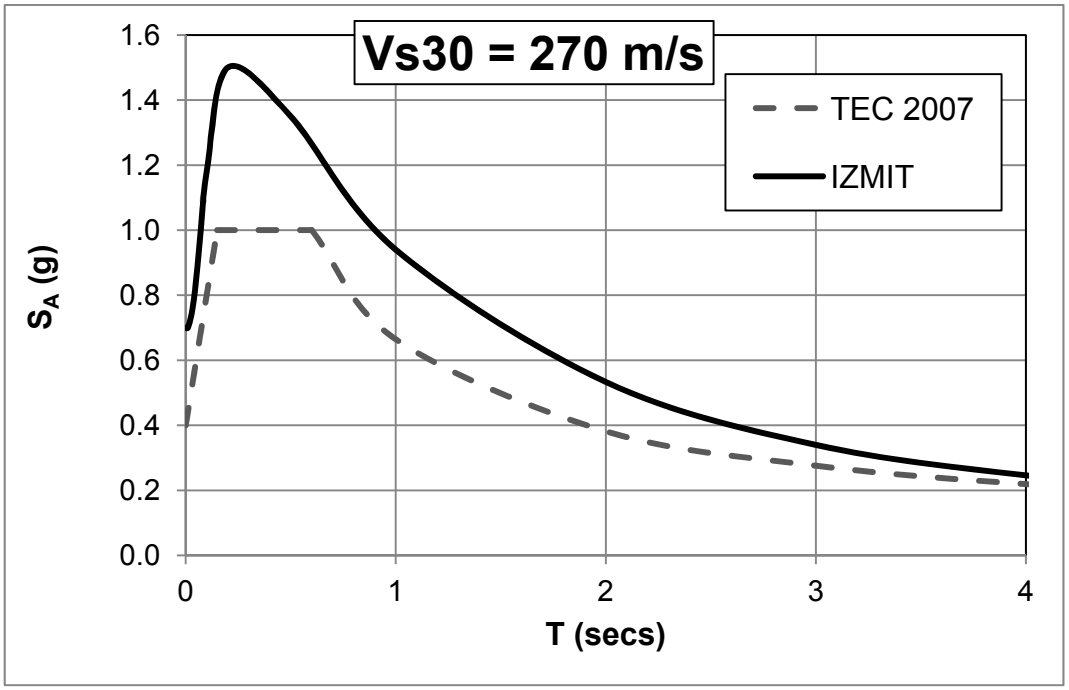

Figure 5.34 Uniform Hazard Spectra for İzmit

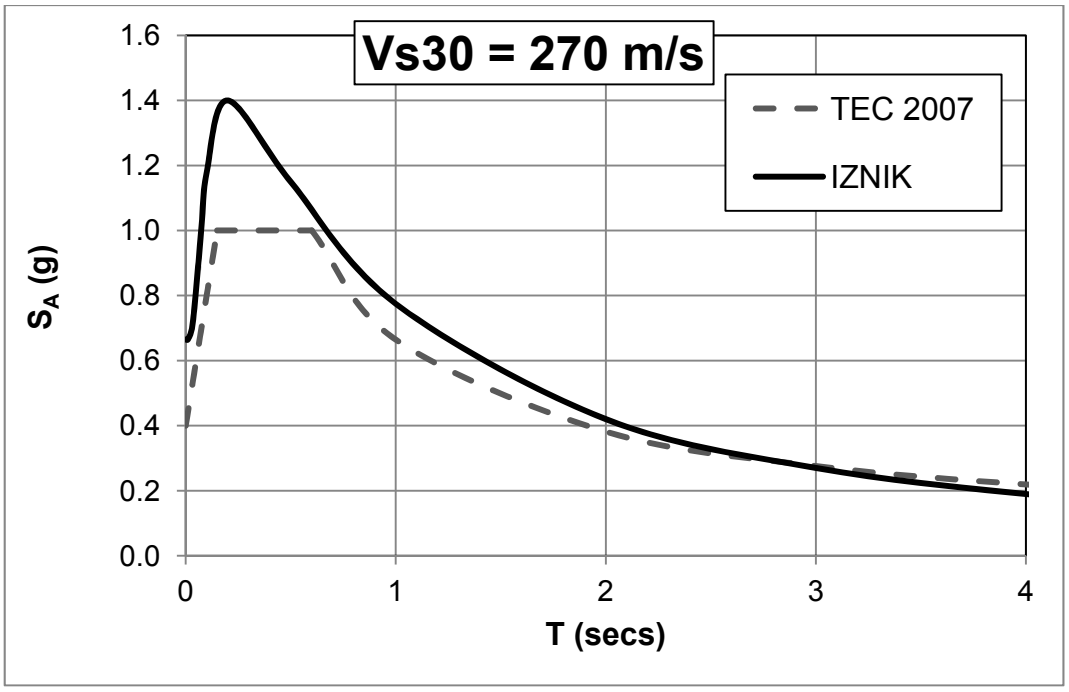

Figure 5.35 Uniform Hazard Spectra for İznik

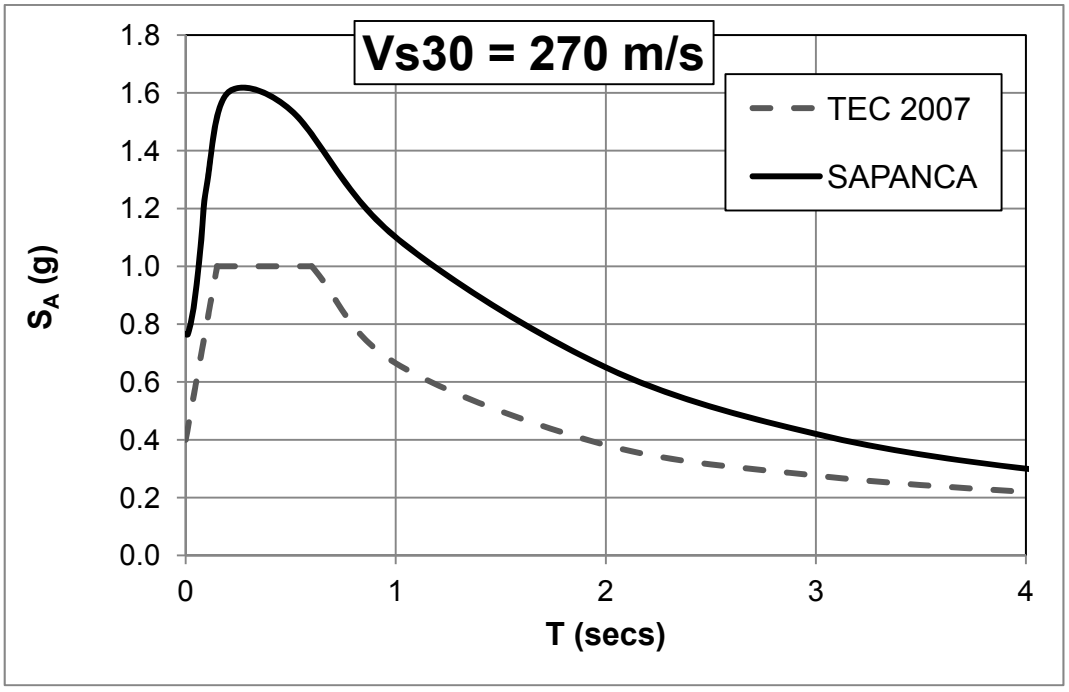

Figure 5.36 Uniform Hazard Spectra for Sapanca

5.3 Hazard Maps for Eastern Marmara Region

The seismic hazard maps for the region are developed for PGA, T=0.2 second and T=1 second spectral periods for the rock site conditions for the acceptable risk levels in Turkish Earthquake Code (2007). For this purpose, 260 grid nodes were defined in the study area (0.1° to 0.1°) as shown in Figure 5.37 and the hazard assessment was performed at each grid node. The density of grids that fall between the faults is increased (0.1° to 0.05°) for more accurate results.

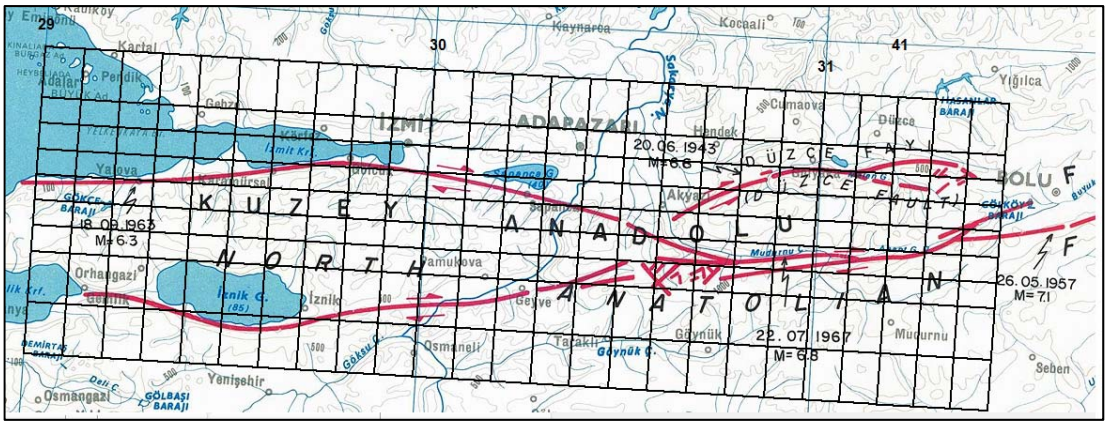

Figure 5.37 Grids assigned to region

The seismic hazard maps for PGA for rock site conditions (Vs30 = 760 m/s) at 2%, 5% and 10% level of exceedance at 50 years are provided in Figure 5.38 to Figure 5.40. Generally, the contours of the maps follow the fault lines as expected. Hazard levels increase at the intersection points of the seismic sources and at the defined segmentation points on the faults. The highest value of PGA is around 1.7g for 2475 years return period and smaller than 1.0g for 72 years return period. The seismic hazard maps for 0.2 and 1 seconds spectral periods for rock site conditions (Vs30 = 760 m/s) at 2%, 5% and 10% level of exceedance at 50 years are provided in Figure 5.41 to

Figure 5.44. High spectral accelerations at 0.2 second spectral period were observed at high return periods for sites very close to the active faults. Detailed discussion on these results is provided in Chapter 6.

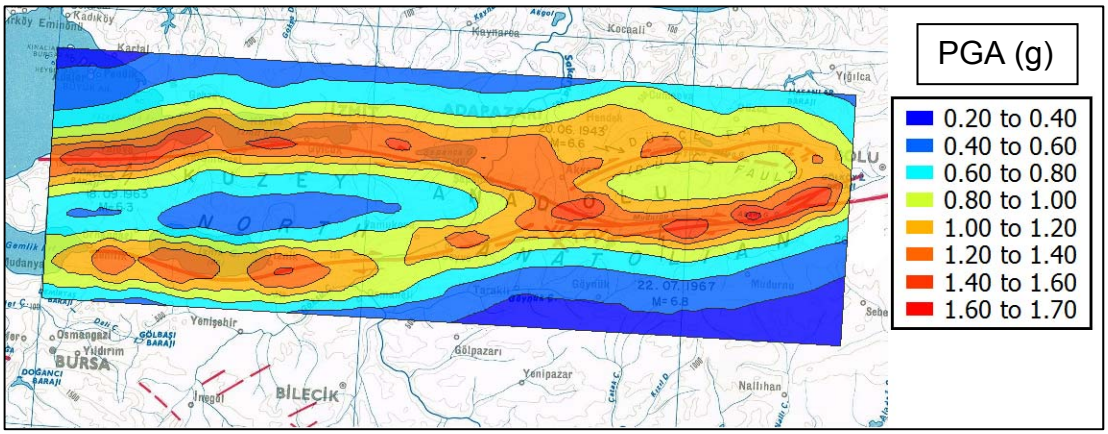

Figure 5.38 Hazard Map for PGA for a hazard level of 2% probability of exceedence in 50 years (g)

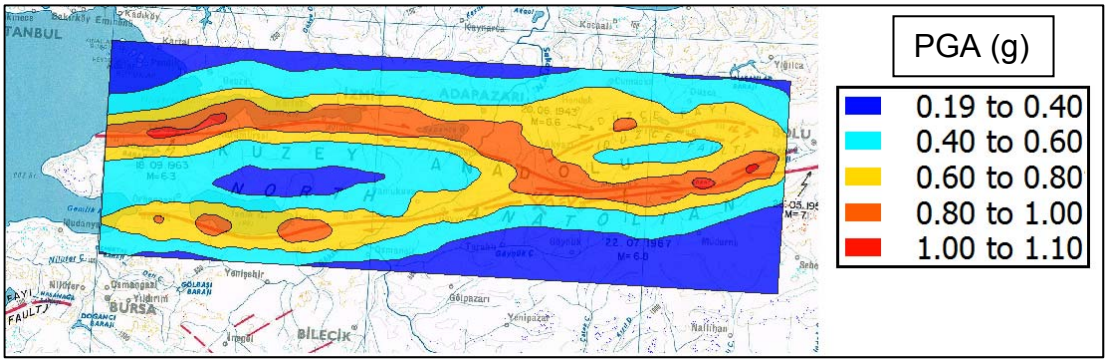

Figure 5.39 Hazard Map for PGA for a hazard level of 10% probability of exceedence in 50 years (g)

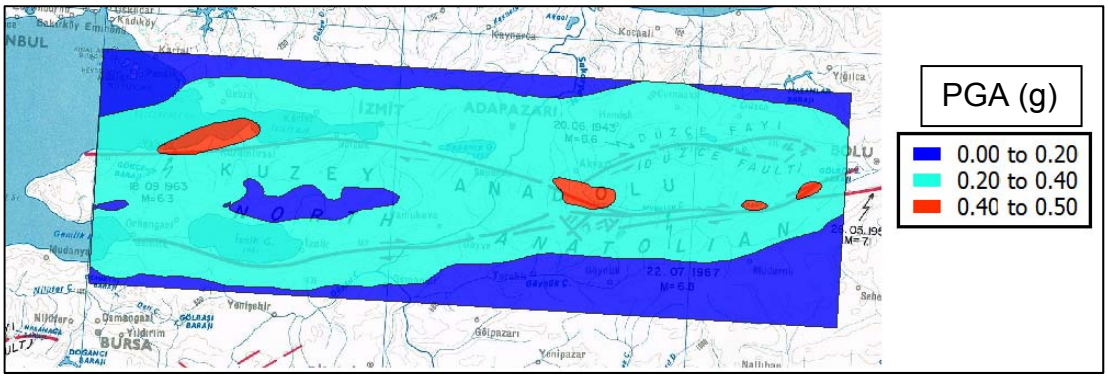

Figure 5.40 Hazard Map for PGA for a hazard level of 50% probability of exceedence in 50 years (g)

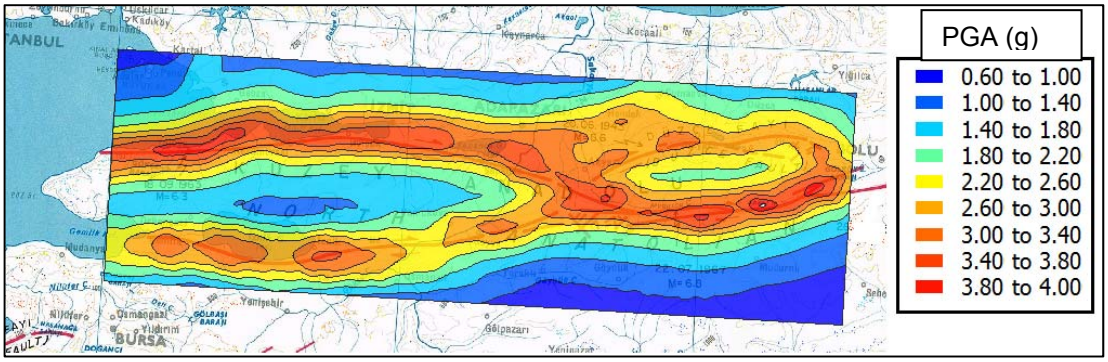

Figure 5.41 Hazard Map for T=0.2 secs for a hazard level of 2% probability of exceedence in 50 years (g)

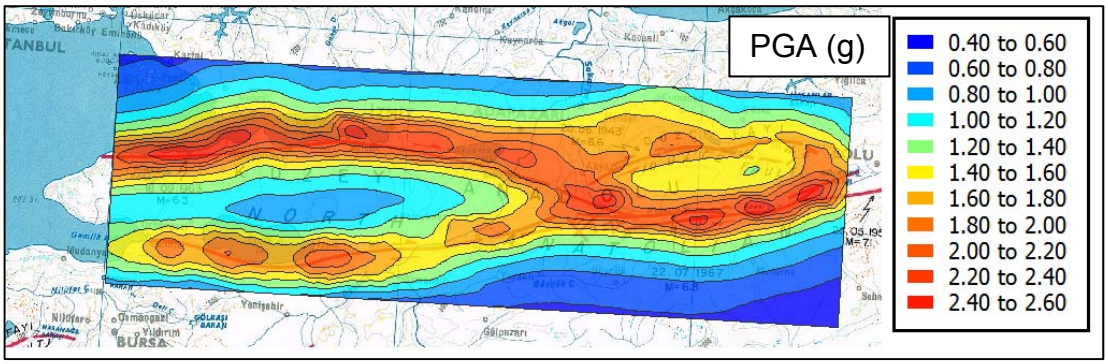

Figure 5.42 Hazard Map for T=0.2 secs for a hazard level of 10% probability of exceedence in 50 years (g)

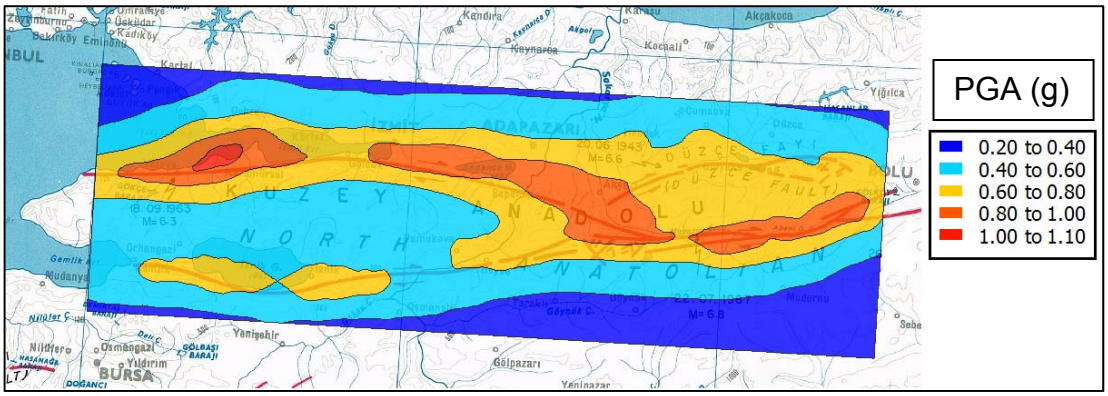

Figure 5.43 Hazard Map for T=0.2 secs for a hazard level of 50% probability of exceedence in 50 years (g)

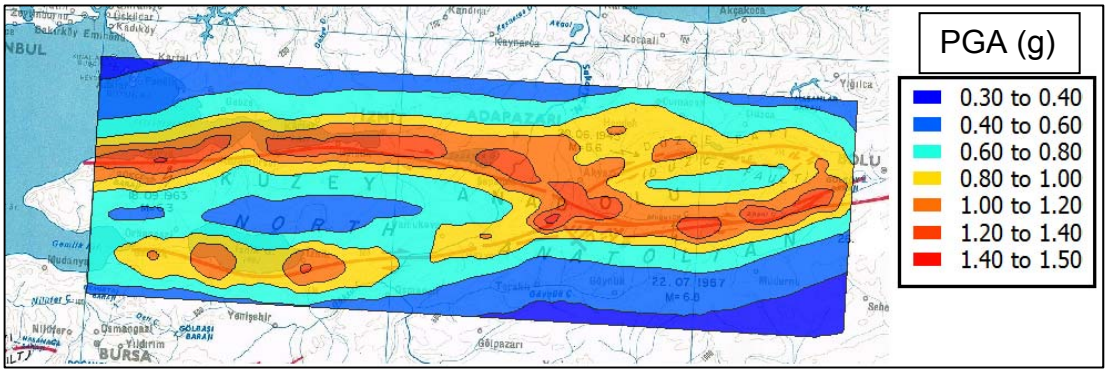

Figure 5.44 Hazard Map for T=1.0 secs for a hazard level of 2% probability of exceedence in 50 years (g)

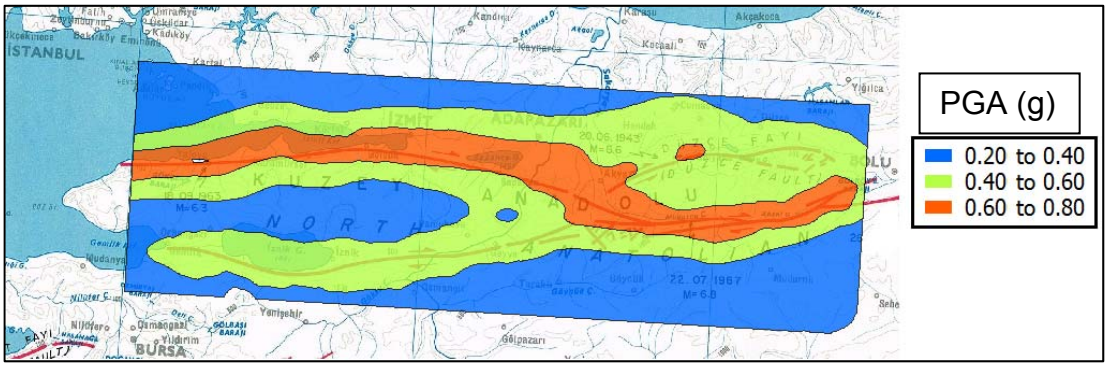

Figure 5.45 Hazard Map for T=1.0 secs for a hazard level of 10% probability of exceedence in 50 years (g)

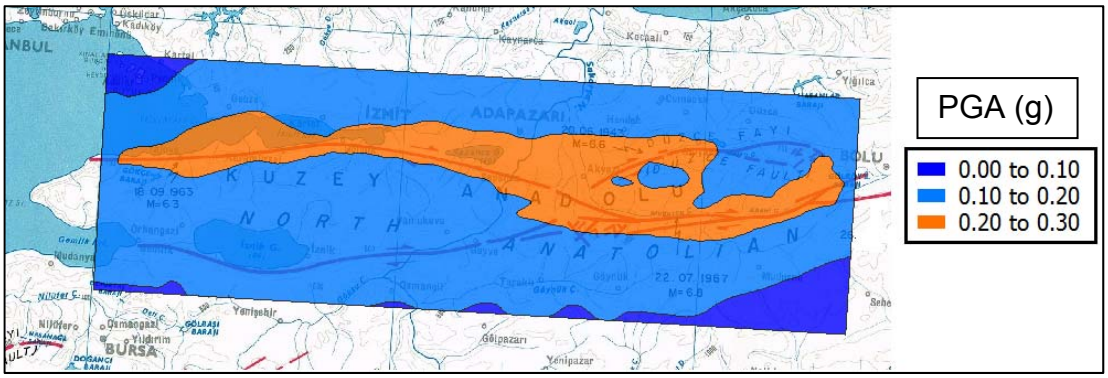

Figure 5.46 Hazard Map for T=1.0 secs for a hazard level of 50% probability of exceedence in 50 years (g)

CHAPTER 6

SUMMARY AND CONCLUSION

The formation of the Anatolia is shaped up by the tectonic interaction between African, Arabian and Eurasian plates, and this interaction results in seismic activity of the faults that exist in Turkey. As the interaction between the plates continues which means permanent seismic activity in Turkey, special care must be taken to reduce the hazard caused by earthquakes since earthquakes have been accepted as one of the most important hazard affecting the human life and structures.

In this study the seismic hazard assessment of Eastern Marmara Region is performed. For performing the hazard analysis probabilistic methodology is followed. The main components of the probabilistic seismic hazard framework are the seismic source characterization and the ground motion prediction models. The total seismic hazard calculated for a site is quite sensitive to the parameters of these models thus; proper modeling of the seismic sources and selecting suitable and unbiased ground motion models will reduce the uncertainty in the hazard significantly.

The improved source geometry model that includes the exact locations of the sources is generated by Cambazoğlu (2011) using satellite images and available fault maps, and with the help of this information linear fault sources are defined for the seismic sources in this study. Four linear faults sources are identified; North Anatolian Fault Northern Strand (NAF_N), North Anatolian Fault Southern Strand (NAF_S), Düzce Fault, and Geyve-Iznik Fault.

Segmentation points delineated by Cambazoglu (2011) are used to define the segments, seismic sources and rupture scenarios consistent with the definition of USGS Working Group of Earthquake Probabilities (2003). A full rupture model is developed for each source considering single- and multi-segment ruptures. The recurrence of earthquakes is modeled with Youngs and Coppersmith (1985) Composite Model for North Anatolian Fault Northern Strand (NAF_N), North Anatolian Fault Southern Strand (NAF_S), and Düzce Fault. The key feature of this model is; 94% of the seismic moment is released by the characteristic earthquakes, and the rest of the total seismic moment is released by the smaller size earthquakes due to the constraints of the distribution equation. Only for Geyve-Iznik fault, the composite model is modified to represent the weak seismicity of the source by modifying the model parameter ΔM1.

The recurrence models for each source are bounded by minimum and maximum magnitudes. The minimum magnitude is selected as 5.0 considering the engineering interest except Geyve – İznik fault. Due to historical seismicity of Geyve and İznik fault, minimum magnitude is selected as 4.0. The maximum magnitude of Youngs and Coppersmith (1985) characteristic model is estimated by adding 0.25 to the characteristic magnitude calculated by rupture area – magnitude relations proposed by Wells and Coppersmith (1994).

The recurrence parameter b-value is found as 0.75 using maximum likelihood approach and considering the time intervals at which the catalogue is complete. The b-values used by the previous studies in the literature are in good agreement with the value estimated in this study.

Activity rates for each source are also defined for source characterization of the region. The basic parameter to be defined for estimating activity rate is annual slip rate of each source. Total slip of 25 mm/year is distributed to parallel faults with the help of GPS measurements and field research performed for the region (McClusky et al., 2000, Reilinger et al., 2000). With

the help of the geological information (rupture area and slip rate) and historical seismicity (which is provided by Cambazoglu, 2011) weights are assigned to individual and multi-rupture scenarios defined by the segments of the sources defined in the source model.

As indicated the ground motion prediction equations (GMPEs) are used to estimate the strong ground motion due to the earthquake scenarios from each source in terms of source (magnitude, depth, style-of faulting, etc.), path (distance, etc.) and site (site conditions, basin effects, etc.) parameters. Ground motion prediction models introduce the biggest uncertainty in the hazard calculations. In this study the global NGA (2008) models are used since they are based on large databases which decrease the epistemic uncertainty in the models. Also the generation of the NGA (2008) models is based on a methodology, GMRotI50 by which the uncertainty due to the orientation of sensors is taken into account. The applicability of the models to the region is checked by comparison with the Turkish Database. Since the ground motion prediction models are log - normally distributed, the natural logarithms of the residuals are examined in terms of magnitude, distance and soil conditions (Vs30).

The distribution of residuals is unbiased within the magnitude range at which the NGA models are considered to be available since no trend is observed along the zero line. However, the predictions are consistently higher than the actual values. Similarly, the distributions of residuals with respect to Vs30 are balanced along the zero line, again with small overestimate of the actual data by NGA models. However, a trend is observed in the distribution of residuals with respect to distance (especially in short distances) in each model indicating the differences in regional attenuation characteristics. The variables in the distance scaling of each model should be modified to fix the trend; however, it is out of the scope of this study. The results of this preliminary analysis indicated that the hazard is slightly overestimated the

especially in the near fault regions. These results may be improved by modifying the distance scaling of the NGA ground motion models.

The hazard curves and uniform hazard spectra for different soil conditions (soil and rock) and for different hazard levels (2%, 10% and 50% probability of exceedence in 50 years) are provided in Chapter 5 for the for six specific locations in the region (Adapazarı, Düzce, Gemlik, İzmit, Iznik and Sapanca). In Turkish Earthquake Code (2007), different design acceleration values are proposed for each earthquake regions and Eastern Marmara region examined in this study is assigned the first earthquake region with a PGA value of 0.4g considering 10% probability of exceedence in 50 years. Also a design spectrum is provided that can be used for different soil site conditions in TEC-2007.

The normalized uniform hazard spectra of the selected sites (Adapazarı, Düzce, Gemlik, İzmit, İznik and Sapanca) for rock site conditions (V_{s30}=760 m/s) at 10% probability of exceedance risk level are presented in Figure 6.1. Similarly, the uniform hazard spectra of the selected sites for soil site conditions (V_{s30}=270 m/s) are provided in Figure 6.2. The TEC-2007 design spectrum for rock or soil site condition is plotted with the UHS to allow the comparison of the results with the code specifications. Soil class is selected as Z1 to represent rock site conditions (V_{s30} = 760 m/s) and Z3 to represent the soil site conditions (V_{s30} = 270 m/s) for TEC 2007 design spectrum. For each location, the spectral acceleration gets its highest value at T = 0.2 second spectral period, and this value is 2.5 times the value obtained at PGA for rock sites (Vs = 760 m/s), but 2.2 times the value obtained at PGA for soil sites (Vs = 270 m/s). Along with these ratios, the width of the peak plateau also changes for different soil classes where a wider plateau is accepted for soil sites. The parameters of this modification are provided in Table 6.1.

In TEC 2007, the ratio of maximum spectral acceleration to PGA is 2.5 regardless of the soil class. The results of this study performed for rock conditions satisfy the ratio of TEC 2007.

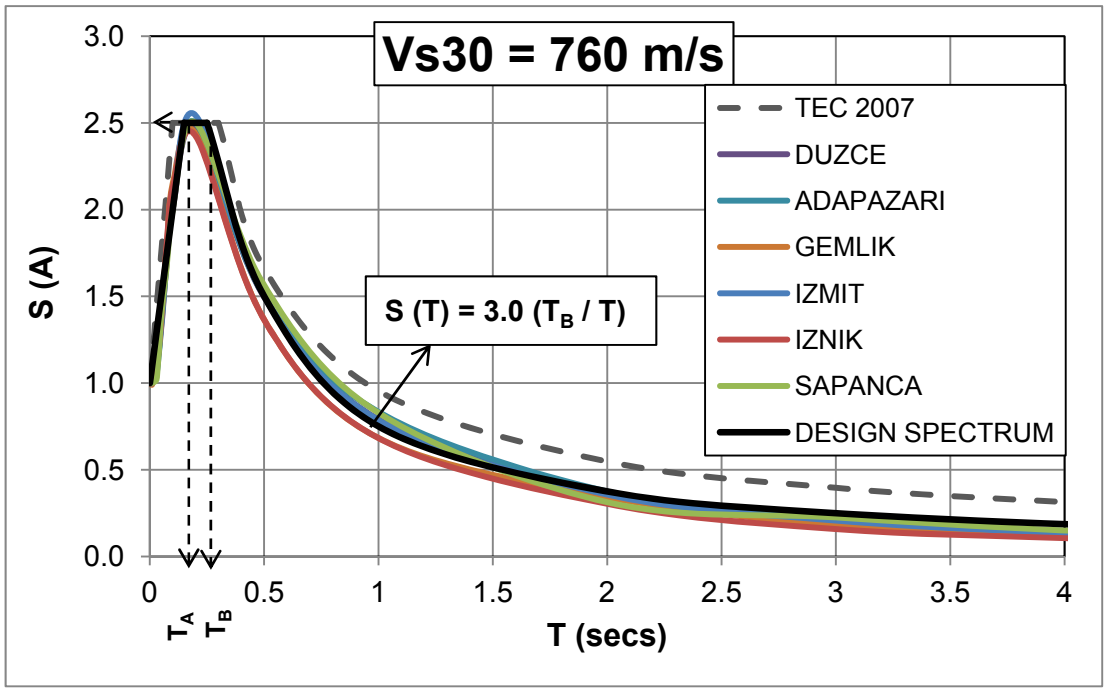

Figure 6.1 Design Spectrum for Rock Sites (Vs30 = 760 m/s)

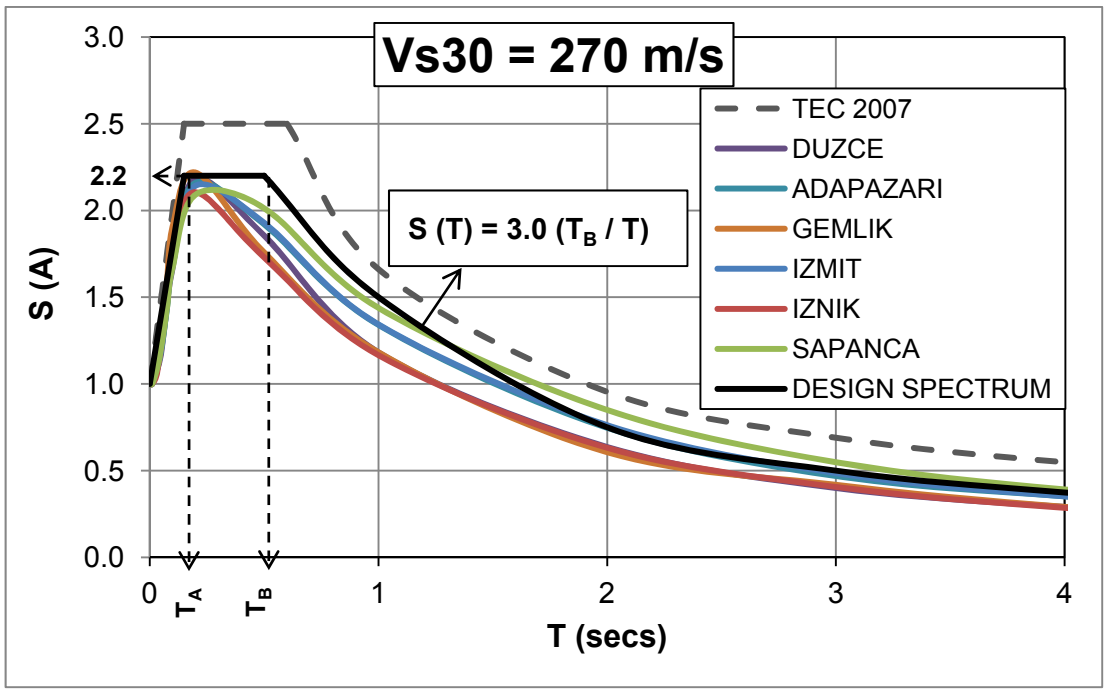

Figure 6.2 Design Spectrum for Soil Sites (Vs30 = 270 m/s)

The seismic hazard maps for the region are developed for PGA, T=0.2 second and T=1 second spectral periods for the rock site conditions for the acceptable risk levels in TEC-2007. Generally, the contours of the maps follow the fault lines as expected. Hazard levels increase at the intersection points of the seismic sources and at the defined segmentation points on the faults. The highest value of PGA is around 1.7g for 2475 years return period and smaller than 1.0g for 72 years return period. High spectral accelerations at 0.2 second spectral period were observed at high return periods for sites very close to the active faults.

The uncertainty level assigned to the ground motions for this study is median± 3σ as the new seismic hazard practice command which is significantly higher than the uncertainty level in TEC-2007. A part of a possible overestimation of the hazard comes from the ground motion prediction equations used in the analysis, especially for near fault sites.

The results of the study will provide a basis for seismic design of special structures in the area. Hazard maps of the region for rock site conditions at the accepted levels of risk by TEC-2007 may be used to perform site-specific hazard assessment for local site conditions and develop site-specific design spectrum. These results may be improved by assessing the contribution of seismic sources outside the study area and modification of the ground motion model variables for seismo-tectonics properties of the region.

Table 6.1 Parameters for Design Spectra

SOIL TYPE	T_A	T_B
ROCK	0.15	0.25
SOIL	0.15	0.50

REFERENCES

Abrahamson, N. A. (2000) State of The Practice of Seismic Hazard Evaluation

Abrahamson, N.A. (2006) Seismic Hazard Assessment: Problems With Current Practice And Future Developments, First European Conference on Earthquake Engineering and Seismology (a joint event of the 13th ECEE & 30th General Assembly of the ESC) Geneva, Switzerland, 3-8 September 2006

Abrahamson, N. A. and Silva, W. (2008) Summary of the Abrahamson & Silva NGA Ground-Motion Relations, Earthquake Spectra, Volume 24, No. 1, 67 – 97.

Aki, K. (1965). Maximum likelihood estimate of b in the formula log N = a - bM and its confidence limits, Bull. Earthquake Res. Inst., Tokyo Univ. 43, 237-239.

Akkar,S. and Cagnan,Z. (2010) A local ground-motion predictive model for Turkey and its comparison with other regional and global ground-motion models

Akyüz, H.S., Hartleb, R., Barka, A., Altunel, E., Sunal, G., Meyer, B. and Armijo, R. (2002). Surface Rupture and Slip Distribution of the 12 November 1999 Duzce Earthquake (*M* 7.1), North Anatolian Fault, Bolu, Turkey, Bull. Seism. Soc. Am. 92, no. 1, 61-66.

Ambraseys, N. N. (1970). Some characteristic features of the Anatolian fault zone, Tectonophysics 9, 143–165.

Armijo, R., Meyer, B., Hubert, A., Barka, A. (1999) Westward propogation of the North Anatolian fault into the nothern Aegean: Timing and kinematics, Geology, vol. 27,no. 3, 267-270.

Atakan, K., A. Ojeda, M. Meghraoui, A. A. Barka, M. Erdik, and A. Bodare (2002). Seismic hazard in Istanbul following the 17 August 1999 Izmit and 12 November 1999 Düzce earthquakes, Bull. Seismol. Soc. Am. 92, no. 1, 466–482.

Ayhan, M.A., Demir, C., Kilicoglu, A., Sanli, I., Nakiboglu, S.M. (1999). Crustal motion around the western segment of the north Anatolian fault zone: geodetic measurements and geophysical interpretation. Abstr. Int. Union Geod. Geophy. 99, 77–78.

Ayhan, M.E., Bürgmann, R., McClusky, S., Lenk, O., Aktug, B., Herece, E., Reilinger, R.E. (2001). Kinematics of the Mw=7.2, 12 November 1999, Düzce, Turkey earthquake. Geophys. Res. Lett. 28 (2), 367–370.

Barka, A. A. (1996), Slip distribution along the North Anatolian fault associated with large earthquakes of the period 1939 to 1967, Bull. Seismol. Soc. Am., 86, 1234–1238.

Barka, A. A., et al. (2002), The surface rupture and slip distribution of the 17 August 1999 Izmit earthquake (M 7.4), North Anatolian Fault, Bull. Seismol. Soc. Am., 92, 43– 60.

Bazzurro, P. and Cornell, C. A. (1999) Disaggregation of Seismic Hazard, Bull. Seism. Soc. Am. 89, no. 2, 501–520.

Bender, B. (1983) Maximum Likelihood Estimation Of b Values For Magnitude Grouped Data, Bull. Seism. Soc. Am. 73, no. 3, 831–851.

Boore, D. M., Lamprey, J. W., Abrahamson, N. A. (2006) Orientation-Independent Measures of Ground Motion, Bull. Seism. Soc. Am. 96, no. 4A, 1502 - 1511.

Boore, D. M., Atkinson, G. M. (2008) Ground-Motion Prediction Equations for the Average Horizontal Component of PGA, PGV, and 5%-Damped PSA at Spectral Periods between 0.01 s and 10.0 s, Earthquake Spectra, Volume 24, No. 1, 99 – 138.

Cambazoglu, S., “Preperation of a Source Model for the Adapazarı Region Along the North Anatolian Fault Segments,” Master Thesis, Geological Eng. Program, Middle East Technical University, Ankara, Turkey, expected to be completed in December 2011.

Campbell, K. W. and Bozorgnia, Y. (2008) NGA Ground Motion Model for the Geometric Mean Horizontal Component of PGA, PGV, PGD and 5% Damped Linear Elastic Response Spectra for Periods Ranging from 0.01 to 10 s, Earthquake Spectra, Volume 24, No. 1, 139 – 171.

Chiou, B. Darragh, R., Gregor, N. and Silva, W. (2008) NGA Project Strong-Motion Database, Earthquake Spectra, Volume 24, No. 1, 23 – 44.

Chiou, B. S. J. and Youngs, R. R. (2008) An NGA Model for the Average Horizontal Component of Peak Ground Motion and Response Spectra, Earthquake Spectra, Volume 24, No. 1, 173 – 215.

Cornell, C. A. (1968) Engineering siemsic risk analysis, Bull. Seism. Soc. Am., 58, 1583-1606. Erratum: 59, 1733.

Crowley, H., and J. J. Bommer (2006). Modeling seismic hazard in earthquake loss models with spatially distributed exposure, Bull. Eq. Eng. 4, 249–273

Earthquake Engineering Research Center METU, (2009) Turkish Strong Ground Motion Database

Erdik, M., M. Demircioğlu, K. Şeşetyan, E. Durukal, and B. Siyahi (2004). Earthquake hazard in Marmara region, Turkey, Soil Dyn. Earthq. Eng. 24, 605–631.

Gülerce, Z. and Abrahamson, N. A. (2010) Vector-valued Probabilistic Seismic Hazard Assessment for the Effects of Vertical Ground Motions on the Seismic Response of Highway Bridges, Earthquake Spectra, Volume 26, No. 4, 999 – 1016.

Harris, R.A., Dolan, J. F., Hartleb, R. and Day, S. M. (2002), The 1999 Izmit, Turkey, Earthquake: A 3D Dynamic Stress Transfer Model of Intraearthquake Triggering, Bull. Seismol. Soc. Am. 92, no. 1, 245–255.

Idriss I. M. (2008) An NGA Empirical Model for Estimating the Horizontal Spectral Values Generated By Shallow Crustal Earthquakes, Earthquake Spectra, Volume 24, No. 1, 217 – 242.

Kalkan, E. and Gülkan, P. (2004) Site-Dependent Spectra Derived from Ground Motion Records in Turkey, Earthquake Spectra, Volume 20, No. 4, 1111 – 1138.

Kalkan, E., Gülkan P., Yilmaz N. and Çelebi M. (2009). Reassessment of Probabilistic Seismic Hazard in the Marmara Region, Bull. Seismol. Soc. Am. 99, no. 4, 2127-2146.

Kandilli Observatory, Boğaziçi University (http://www.koeri.boun.edu.tr/sismo/Mudim/katalog.asp, last accessed November, 2011)

Kargıoglu, B., “Applicability of Next Generation Attenuation Models in Probabilistic Seismic Hazard Assessment Studies Performed in Turkey,” Master Thesis, Civil Eng. Program, Middle East Technical University, Ankara, Turkey, expected to be completed in March 2012.

Kramer, S. L., Geotechnical Earthquake Engineering, Prentice Hall, 1996

Langridge, R. M., H. D. Stenner, T. E. Fumal, S. A. Christofferson, T. K. Rockwell, R. D. Hartleb, J. Bachhuber, and A. A. Barka (2002). Geometry, slip distribution, and kinematics of surface rupture on the Sakarya fault segment during the 17 August 1999 Izmit, Turkey, Bull. Seism. Soc. Am. 92, no. 1, 107–125.

McClusky, S.27 coauthors (2000). Global Positioning System constraintson plate kinematics and dynamics in the eastern Mediterranean and Caucasus, J. Geophys. Res. 105, 5695–5719.

Ministry of Publicworks & Settlement, (2007). Turkish Earthquake Resistant Design Code - TEDRC, Ankara, Turkey.

Nigam, N. C. and Jennings, P. C. (1969) Calculation Of Response Spectra From Strong-Motion Earthquake Records, Bull. Seism. Soc. Am. 59, no. 2, 909–929.

Özbey et al.(2003) An empirical attenuation relationship for Northwestern Turkey ground motion using a random effects approach, Soil Dynamics And Earthquake Engineering, No. 24, 115-125

Parsons, T. (2004). Recalculated probability of M ≥ 7 earthquakes beneath the Marmara Sea, Turkey, J. Geophys. Res. 109, B05304, 1–21.

Power,M., et al. (2008) An Overview of the NGA Project, Earthquake Spectra, Volume 24, No. 1, 3 – 21.

Reilinger, R. E., et al. (2000), Coseismic and postseismic fault slip for the 17 August, M = 7.5, Izmit, Turkey earthquake, Science, 289, 1519– 1524.

Schwartz, D. P. and K. J. Coppersmith (1984). Fault behavior and characteristic earthquakes: examples from the Wasatch and San Andreas faults, J. Geophys. Res. 89, 5681-5698

Stein, R. S., Barka, A. A. and Dieterich, J. H. (1997), Progressive failure on the North Anatolian fault since 1939 by earthquake stress triggering, Geophys. J. Int., 128, 594– 604.

Stepp, J.C. (1972). Analysis of completeness of the earthquake sample in the Puget Sound area and its effects on statistical estimates of earthquake hazard, Proc. Microzonation Conf., Seattle, WA, 897- 909.

Thomas,P., Wang, I. and Abrahamson, N. A. (2010), HAZ38, Verification of Probabilistic Seismic Hazard Analysis Computer Programs, Pacific Earthquake Engineering Research Center,, No. 106, May 2010.

Weichert, D. H. (1980), Estimation Of The Earthquake Recurrence Parameters For Unequal Observation Periods For Different Magnitudes, Bull. Seismol. Soc. Am. 70, no. 4, 1337–1346.

Wells, D. L., and K. J. Coppersmith (1994). New empirical relationships among magnitude, rupture length, rupture width, rupture area, and surface displacement, Bull. Seismol. Soc. Am. 84, no. 4, 974–1002.

Working Group for Earthquake Probabilities (USGS Working Group) (2003). Earthquake Probabilities in the San Francisco Bay Region: 2002–2031, U.S. Geological Society Open File Report 03-214.

Youngs, R. R., and K. J. Coppersmith (1985). Implications of fault slip rates and earthquake recurrence models to probabilistic seismic hazard estimates, Bull. Seismol. Soc. Am. 75, no. 4, 939–964.